A SELF-ACTUATED CELLULAR PROTEIN DELIVERY MACHINERY

A DISSERTATION SUBMITTED TO

THE GRADUATE SCHOOL OF ENGINEERING AND SCIENCE

OF BILKENT UNIVERSITY

IN PARTIAL FULFILLMENT OF THE REQUIREMENTS FOR

THE DEGREE OF

MASTER OF SCIENCE

IN

MATERIALS SCIENCE AND NANOTECHNOLOGY

By

RECEP ERDEM AHAN

August 2018

A SELF-ACTUATED CELLULAR PROTEIN DELIVERY MACHINERY

By Recep Erdem Ahan

August 2018

We certify that we have read this dissertation and that in our opinion it is fully adequate, in scope and in quality, as a thesis for the degree of Master of Science.

_____

Urartu Özgür Şafak Şeker (Advisor)

_____

Murat Alper Cevher

_____

Mesut Muyan

Approved for the Graduate School of Engineering and Science:

_____

Ezhan Karaşan
Director of the Graduate School

ABSTRACT

A SELF-ACTUATED CELLULAR

PROTEIN DELIVERY MACHINERY

Recep Erdem Ahan

M.S. in Materials Science and Nanotechnology

Advisor: Urartu Özgür Şafak Şeker

August, 2018

Owing to increase the knowledge on biology and available tools for genetic manipulations, biological systems are engineered to perform complex tasks. They can be designed to degrade toxic molecules in environment, produce and deliver complex biological drugs, or process and synthesize valuable materials. Hence, the cellular machines hold great promises to solve world problems such as global warming, world hunger, cancer and so forth. However, most of the complex tasks require protein release to extracellular space in a controlled manner. Development of efficient cellular machines is hampered by lack of convenient strategy for controlled protein release as many of proposed secretion systems are limited in a narrow focused application. In this thesis, we are proposing a novel bifunctional self-exciting protein delivery system for broader applications. The proposed protein delivery machine harbours a genetic circuit that is able to display protein-of-interest on cell surface and to secrete to extracellular space in case of need. To do so, we engineered the autotransporter protein Ag43 to display POI with TEV protease recognition site on the cell surface of *Escherichia coli* (*E. coli*). The release of displayed POI was achieved and systematically optimized *in vitro* via

addition of purified TEV protease. To accomplish the self-exciting and controlled release of POI by cells, TEV protease was aimed to be expressed and translocated to extracellular space to cleave the recognition site between POI and Ag43 protein. Four different secretion strategies was employed to secrete TEV protease to extracellular space. While cleavage of POI from cell surface can't be accomplished through secretion of TEV protease by type I system, YebF fusion, and co-expressing lysis gene, codisplaying TEV protease on the cell surface can release the POI. Our data revealed that release of POI can be tuned with controlling the amount of TEV protease on the cell surface. Considering the simplicity of protein display as well as ability to express Ag43 protein in various organisms, the proposed system can be implemented in more complex genetic circuits and used in diverse applications.

Keywords: Protein Secretion, Cellular Machines, Autotransporter protein, Protein Display, TEV Protease

ÖZET

KENDİLİĞİNDEN HAREKETE GEÇEBİLEN HÜCRESEL PROTEİN TAŞIMA ARACI

Recep Erdem Ahan

Malzeme Bilimi ve Nanoteknoloji, Yüksek Lisans

Tez Danışmanı: Urartu Özgür Şafak Şeker

Ağustos, 2018

Biyoloji hakkında bilginin artması ve genetik manipulasyon araçları gelişmesiyle hücreler daha karmaşık görevler yapmak için tasarlanmaktadır. Hücresel makineler küresel ısınma, açlık ve kanser gibi bir çok dünya sorununa çözüm üretmek için umut vadetmektedir. Hücreler makineler çevredeki toksik molekülleri yıkmak, karmaşık biyolojik ilaçları üretmek ve vücut içine dağıtımı veya materyal üretimi ve proses edilmesi için tasarlanabilir. Ancak bunlara benzer bir çok karmaşık görev hücre dışına kontrollü salınımı yapabilen genetik devreler gerekmektedir. Geliştirilmiş çoğu protein salgılama sistemi dar uygulamalarla sınırlı kaldığından etkili hücresel makineler gelişimi aksamaktadır. Bu nedenlerden ötürü yenilikçi bifonksiyonel kendiliğinden salınım yapan bir hücresel protein iletim sistemi geliştirmiştir. Geliştirilen protein iletim sistemi genetik devreler kullanarak proteinleri hücre yüzeyinde gösterimi yapabilmekte ve gerektiğinden salınımı gerçekletirebilmektedir. Sistemde bir ototransporter proteini olan Ag43 istenilen proteiniyle beraber TEV proteaz tanınma bölgesinin gösterimini yapabilmesi için tekrar tasarlanmıştır. İstenilen proteini salınımı *in*

vitro da sistematik olarak saf TEV proteaz enzimi eklenmesi ile optimize edilmiştir. Hücrenin kendiliğinden istenilen durumda protein salınımı yapabilmesi için TEV proteaz hücre dışına salgılanması planmış ve bu amaçla dört farklı salgılanma sistemi denenmiştir. Tip 1 salgılama sistemi, YebF proteiniyle füzyon edilerek ve hücre lize edici proteinlerin beraber ifadesi ile salgılama yöntemlerinde salgılanan TEV proteaz gösterimi yapılan protein salımını gerçekleştirememiştir. Fakat, hücre yüzeyine gösterimi yapılan protein TEV proteaz ile beraber hücre yüzeyinden gösterildiğinde salınım gerçekleşmiştir. Elde ettiğimiz verilere göre protein salınımı TEV proteazın hücre yüzeyinde miktarını kontrol edilmesiyle ayarlanabilmektedir. Salınım basitliği ve Ag43 proteinin bir çok organizmada üretilebilmesini göz önüne alındığında önerilen sistem daha karmaşık genetik sistemlere entegre edilebilir ve geniş uygulama alanda kullanılabilir.

Anahtar kelimeler: Protein Salgılanması, Hücresel Makineler, Ototransporter proteinler, Protein Gösterimi, TEV proteaz

Acknowledgements

I would like thank all the people who supported and helped me during my Master's thesis. It took almost 3 years to finish education in UNAM MSN program, Bilkent, Ankara. During this period, I had many delightful and memorable moments. Despite mainstream opinions, I believe and see that Ankara is a charming place for living with its own dynamics.

I want to start to show my gratitude to Dr. Urartu Seker. As my thesis advisor and mentor, he showed the uttermost support to finish my thesis. He is a very kind, and moral person. He does all possible options to motivate students work with him. I admired his research passion. During under his mentorship, I have improved my professional skills as a scientist. I am very pleased to finish my master education with him. Science is a long journey, I am very lucky to meet a good companion at very beginning of career.

I am grateful to meet with Dr. Esra Yuca during master education. She was a postdoctoral researcher in our laboratory. I believe that she is a walking example of kindship. She helped me to troubleshoot my experiments, and motivated me to continue research.

I am thankful to all current and former members of Synthetic Biosystems Laboratory, UNAM for their friendship, support and understanding. I am aware of that I am not perfect person to work with. I apologize all troubles that I am responsible. I thank my former intern and peer Busra Merve Kirpat, my former intern Nilsu Turan for helping my thesis experiment. I am beholden to work with Sila Kose and Cisil Koksaldi in biosensor project. I always remember their

support in those projects. I thank Ebru Sahin Kehribar for her little chats on everything, Elif Ergun Duman for anecdotes on parenting, Musa Efe Isilak for being an eccentric person, Nedim Haciosmanoglu for scientific news, Ozge Begli for Turkish coffee glasses, and Merve Yavuz for bagels. Most importantly, I thank the members of SBL for making research more fun. In addition, I am happy to meet with Simay Ayhan, Tolga Tarkan Olmez and Ebuzer Kalyoncu. I thank UNAM administrative staff Aysegul Torun, Duygu Kazanci, Mustafa Dogan and Murat Dere for making research easier through their support. Beyond those, I would like to express my gratefulness to UNAM family, and all people who have contributed to National Nanotechnology Research Center. UNAM is the best place in Turkey to do research. I hope that it will continue to grow and become one of the most successful research centers in world.

One of most valuable things that I obtained from my master education is the life-long friendship. I thank Onur Apaydin, Behide Saltepe, Ozlem Ceylan, Cagla Eren and Cemile Elif Ozcelik for their friendship. Especially, I am pleased to Cagla Eren and Behide Saltepe for countless meals that they invited me, Onur Apaydin for life questioning tea times, Ozlem Ceylan for professional support, and Cemile Elif Ozcelik for breakfasts. Even though life may separate us in future, I always remember their memory. Even we are very far from each other, I thank my friends in Istanbul, Deniz Agirdan, Efe Bent and Umut Eskicirak.

Lastly, my deepest gratitude goes to my family for their unrequited love and support. I would like to thank my mother Atikhan AHAN, my father Kadir

AHAN, my big brother A. Oguzhan AHAN, my brother's wife Arzugul Ahan, my little angel Zulfiye AHAN and newest member Rifat Alp Ahan.

This is study was supported by TÜBİTAK Project Number 115M108

Table of Contents

List of Figures

List of Tables

CHAPTER 1

INTRODUCTION

Microorganisms are genetically engineered to perform different tasks as simple as overexpressing a protein and as complex as processing environmental clues to give specific responses. In biotechnological perspective, synthetic microorganisms hold great promises to improve existing applications such as biopharmaceutical production, whole cell catalysis platforms, environmental bioremediation and cell-based therapies (Figure 1).[1]

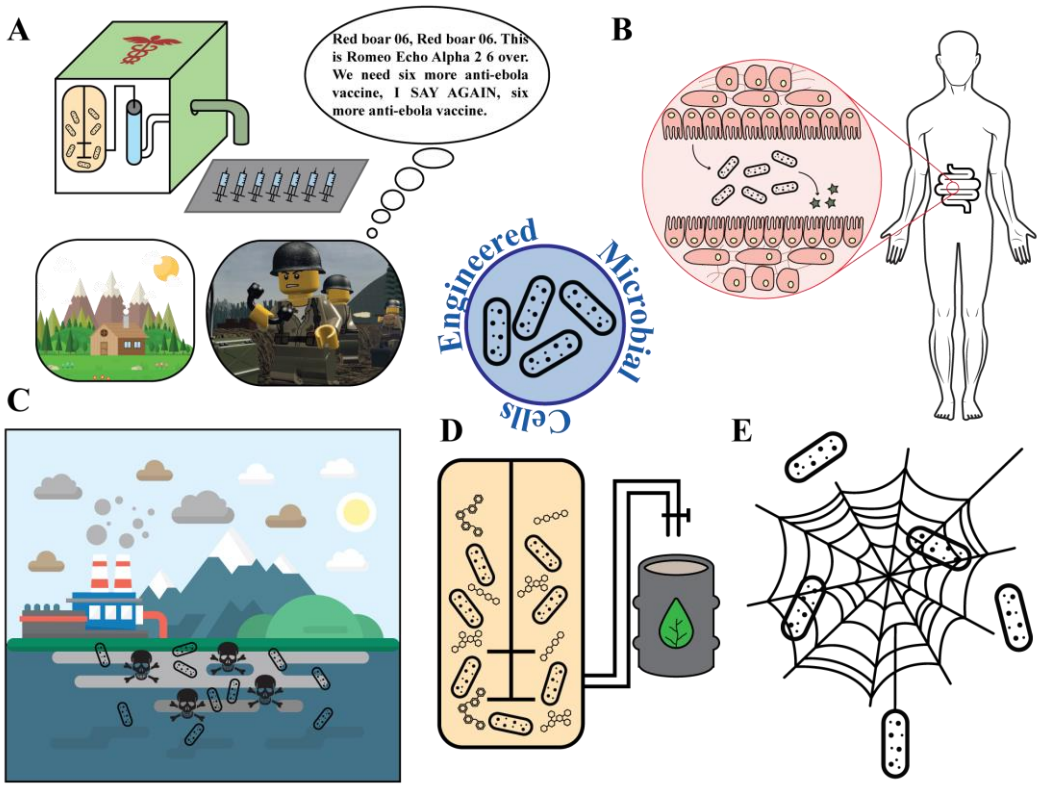

Figure 1: Potential application areas of genetically engineered cell machines. A) Compact point-of-need biopharmaceutical production platforms. B) Intelligent

targeted biologic drugs delivery shuttle. C) Bioremediation applications in polluted areas. D) Degradation of plant debris to produce biodiesel. E) Biomaterial production.

Controlled release of recombinantly expressed proteins is a demanding task and has an uttermost necessity to engineer complex effector microorganisms. Development of better-personalized biomanufacturing platforms, as well as cheaper biopharmaceutical drugs, efficient whole-cell catalysts to process toxic compounds for bioremediation and/or large indiffusible compounds, synthetic cell chassis for production of protein-based materials, and synthetic cell shuttles for protein delivery are dependent on the extracellular production of recombinant proteins.[2-5] Therefore, improving existing strategies and engineering new systems to control the secretion of proteins across cell membranes are crucial for those applications.

Proteins such as toxins, virulence factors, and enzymes are secreted to extracellular medium by a diverse class of microorganisms.[6] Gram-negative bacteria secrete its proteins through two cell membranes that are different in structure and function while secretion in gram-positive bacteria includes only one membrane translocation.[7, 8] There are at least six different types of secretion machinery have evolved for secretion in bacteria. Although secretion systems are distinct compared to each other, their common function is to translocate their substrate through the cellular membranes without leakage of any intracellular molecules.[9, 10] Natural secretion systems are modified and redesigned in order to secrete recombinantly expressed proteins for different purposes.

Downstream processing for purification of secreted proteins is easier as well as cheaper for compared to intracellularly expressed proteins.[11] The cell membrane disruption which may affect the biological activity of proteins is completely omitted as proteins are recovered from extracellular medium.[12, 13] Secreted proteins can be purified with high purity from extracellular medium because compact cells and other contaminants can be easily removed from solution with centrifugation and filtration.[14] In addition, extracellular proteins are protected from intracellular proteolytic degradation and are less likely to form inactive inclusion bodies due to dilution of total protein concentration in extracellular medium.[15] Therefore, extracellular proteins can be recovered from cell medium in high yields. Considering the advantages of extracellularly produced proteins, it may paw the way for the development of efficient personalized biologics production platforms.

Portable platforms for biologic drug production are promising technologies for healthcare systems because current production lines for a biopharmaceutical drug require high-level infrastructure.[2, 16] Moreover, distribution of biologic drugs to remote areas, battlefields, and similar locations face logistical obstacles.[17] Even though transportation is successful, the biological activity of drugs may be decreased during the transport. A previous report indicated that the secreted proteins can be produced and purified at point-of-care with affordable tools in limited time frames. They accomplished to produce near-single-dose recombinant human growth hormone and interferon-α2b in less than 24 hours with milliliter-scale perfusion microfluidic platform.[18] This proof-of-concept study presents

the preliminary achievement of portable platforms that may help people in remote areas to get biopharmaceuticals they need.

Proteins are needed to be secreted to extracellular medium in whole cell catalysis applications to process impermeable substrates, cytotoxic enzyme-catalysed reactions, and toxic compound bioremediation.[19] For instance, a microorganism is engineered to secrete enzymes for degradation of hemicellulose, the major component of plant debris. The resulting sugar molecules are taken up by cells to produce biodiesel.[20] In another study, microorganisms are used to degrade synthetic organophosphates which are poorly transported through cellular membrane and used as pesticides despite their acute neurotoxic effect on humans. The microorganism is engineered to secrete recombinantly produced organophosphorus hydrolases. The secreted enzymes can degrade various different synthetic organophosphorus compounds faster than intracellular expressed enzymes.[21]

In recent years, recombinant production of structural proteins such as silk monomers for development of novel biomaterials for electronic, biomedical and other applications has been drawn attention from scientists because of their superiorities on strength, biodegradability, and elasticity.[22] However, aggregation-prone nature of those proteins makes them impractical to produce intracellularly in a recombinant host.[23, 24] Therefore, many studies focus on the secretion of monomers of protein-based biomaterials have been published. In a previous study, *E. coli* is engineered to secrete conductive amyloid fibers. The secreted amyloid monomers are able to form amyloid fibers yet the intracellular expression of amyloid fiber monomers lead to cytotoxic on the *E. coli*.[25, 26]

Synthetic cell therapies hold great promises to develop next-generation medicine that interacts with the body through implemented genetic circuits to deliver therapeutics in target-sites.[27] Synthesis and delivery of therapeutics by engineered cells have many advantages over traditional administration of drugs such as reduced side effect, and increased efficacy.[28, 29] Most of the cases, the therapeutics that are needed to be delivered are protein-based substances and are required to be secreted by engineered cells. Previous reports demonstrated that cells can be engineered to treat diseases such as diabetes *in vitro* epithelial cell models and *in vivo* mouse models.[30] For instance, *E. coli* is engineered to sense glucose concentration and to secrete insulinotropic proteins fused cell penetrating peptide based on glucose concentration. Addition of cell supernatant from glucose-treated cells is lead to the expression of insulin from Caco-2 cells based on *in vitro* experiments.[31] Programmed cells as therapeutics have potential to be long-lasting treatment for diseases that can't be addressed with current medication.[32]

1.1. Secretion of Recombinantly Expressed Protein in *Escherichia coli*

E. coli is the work-horse microorganism for recombinant production of industrially and pharmaceutically important proteins.[33] This gram-negative bacterium is widely used in mass production due to its relatively fast growth rate and simple cultivation techniques. Moreover, lots of genetic tools have been developed for *E. coli* to alter its genomic information such as modified strains, vector plasmids, promoter and regulatory elements.[24, 34]

The *E. coli* bacterium is able to express foreign proteins in an amount equivalent to half of its protein pool upon induction.[24] Due to its high performance in recombinant protein production, a significant amount of research has been done to develop secretory protein production for *E. coli*.[33] The proteins can simply be secreted to periplasm by SecYEG and TAT transporters.[35] However, the main challenge for secretory production of heterologously expressed proteins is the translocation through outer membrane.[36] Primary studies utilize the dedicated secretion systems, which are evolved for the secretion of toxic protein molecules such as HlyA, to transport recombinant proteins to extracellular space. The secretion machineries found in pathogenic strains are engineered and heterologously expressed in non-pathogenic laboratory strains of *E. coli*. Recombinant proteins are fused with part of the natively secreted proteins to target to secretion machineries.[37] The finding of naturally secreted proteins by non-pathogenic strains such as YebF and OsmY gives an alternative way to secrete recombinant proteins. The recombinant proteins can be secreted through membranes fused with those carrier proteins.[38, 39] In addition to carrier proteins and dedicated secretion systems, the recombinant proteins can be translocated to periplasm; then, can be secreted to extracellular space through outer membrane leakage. The leakage can be established with co-expressing or knock-outing certain proteins that are interacting and/or disturbing the outer membrane.[40, 41] Moreover, the autotransporter proteins are used translocate recombinant proteins to the outer membrane. Unlike other systems, autotransporter proteins are embedded in the outer membrane and the fused proteins are not truly secreted to extracellular medium but are displayed on the

cell surface yet it is possible to release proteins to extracellular milieu (Figure 2).[42, 43]

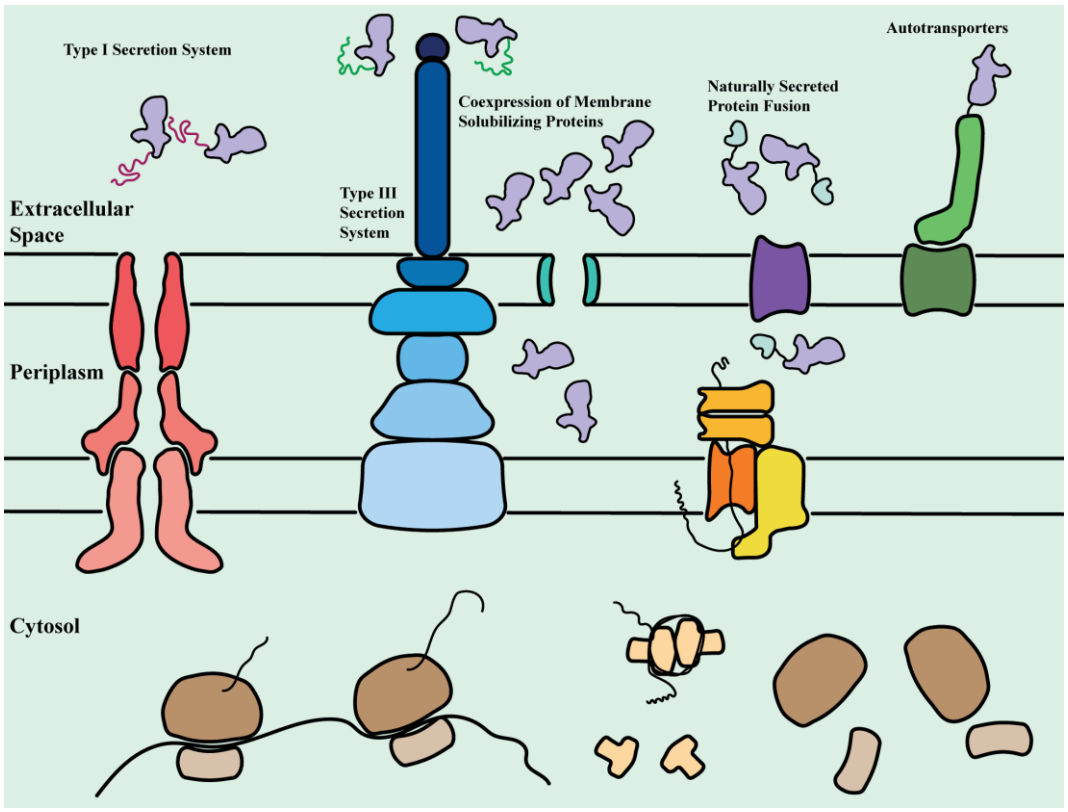

Figure 2: Strategies to secrete recombinant proteins in *E. coli*

Site-specific proteases such as TEV protease are used to cleave the fusion partners however those strategies can't be employed by themselves to delivery therapeutics.

1.2. Type I Secretion System Based Strategies

E. coli utilizes the type I secretion system (TISS) to secrete large toxins and exoenzymes.[44] Type I system involves a single step for transporting proteins to extracellular space. The translated proteins partially fold in the cytosol and recognized by the system for secretion. During secretion process, translated

proteins are directly secreted to extracellular space without passing periplasm.[45] The type I secretion machinery is composed of two effector protein belonging to ATP binding cassette transporter family.[46] The HlyA secretion cassette is most engineered transporter system to secrete recombinant proteins. The information required for secretion is encoded in the C-terminal region of HlyA protein. Previous reports show that at least 62 amino acids from C-terminal of HlyA are required to fuse to recombinant protein for secretion.[47] The C-terminal region is recognized by HlyB and HlyD proteins. Another protein called TolC binds the protein complex to facilitate secretion. Upon hydrolysis of ATP by HlyB protein, the recombinant protein is secreted into extracellular space.[48] During secretion, disulfide bridges are formed independently from Dsb system.[44] TISS is capable to secrete proteins as large as 4000 amino acids, and %5 of the total protein pool. The main drawback of TISS is that HlyB and HlyD transporters proteins are needed to co-express with recombinant proteins.[49] Co-production of transporters proteins may cause a burden on cellular metabolism. In addition to metabolic burden, the fused C-terminal region of HlyA is not cleaved during the secretion. Further cleavage after secretion is required to remove the region.

Although the metabolic burden and extra processing requirement, the HlyA system was used to secrete various proteins including interleukin-6 and scFv antibodies.[50, 51] Furthermore, research efforts continue to make hypersecretory cells with hemolysin transport system.[52, 53]

1.3. Type III Secretion System Based Strategies

The type III secretion system (TIIISS) is the most complex bacterial secretion system. The system composed of at least 30 different structural and regulatory proteins to control and facilitate the secretion.[54] Generally, pathogenic strains of different bacteria utilize this system to transport virulence effector proteins into mammalian hosts. The structural proteins of TIIISS form a syringe-like nanomachine to connect intracellular space of bacteria to mammalian cell cytoplasm.[55] The expression of machinery, as well as secretion, is well regulated with transcription factors and chaperone proteins as the production of TIIISS is metabolically expensive.[56] The TIIISS have similarities with bacterial flagella. Previous studies reported that the deletions of FliC, FliD genes from the laboratory strain of *E. coli* lead to secretion of recombinant proteins. To secrete recombinant proteins, the gene is cloned with 173 bp untranslated DNA region of FliC as well as transcription terminator of FliC gene.[57]

In addition to modifications of bacterial flagella for secretion, TIIISS of Shigella flexneri is reconstituted in *E. coli* to secrete various proteins into mammalian cells. The region that encodes the TIIISS from Shigella 220 kb virulence plasmid was inserted into the genome of *E. coli* DH10ß strain. The expression of the cassette is controlled through cloning the transcription activator of secretion genes under an inducible promoter. The secretion signal screening results indicate that recombinant proteins fused with first 50 amino acid of eleven distinct effectors are translocated to extracellular medium.[58] In another study, the TIIISS of Salmonella bacteria is engineered to secrete silk monomers fused with N-terminal

secretion signal of effector protein called SptP. The system is able to secrete silk monomers at the rate of 1.8mg.l^{-1}.h^{-1}.[59]

1.4. Naturally Secreted Protein Fusions

Recombinant proteins can be secreted to extracellular medium with carrier proteins such as YebF and OsmY. Both of the proteins are native *E. coli* proteins transported to extracellular space. During the secretion processes, YebF and OsmY proteins are firstly translocated to periplasm by SecYEG translocon. The transportation of YebF across outer membrane is facilitated by OmpF and OmpC proteins while translocation mechanism of OsmY is still unknown. The recombinant proteins are fused to C-terminal of the YebF or OsmY for extracellular secretion. The expression of either protein does not affect the outer membrane integrity.[38, 39] The main disadvantage of the carrier proteins is low secretion although many studies are reported for improving the secretion yield.[19]

A systematic study shows that epidermal growth factor, growth hormone, interleukin-2, and granulocyte colony-stimulating factor are successfully secreted to extracellular medium fused with YebF and OsmY. The secreted proteins are isolated in their active form with yield in the range of 1 to 350mg. The report concludes that many of the hard-to-expressed eukaryotic proteins can be expressed as YebF or OsmY fusions and can be isolated from extracellular medium.[60]

1.5. Strategies Involving Leaking Membrane Mutants and Lysis-Inducing Protein Co-Expressing Cells

Decreasing the outer membrane integrity to induce leakage is exploited for the production of extracellular proteins. The recombinant proteins are targeted to SecYEG or Tat translocon with N-terminal signal sequences of native periplasmic proteins such as Dsb, ALP, OmpA.[61-63] The translocated proteins freely diffuse due to loss of outer membrane integrity and can be recovered from extracellular medium. There are several methods to disturb outer membrane structure. Deletion of certain genes such as *lpp* increases the diffusion of periplasmic proteins.[33]

A previous report indicates that the protein secretion in *lpp* gene mutant cells is not caused by cell lysis. The mutant cells are able to grow in all stages of the growth phase. In their experimental set-up, all three model proteins which are MalE, xylanase, and cellulase are secreted in higher amounts compared to non-mutant cells.[64] In another extreme example, L-forms cell mutants that lack cell wall can be used for extracellular protein production yet the mutant cells are highly sensitive to physical stress which make them inconvenient to large batch fermentation.[65]

Beyond the cell mutants, outer membrane disrupting genes such as *kil* gene can be co-expressed to increase the permeability of the outer membrane. The previous report shows that the encoding protein interacts with FtsZ protein and inhibits assembly of FtsZ ring structure required for proper cell division. Due to interaction with a vital process in cell division, expression of kil gene is needed to

optimize for maximum production efficiency.[66] Many examples of secretory protein production using kil gene co-expression are reported. For instance, a study shows that human growth factor can be isolated in high purity from the extracellular medium using this approach. The human growth factor is secreted to periplasm with OmpA signal peptide, and extracellular diffusion is triggered upon induction of *kil* gene. The authors indicate that after single step purification, they manage to obtain the protein with >98% purity.[67]

1.6. Type V Secretion System Based Strategies

Type V secretion system (TVSS), also called as autotransporters, is diverse protein family found in gram-negative bacteria. Although TVSS family proteins have different classes, they share common mechanism secrete its partner domain to the outer surface of bacteria. The autotransporter proteins are consist of N-terminal periplasmic localization signal, secreted partner domain, and outer membrane translocation domain. The unfolded translated protein chain is transported across inner membrane to periplasmic space. The outer membrane translocation domain is embedded into outer membrane and forms the ß-barrel structure. The secreted partner domain is transported to the outer surface of bacteria by translocation domain. During the transport, the partner domain may be cleaved by internal proteases motif and remains attached to surface with non-covalent interactions. Despite fact that many years researchers convinced that all information required for transportation is encoded in protein structure, recent studies show that the periplasmic proteins such Bam and Tam complexes interact with autotransporters to facilitate secretion.[68, 69]

The protein secretion and surface display with autotransporters are possible with replacing the native partner protein with recombinant proteins.[70] Mainly, autotransporter proteins are used in the bacterial surface display of enzymes, and motifs for high-throughput techniques.[71] In addition to using as display technology, a study shows that deletion of certain parts of partners protein that are mainly responsible for attachment cell surface leads to release of the recombinant proteins to extracellular medium.[72]

1.7. Site-Specific Proteases in Recombinant Protein Processing

The site-specific proteases which have key roles on fundamental biological reactions recognize and cleave a certain motif in proteins.[73] For instance, protease domain obtained from nuclear inclusion a protein from tobacco etch virus (TEV protease) recognizes the consensus sequence ENLYFQG and cleaves peptide bond between Q and G residues.[74] The protease domain is important for processing translated polypeptide into active viral proteins[75]. Besides their biological importance, the site-specific proteases are engineered to be utilized biological technological tools.[76, 77] For example, the unwanted functional tags are cleaved with site-specific proteases such as TEV protease, Factor Xa, human rhinovirus protease and many others.[78] Moreover, site-specific proteases are utilized to build post-translational logic gates in recent reports. [79]

Many of bacterial secretion strategies require downstream processing to remove uncleaved tags from recombinant proteins. The fusion partners are left covalently attached to recombinant protein in most of the systems after secretion processes.

Therefore, downstream processing are needed to cleave the fusion partners as a remaining domain may affect protein folding and activity.[80-82] In case of YebF protein for example, it carries two cysteine residues that may cause the formation of unspecific disulfide bridges with secreted protein during maturation.[33] Though cleavage reaction is efficient to cleavage tags in vitro, additional purification step often is necessary to remove the protease which leads to decrease in total purified protein yield. In addition, the biological activity of protein might be affected during cleavage and/or further purification step.[83] Site-specific proteases can be expressed in cells to process recombinant protein in the cytosol which ease the burden on following steps.[80] Moreover, self-processing is required for protein-based therapeutics delivery by cells because it isn't convenient to add pure site-specific protease with cells into body.

Considering features of site-specific proteases, they can be engineered to build autonomous cellular system that is able to control recombinant secretion and to process secreted protein at the same time.

1.8. The Aim of Study

Although there are many different strategies to secrete proteins to extracellular space, most of them are developed for specific purposes, and can't be utilized in other applications. In this thesis, we aim to develop a novel protein secreting cell system for addressing many drawbacks in extracellular protein production. For this purpose, an engineered cellular system that is capable of display and release proteins in defined conditions is proposed. The proposed strategy involves the display of recombinant proteins on the cell surface via engineering the Ag43

native autotransporter protein. The displayed protein is aimed to release to medium upon cleavage with a site-specific protease (TEV) (Figure 3). To release the displayed proteins, site-specific protease is secreted to extracellular medium with four different secretion strategies. The release of displayed proteins is accomplished with co-displaying the site-specific protease. As the release of recombinant proteins are controlled with the expression of two different gene cassette, it is possible to build two-input Boolean logic operations for defining the release conditions. The proposed system provides a better platform to develop efficient cellular machinery for biologic delivery, bioremediation and bioprocessing applications as well as onsite biologics manufacturing systems.

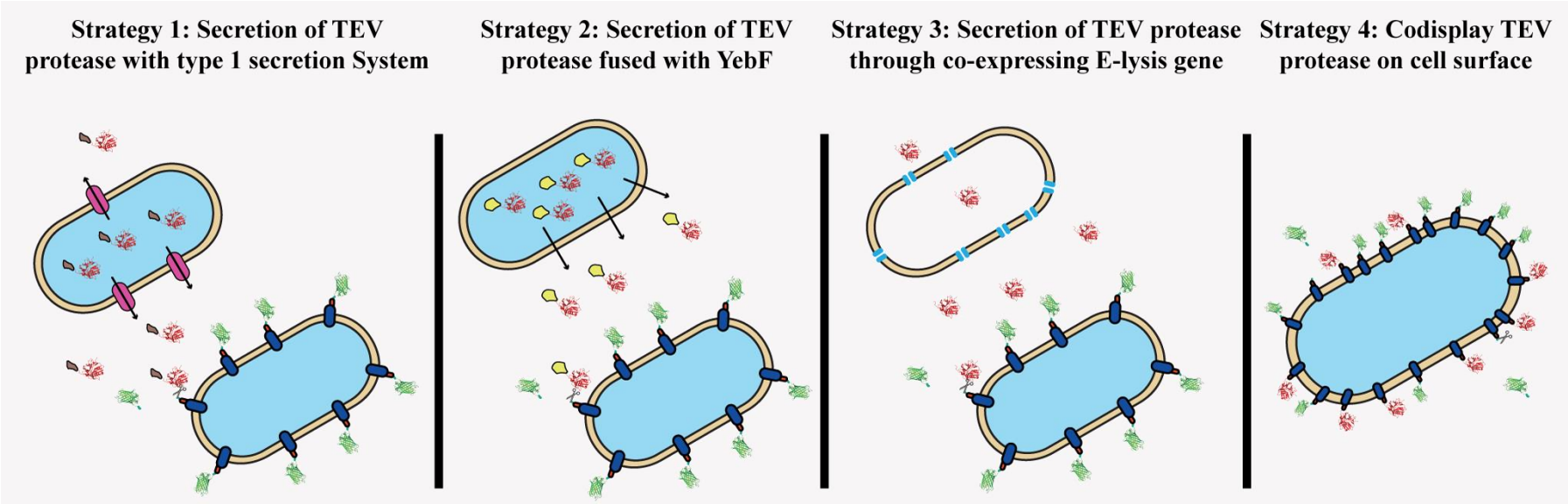

Figure 3: Four different secretion strategy for TEV protease to release displayed POI

CHAPTER 2

MATERIALS AND METHODS

2.1. Cell Strains, Growth, Cell Maintenance, and Transformation

E. coli DH5α PRO strain was used for cloning purposes. Cell stocks are maintained at -80 ˚C in %25 glycerol in Lysogeny Broth (LB) solution. This strain contains PRO cassette which encodes elements for constitutively active expression of TetR and LacI repressor and resistance gene to spectinomycin. For protein expression and purification, *E. coli* BL21 (DE3) strain was used. This strain carries T7 polymerase gene under control of Lac promoter.

Unless otherwise stated, plasmids are transformed into the bacterial cell with chemical transformation. To prepare chemical competent cells, cells were inoculated in fresh LB with appropriate antibiotics from -80 ˚C cell stock and grown for overnight. Next day, cells were reinoculated in fresh LB with 1:100 dilution. When OD600 reached 0.2-0.5, cells were cooled in ice for 10 minutes. After cooling, cells were collected by centrifugation at 1000xg for 10 minutes at 4 ˚C. The cell pellet was resuspended in TSS Buffer (1:10 volume of original growth) and aliquoted into 100µl per micro-centrifuge tube. The aliquots were stored -80 ˚C.

The aliquoted cell stock was thawed on ice for 30 minutes in order to transform the plasmids. For transformation, 100 ng of intact plasmid or whole Gibson assembly reaction or whole T4 ligation reaction was added to thawed cells and incubated on ice for 20 minutes. The cells were shocked at 42 ˚C for 45 seconds. After the heat shock, cells were incubated on ice for 2 minutes. 250µl of LB was added onto the cells and incubated at 37 ˚C for 45 minutes in shaking incubator (200rpm). After incubation, cells were centrifuged. 250µl of the supernatant was discarded, and the cell pellet was resuspended with remaining supernatant. The resuspended cells were spread onto LB-agar with appropriate antibiotics.

2.2. Plasmid Constructions and Cloning

In order to construct the pET22b PelB 6H Ag43 160N sfGFP vector, 1000ng of pET22b vector was digested with XhoI and NcoI enzymes at 37 ˚C for 3 hours. sfGFP gene was amplified with R3 and R4 primers from the pJT119b plasmid (kindly gifted by Jeffrey Tabor, Addgene plasmid #50551).[84] The PCR product was reamplified with R3 and R5 to add TEV recognition site flexible linker to sfGFP protein. The truncated Ag43 gene was amplified with R1 and R2 primers from *E. coli* DH5α strain. PCRs were performed with Q5 polymerase enzyme in recommended conditions by the manufacturer (given in Appendix E).

The PCR products and restriction digestion reaction were loaded in %1 agarose gel and run for 25 minutes at constant 140V. The DNA products were sliced from agarose gel and were isolated from agarose using MN PCR clean-up kit. The isolated DNA pieces were assembled with Gibson Assembly reaction prepared in our laboratory (reaction mix is given in Appendix E). Approximately 50 ng

digested vector and the equal molar to digested vector of each DNA pieces added into 1,33x Gibson reaction mix. If the reaction mix was not diluted to 1x upon addition DNA pieces, ddH2O should have been added into the reaction to dilute reaction to 1x. The reaction mix was incubated at 50 ˚C for 1 hour. Then; the assembled vectors were transformed into *E. coli* DH5α PRO strain as described above.

To clone TEV protease into pET22b PelB 6H Ag43 160N vector, YebF-TEV pZA vector was cut with AflII and BamHI enzymes to obtain TEV protease gene. The pET22b PelB 6H Ag43 160N sfGFP vector was digested with same restriction enzymes to obtain the vector. The restriction digestion products were loaded in %1 agarose gel and run for 25 minutes at constant 140V. DNA from sliced gels obtained same as described above. The purified DNA products were ligated with T4 ligation reaction. 50 ng of vector and 3 fold excess molar of the digested insert was mixed in T4 reaction. The reaction recipe is given in Appendix E. The reaction mix was incubated at room temperature for 15 minutes and subsequently transformed into *E. coli* DH5α PRO strain as described above.

pZA nTetO PelB 6H Ag43 160N TEV vector was constructed by assembling native TetO promoter, PelB 6H Ag43 160N TEV gene, and pZA vector. Native TetO promoter was amplified along with TetR repressor from the pdCas9-bacteria plasmid [85] (kindly gifted by Stanley Qi, Addgene plasmid #44249) using R8 and R9 primers. The PelB 6H Ag43 160N TEV gene was obtained via PCR using R6 and R7 primers. pZA vector was digested with NotI-HF and MluI-HF restriction enzymes as in conditions described above. The products were loaded in the agarose gel and purified as described above. The equal molar of each DNA

segment was assembled with Gibson Assembly reaction, and transformed into *E. coli* DH5α PRO strain as described above.

To construct the pET22b 6H GST-TEV vector, pET22b vector was digested with XbaI and XhoI restriction enzymes. The GST gene was amplified from pGEX-6P-1 vector using R12 and R13 primers. The resulted PCR product was amplified again using R12 and R14 to add the N-terminal 6x His-tag and ribosome binding site to GST gene. The TEV protease gene was amplified from pUC57-TEV protease (synthesized from Genewiz) via PCR using R10 and R11. The products were loaded in the agarose gel and purified as described above. The equal molar of each DNA segments were assembled with Gibson Assembly reaction, and transformed into *E. coli* DH5α PRO strain as described above.

For construction of pET22b nTetO 6H HlyA tagged GST-TEV vector, the DNA region encoding GST-TEV fusion protein was amplified with R15 and R16 primers along with Gibson overhangs. The C-terminal region of HlyA toxin was amplified from BBa_K554002 vector (iGEM collection) with R17 and R18 primers. The pET22b nTetO vector was linearized with KpnI and XhoI digestion. The DNA fragments were run and purified from agarose gel. The purified DNA fragments assembled in Gibson Assembly reaction, and transformed into *E. coli* DH5α PRO strain as described above.

In order to clone the YebF gene at the upstream of TEV protease coding region, the region encoding the YebF gene was amplified with R19 and R20 primers from *E. coli* DH5α genome. The pZA TetO TEV 6H vector was digested with KpnI and BamHI. The DNA fragments were run and purified from agarose gel. The purified

DNA fragments assembled in Gibson Assembly reaction, and transformed into *E. coli* DH5α PRO strain as described above.

To change the sec translocon peptide of YebF protein pZA TetO YebF-TEV 6H vector, the vector was amplified with R21 and R22 for DsbA signal peptide, and with R23 and R24 for OmpA signal peptide. The amplified vectors were self-assembled in Gibson Assembly reaction, and transformed into *E. coli* DH5α PRO strain as described above.

The E-lysis gene was cloned into pZA nTetO vector. The pZA nTetO vector was digested with KpnI and XhoI enzymes. The E-lysis gene was amplified with R25 and R26 from pCSaE500 vector (kindly gifted by Lingchong You, Addgene plasmid #53182)[86]. The DNA fragments were run and purified from agarose gel. The purified DNA fragments assembled in Gibson Assembly reaction, and transformed into *E. coli* DH5α PRO strain as described above.

All vectors were sequenced with Sanger sequencing (Genewiz) to verify successful cloning.

2.3. Sequence Alignments with Geneious Software

The vector sequences were constructed and obtained Benchling.com. The sequence files obtained from Genewiz company and .gb files exported from Benchling.com of vectors were imported by choosing file>import>from file option. Clicking the option opens to a new window for navigating the files. The folder containing .abi were selected to import all files. To align the two specific sequences, sequences were selected to main working windows. After selection,

choosing to align/assemble>pairwise alignment from upper panel opens new windows. At this window, the user may define specific parameters to align the sequences. We selected to automatic determination of directions, global alignments with free and gaps, and %65 similarity options to align the sequences.

2.4. Expression and Labelling of Surface Displayed sfGFP and TEV protease

Sequence verified pET22b PelB 6H Ag43 160N sfGFP or TEV protease vector was transformed into *E. coli* BL21 (DE3) strain with chemical transformation. Single colonies from each plate were picked and inoculated into 5ml of LB medium with appropriate antibiotics. The overnight grown cells were subcultured 1:100 into 10ml of fresh LB supplemented with %1 (w/v) glucose and antibiotics. At mid-log phase (OD600: 0.4-0.6), the gene was induced with 1mM IPTG at 18 ˚C for overnight.

Induced cells harboring pET22b PelB 6H Ag43 160N sfGFP or TEV protease vector was collected in next day. 250µl of cells in LB medium was centrifuged at maximum speed for 3 minutes. The pellet was washed with 1ml of 1x PBS once and resuspended in 250µl of %1 BSA dissolved in 1x PBS solution. For blocking, cells were incubated at RT for 2 hours. Subsequent to incubation, cells were centrifuged at maximum speed for 3 minutes, and blocking solution was discarded. The cell pellet was resuspended in anti-his primary antibody diluted with 1:250 ratio in %1 BSA dissolved in 1x PBS solution and incubated at 4 ˚C for overnight. The cells were washed three times with 1x PBS solution after the incubation. Following the washing step, cells were treated with anti-mouse

secondary conjugated DyLight550 dye diluted with 1:500 ratio in %1 BSA dissolved in 1x PBS solution. The solution was incubated at room temperature for 2 hours. The cells were washed two times with 1x PBS solution. The labeled cells were examined under the epifluorescence microscope.

2.5. Gold Nanoparticle Labeling of Surface Displayed sfGFP

Cells were induced as described above. Subsequent to induction, cells harboring surface displayed sfGFP with 6x His tag were tagged with Ni-NTA conjugated gold nanoparticles (5nm, Nanoprobes) with the modified version of protocol in [4]. Briefly, TEM formvar-carbon coated 200 mesh nickel grids (Electron Microscopy Sciences) was used to blot sfGFP displayed. The coated surface of the grid was incubated onto 20 µl droplet of suspended cells on parafilm for 5 minutes. Following the blotting, the TEM grids were washed with, respectively, 30µl of ddH2O and selective binding buffer (1x PBS, 300mM NaCl, 80mM imidazole, 0.2% (v/v) Tween-20) for 5 minutes, each. The remaining cells on the grid were labeled NiNTA-AuNP. To label the cells, TEM grids were incubated onto 90µl droplet of 10nM Ni-NTA dissolved in selective binding buffer for 90 minutes at room temperature. To reduce the evaporation of liquid during incubation, droplet and TEM grid were covered with a petri dish. Subsequent to tagging step, the TEM grids were washed 9 times with 30µl of selective binding buffer for 5 minutes, each. Additionally, the grids were washed further 2 times with 30µl of 1x PBS, and 2 times with 30µl of ddH2O. The washed TEM grids were stained with 20 µl of 2% (w/v) uranyl acetate for 15-30 sec. All liquids on

TEM grids was evaporated with air drying. In the all steps, excess liquid onto TEM grids was removed with Watmann paper. The TEM grids are examined under transmission electron microscope TEM (FEI Tecnai, USA) at 200 kV. Energy Dispersive X-Ray Spectroscopy (EDS) analysis was also performed to verify the presence of gold nanoparticles. (EDAX, USA).

2.6. Trypsin Protease Digestion of Surface-Exposed sfGFP

Prior to trypsin treatment, cells were induced as described above. The fresh induced cells were collected and centrifuged at 8000xg for 5 minutes. The supernatant was discarded and suspended in 1x PBS for further use. For trypsin treatment, 5x108 cells were taken and suspended with 200µl 1x PBS. 10 µg trypsin protease (Sigma- Aldrich) was added and incubated 37 ˚C for 2 hours. After incubation, cells were centrifuged and washed twice with 1x PBS. The washed cells were resuspended in 200µl of PBS. The fluorescence emission of cells was measured with the M5 spectrophotometer.

2.7. Heat Release of Surface Displayed sfGFP and TEV protease

To release surface displayed proteins (either TEV or sfGFP), 5x108 cells were taken and suspended with 200µl 1x PBS. The suspended cells were briefly heated at 60 ˚C for 5 minutes. Following the heat shock, cells were immediately centrifuged at maximum speed for 5 minutes. The supernatants were collected to

further analysis. For sfGFP displaying cells, the fluorescence emission of supernatants was measured with the M5 spectrophotometer. Western blot analysis was performed to verify the presence of sfGFP and TEV protease fused with truncated passenger domain of Ag43.

2.8. Expression, Purification, and Quantitation of GST-TEV protease

The sequence-verified pET22b 6H GST-TEV vector was transformed into chemically competent *E. coli* (DE3) strain as described above. The cells were spread onto agar plate containing appropriate antibiotic and was incubated overnight at 37 ˚C for overnight. In the next day, a single colony was chosen to inoculate into LB medium supported with appropriate antibiotic. The inoculated cells were grown in shaking incubator for overnight at 37 ˚C, 200 rpm. The grown cells were diluted into LB medium in the next morning. When optical density of the medium (600nm) reached to approximately 0.6 (mid-log phase), the production of GST-TEV protease was induced with 1mM of IPTG (isopropyl β-D-1-thiogalactopyranoside). The cells were further incubated in shaking incubator for 6 hours at 30 ˚C, 200 rpm. After the incubation, the cells were centrifuged and the pellet was solved with binding buffer (20 mM sodium phosphate, 0.5 M NaCl, 20 mM imidazole, pH 7.4). 1mM of PMSF and 100 µg/µl of lysozyme was added into suspended cells. The cells were burst with five cycles of freeze & thawing with liquid nitrogen. The total protein lysate was collected by centrifugation at 4 ˚C, 21500xg for 1 hour. GST-TEV protein was purified with IMAC column purification.

The IMAC column (HisTrap HP 1ml, GE Healthcare) was washed with 5 volumes of distilled water prior to use at flow rate 5ml/min. To equilibrate the column, at least 5 volume of binding buffer was used to wash. The total protein lysate was filtered twice with 0.45 μm filter, and His-tagged proteins were bound to the column with same flow rate. After binding, the column was washed until the protein absorbance reached the steady baseline. Bound GST-TEV proteins were eluted with 5 volume of elution buffer (20 mM sodium phosphate, 0.5 M NaCl, 500 mM imidazole, pH 7.4). The purified proteins were dialyzed two times with SnakeSkin Dialysis Tubing 3K MWCO (Thermo Fisher) to 100 mM Tris-HCl pH 7.5, 2 mM EDTA, and 0.1% (w/v) Triton X-100 solution at 4 ˚C. After dialysis, the solution was concentrated with ultracentrifugation. One volume of pure glycerol and 5mM DTT were added to the final solution. The SDS-PAGE analysis was performed to determine the concentration of GST-TEV after buffer exchange.

20μL of purified and buffer exchanged GST-TEV proteins, and BSA stocks (2mg/ml, 1mg/ml, and 0.5mg/ml) were mixed with 4μL 6x SDS-PAGE loading dye. The samples mixed with dye solutions were incubated at 95 ˚C for 5 minutes. The heat samples were load into 12% SDS-PAGE gel wells, and run at 120V for 1.5 hours. Subsequent to running, the gel was stained with Coomassie blue. To stain the gel, the Commassie dye solution was poured onto the gel in a container, and heated in a microwave for 1 minutes. The dye solution poured, and the gel was washed plenty of tap water. The destaining solution was poured on the gel and incubated at room temperature until the bands appear. The imaging and

quantitation of bands were performed in Chemidoc Imaging System (Bio-Rad) and ImageLab software (Bio-Rad).

2.9. Biochemical Release of Surface Displayed sfGFP with TEV protease and TEV Protease Activity in Different Growth Media

5x108 fresh sfGFP displayed cells were centrifuged and washed with TEV protease buffer (50mM Tris-HCl pH=8, 0.5mM EDTA) without DTT. Cells were resuspended in 200 µl of TEV protease buffer, and approximately 6µg of GST-TEV protease was added. The cleavage reaction was incubated at 4 ˚C for overnight. Cells were centrifuged at full speed for 5 minutes. Supernatants were collected. The pellets were resuspended in 200µl of PBS. The fluorescence emissions of collected supernatants and resuspended cells were measured with the M5 spectrophotometer.

To assess the activity of TEV protease in different media, 400µl of freshly induced cells were taken and centrifuged at maximum speed for 5 minutes. The cell pellets were washed twice with either LB or M63 defined medium or MOPS defined medium. After washing, cells were resuspended in different growth media in different pH. LB (pH= 5.2, 7.0, 8.2), M63 defined media (pH= 5.2, 6.0, 7.0, 8.2), and MOPS defined media (pH= 5.2, 6.0, 7.0, 8.2) was used. 6µg of GST-TEV protease was added into suspended cells and incubated at 4 ˚C for overnight. Following the incubation, cells were centrifuged at maximum speed for 5 minutes.

The fluorescence emissions of collected supernatants were measured with the M5 spectrophotometer.

2.10. Expression of HlyA Tagged GST-TEV

Sequence verified pET22b nTetO 6H HlyA tagged GST-TEV and pVDL9.3 vectors were co-transformed in *E. coli* BL21 (DE3) strain. A single colony was picked and was grown for overnight in LB medium supplemented with appropriate antibiotics. The overnight grown culture was re-inoculated in fresh LB medium with 1:100 dilution. The expression of Hly transpoter genes and HlyA tagged GST-TEV were induced same time with IPTG and aTc, respectively, at mid-log phase. The cells were incubated at 30 ˚C for six hours. Following the incubation, supernatants were collected by centrifugation (8000xg, 5 minutes) for analysis.

2.11. Expression and Co-seeding of YebF-TEV Fusion Proteins

Sequence verified pZA TetO YebF-TEV 6H vector was transformed into *E. coli* DH5α PRO strain. A single colony was picked and was grown for overnight in LB medium supplemented with appropriate antibiotics. The overnight grown culture was re-inoculated in fresh LB medium with 1:100 dilution. The YebF-TEV gene was induced with aTc at 30 ˚C for six hours. Subsequent to the induction, supernatants were collected by centrifugation (8000xg, 5 minutes) for analysis.

For co-seeding of YebF-TEV carrying cells, and display cassette carrying cells, single colonies were picked and grown overnight for each one. The overnight grown cells were inoculated into same modified MOPS defined medium with defined ratio at final cell dilution of 1:100. At mid-log phase, the display cassette was induced with IPTG while the YebF-TEV gene was induced with aTc. The cells were induced at 18 ˚C for 24 hours. After the induction, supernatants were collected by centrifugation (8000xg, 5 minutes) for analysis.

2.12. Expression and Analysis of E-lysis Related Experiments

The sequence verified pZA nTetO E-lysis vector was transformed into *E. coli* BL21 (DE3) strain. A single colony was picked from agar plate and grown for overnight. The overnight grown cells were diluted with 1:100 ratio in fresh LB medium with appropriate antibiotics. The E-lysis gene was induced at mid-log phase with aTc. The growth of culture were monitored during induction with measuring the absorbance at 600nm.

To count the viable cells after the induction, 100µl of culture was spread onto agar plate and grown for overnight. Next day, the single colonies were counted on agar plates.

To visualize the pores on cells after E-lysis induction, environmental scanning electron microscope (ESEM) was utilized. The cells were fixed onto silica wafer with %2,5 glutaraldehyde solution in PBS for overnight at 4 ˚C. Following the incubation, silica wafers were washed two times with PBS, and two times with

pure water for 5 minutes each. The silica wafer washed one time with %25 EtOH for 5 minutes, one time with %50 EtOH for 5 minutes, one time with %75 EtOH for 5 minutes and three time with pure EtOH. Following the washing steps, the silica wafer was dried with Critical Point Dryer (Tousimis). The silica wafers were coated 8nm with Au/Pd alloy. The silica wafers were examined under ESEM (Tecnia) at 15 kV, 3.0 spot size.

2.13. Co-seeding of Display Cassette Carrying Cells and E-lysis/GST-TEV Carrying Cells

Sequence verified pZA nTetO E-lysis and pET22b 6H GST-TEV vectors were sequentially transformed into *E. coli* BL21 (DE3) strain. Meawhile, pET22b PelB 6H Ag43 160N sfGFP and mock CmR pZA vectors sequentially were transformed *E. coli* BL21 (DE3) strain. Single colonies were picked and grown overnight for each one. The overnight grown cells were inoculated into same modified MOPS defined medium with defined ratio at final cell dilution of 1:100. At early-log phase, the display cassette and the GST-TEV gene were induced with IPTG. The e-lysis gene was induced at mid-log phase with aTc. The cells were incubated for overnight at 18 ˚C. Following the incubation, supernatants were collected by centrifugation (8000xg, 5 minutes) for analysis.

2.14. Protein Precipitation and Western Blotting

Western blot analysis was performed after heat and biochemical release of surface displayed proteins to verify their presence in supernatants. The proteins were precipitated from the supernatant using acetone. 5 volume of acetone was added

into supernatants to precipitate supernatants. The solutions were incubated at -20 ˚C for overnight. The precipitated proteins were centrifuged at maximum speed, 4 ˚C for 1 hours. The solution was discarded and protein pellet was air dried. Pellets weren't over dried in this process otherwise it is hard to resuspend. The pellets were dissolved in 1 x SDS-PAGE loading dye following the drying.

The dissolved samples run in SDS-PAGE gel same as described above. The proteins were blotted onto PVDF membrane via Trans-Blot Turbo (Bio-Rad). The PVDF membrane was activated with brief methanol treatment, and blot papers were wetted with Trans-Blot Transfer Buffer (Bio-Rad). The transfer cassette was prepared by sandwiching SDS-PAGE gel and PVDF membrane between two transfer papers. (The bottom-to-top order of sandwich was transfer paper, PVDF membrane, SDS-PAGE gel, transfer paper). The transfer was performed with predefined transfer protocol in Trans-Blot Turbo transfer system for total proteins. Subsequently, the membrane was incubated in %5 milk powder dissolved in TBST buffer to block non-specific bindings. The membrane was incubated for overnight in 1:5000 diluted anti-his primary antibody (ThermoFisher) in %5 milk powder TBST buffer following the blocking. The membrane was washed with TBST buffer twice for 10 minutes and once for 5 minutes. The Membrane was incubated in 1:10000 diluted anti-mouse secondary antibody conjugated with horseradish peroxidase (Abcam) in %5 milk powder TBST buffer. The membrane was washed same as above. The membrane was treated with luminescence substrate kit (Bio-Rad) and visualized with ChemiDoc Imaging System (Bio-Rad).

2.15. Molecular Modelling of TEV Protease Fusions

The 3D structure of TEV-protease-truncated passenger domain fusion protein was predicted with I-Tasser[87-89]. The protein sequence without pelB secretion tag was uploaded to https://zhanglab.ccmb.med.umich.edu/I-TASSER/ website in default mode. One of the predicted 5 protein structure was selected to align with native TEV protease structure with PyMol protein structure alignment tool.

2.16. Co-expression of Ag43 160N sfGFP and TEV Protease and Release Kinetics

pET22b PelB 6H Ag43 160N sfGFP and pZA nTetO PelB 6H Ag43 160N TEV vectors were co-transformed sequentially into *E. coli* BL21 (DE3) strain with chemical transformation. A single colony was picked from the agar plate and grown for overnight in LB with appropriate antibiotics. The cells inoculated in modified MOPS defined medium (80mM MOPS, pH=8.2) with 1:100 dilution, and grown at 37 ˚C, 200 rpm until OD600 reached to 0.4. The cells were induced IPTG and aTc. The induced cells were grown at 18 ˚C, 200 rpm for overnight. In the next day, cells were collected and centrifuged at maximum speed for 5 minutes. The fluorescence emission of supernatants was measured with the M5 spectrophotometer.

To find release kinetics upon TEV protease display, the freshly induced cells were centrifuged at 3000xrpm for 10 minutes. The medium of cells was changed while the inducer conditions remained constant. The cells were incubated at 18 ˚C, 200 rpm. In every four hours, 400µl of cells were taken and centrifuged at maximum

speed for 5 minutes. The supernatants were taken for fluorescence measurement. The remaining pellets were resuspended in 1x PBS for whole fluorescence measurements. All fluorescence measurements were performed with the M5 spectrophotometer.

CHAPTER 3

RESULTS AND DISCUSSION

3.1. Protein Display on Cell Surface and Release

Ag43 autotransporter protein was engineered to display POI on the cell surface. Previous reports showed that auto-aggregation activity of Ag43 protein α-domain is dependent on electrostatic interaction of first 160 amino acid with other α-domains.[90] To display cargo proteins, first 160 amino acid of Ag43 α-domain was deleted and replaced with cargo proteins (Figure 4).

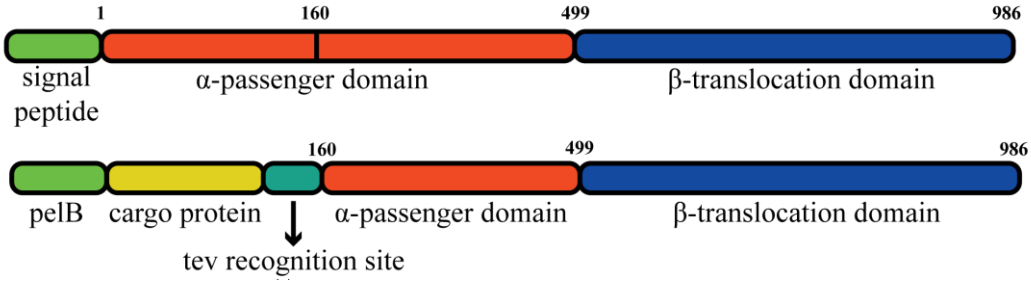

Figure 4: Topology of native Ag43 autotransporter protein (top) and engineered Ag43 gene for protein display (bottom).

For translocation of engineered Ag43 proteins, pelB secretion signal in pET22b vector was used. The sfGFP was determined as reporter protein to characterize the display system. sfGFP gene was fused with truncated Ag43 coding sequence along with TEV recognition to construct display cassette named as pET22b PelB 6H Ag43 160N sfGFP vector.

3.1.1. Construction of pET22b PelB 6H Ag43 160N sfGFP vector

To construct the display cassette, sfGFP gene was amplified from pJT119b vector with two PCR. In the first round, the gene was amplified with N-terminal 6 His-tag and C-terminal TEV recognition site (Figure 5). The PCR product was purified and used as template in the second round. A GGGGS flexible linker at C-terminal of sfGFP and homolog sequence was added in the second PCR (Figure 5). The truncated Ag43 gene were amplified from *E. coli* genome with Gibson Assembly overhangs to assemble with sfGFP coding sequence (Figure 6). The coding sequence corresponds to first 160 amino acid after secretion signal of Ag43 protein was excluded from PCR amplification.

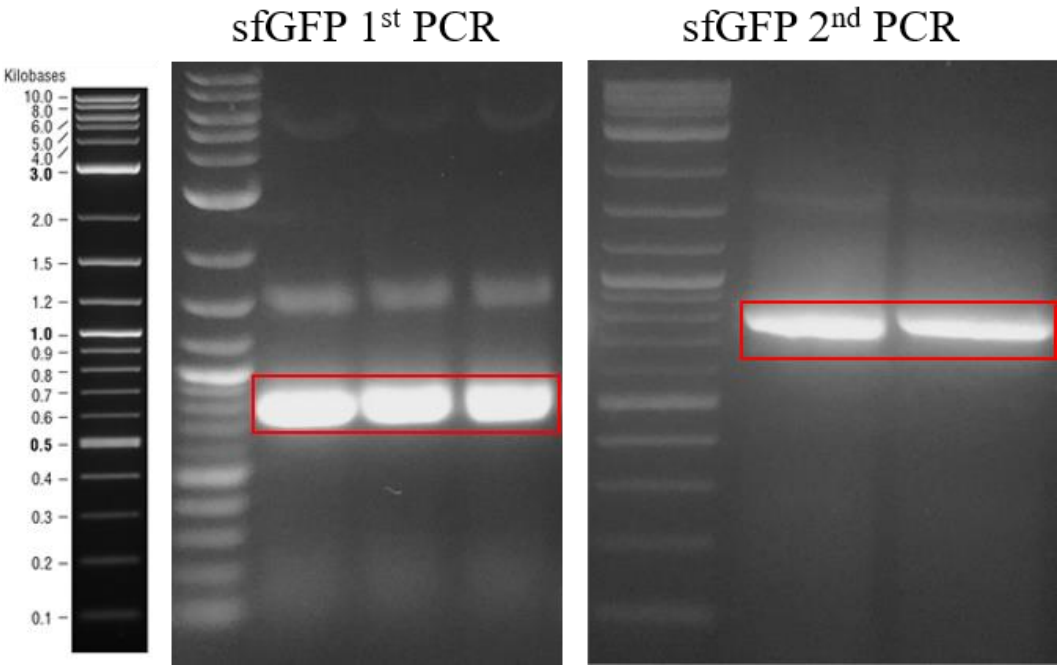

Figure 5: Agarose gel images of PCR products to obtain sfGFP gene for display cassette. Expected bands are 802 bp for first reaction, and 853 bp for second reaction.

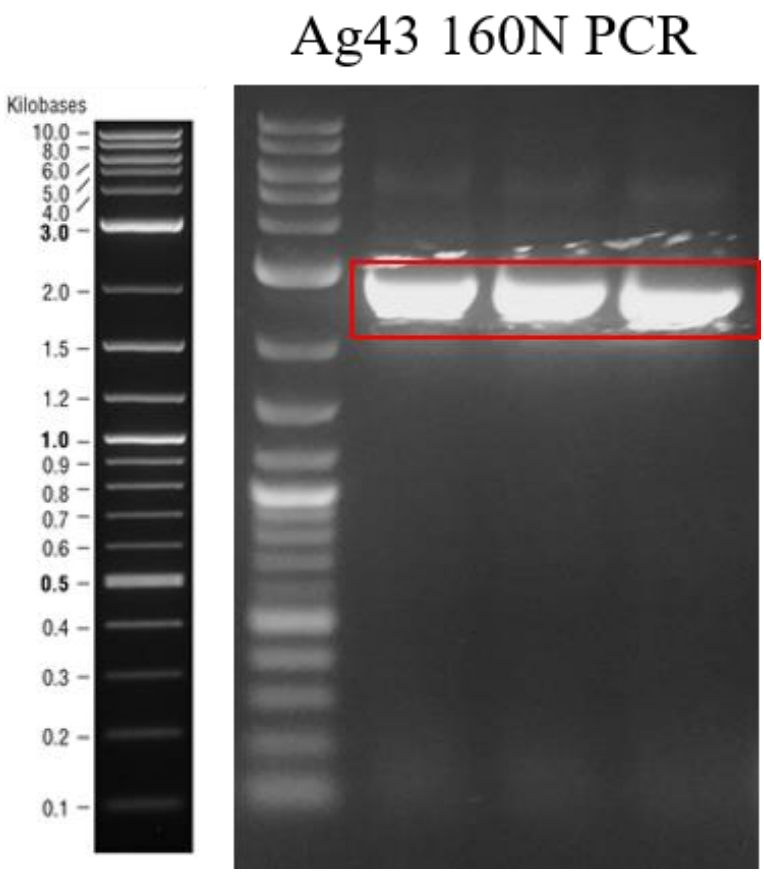

Figure 6: Amplification of Ag43 gene without native signal sequence and first 160 amino acid coding region. Expected bands are 2544 bp.

pET22b was used as the vector backbone in the Gibson Assembly reaction. pET22b vector was linearized with NcoI-XhoI digestion. (Figure 7). Two nucleotides were inserted between coding sequences of the pelB secretion signal and fusion protein to prevent frameshift. Addition of two nucleotides led additional glycine residue between pelB secretion signal and the fusion protein. The DNA segments were assembled with Gibson Assembly. The sequence verification was determined with Sanger sequencing (Appendix D).

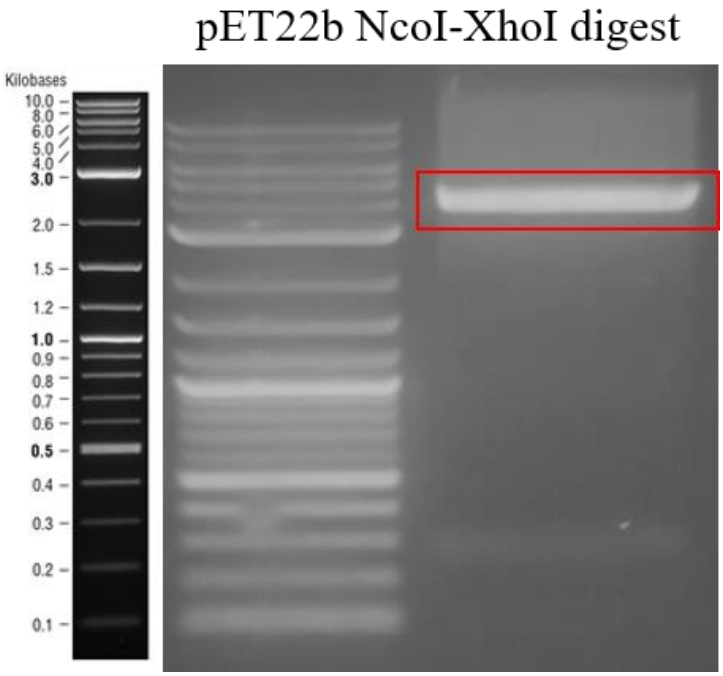

Figure 7: Digestion of pET22b vector with NcoI and XhoI restriction enzymes. Expected band is 5437 bp.

3.1.2. Cell Surface Display of sfGFP via Ag43 Autotransporter Protein

The verified pET22b PelB 6H Ag43 160N sfGFP vector was transformed in BL21 (DE3) strain and the display cassette was induced with IPTG at mid-log phase. The induction was carried out at low temperature because translocation of sfGFP to cell surface with Ag43 protein requires multiple steps including secretion of unfolded translated protein to periplasmic space and insertion of ß-barrel domain to outer membrane.[90] The cell surface localization of sfGFP was verified with labelling the His-tagged sfGFP using His-tag specific antibodies conjugated with DyLight550. The antibody labelled cells were analysed under confocal scanning microscope with green and blue lasers. The clear red signal from labelled cells

indicates that sfGFP molecules are on the cell surface as antibodies can't freely diffuse through cellular membrane without any membrane solubilizing agents (Figure 8). The anti-his binding epitope for the antibody need to be surface exposed. Furthermore, cells without any surface displayed sfGFP molecules were not labelled with anti-his antibody (Appendix F).

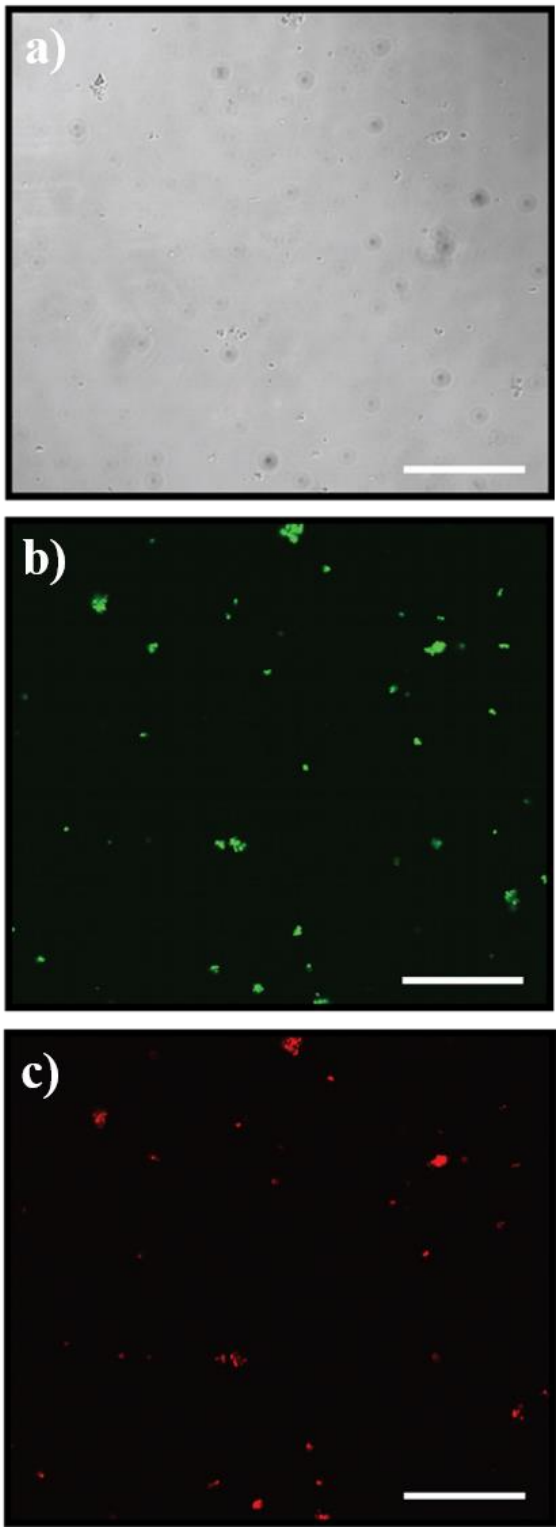

Figure 8: Immunostaining of cells expressing the display cassette with anti-his antibody conjugated with Dylight 550. Cell images under a) bright field, b) blue light/green filter c) green light/red filter. (white bars represent 40μm)

His-tagged sfGFP molecules were also labelled with Ni-NTA conjugated gold nanoparticles. As Ni-NTA conjugated nanoparticles can diffuse intracellular space and bind unspecifically to other proteins, cells were washed with high concentration imidazole solution for several times. The TEM examination showed that only cells harbouring the display cassette were labelled with gold nanoparticles (Figure 9a). The presence of gold nanoparticles on cells shown in figure 8b was verified with EDS analysis (9b). The clear Au peaks were observed in the EDS spectrum.

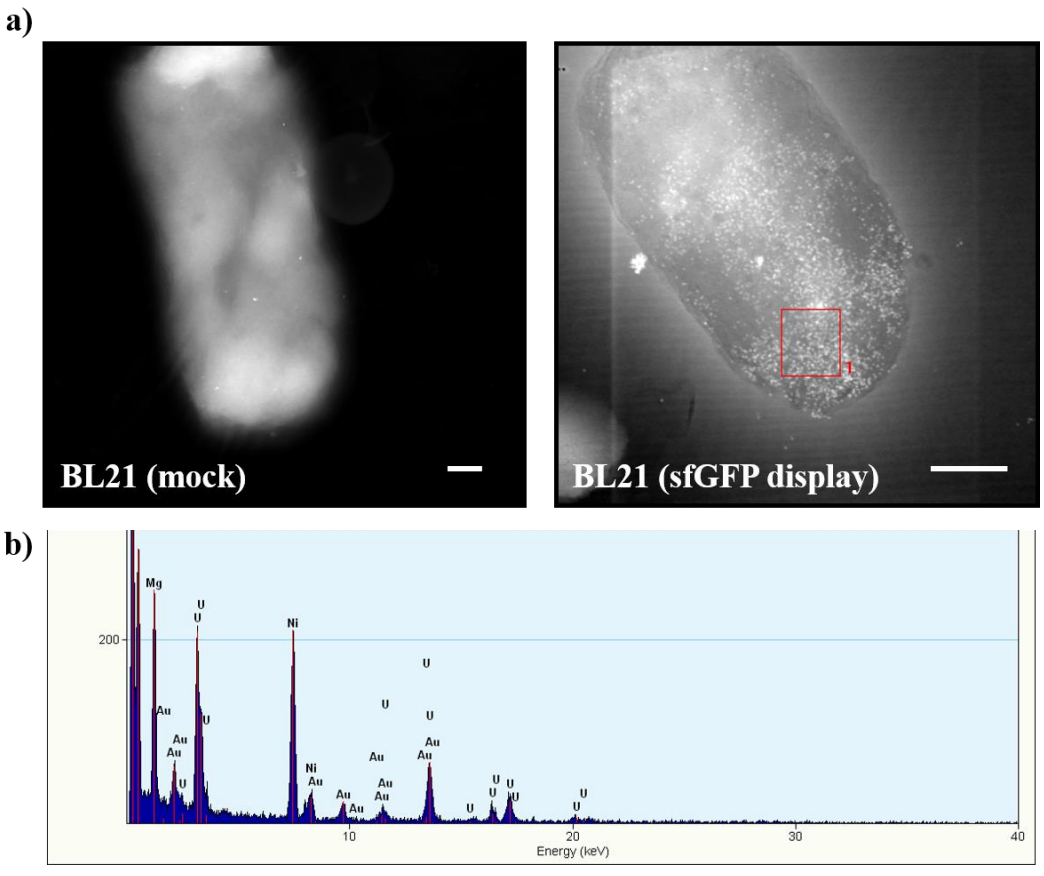

Figure 9: Ni-NTA conjugated gold particle labelling of cells. a) TEM images of empty cells (left) and cells expressing display casette (right). b) The EDS analysis for the region indicated as red box. (white bars represent 200nm).

The localization of sfGFP molecules on the cell surface was further verified with trypsin protease accessibility assay. The trypsin protease can digest the surface exposed proteins and domains. The protease treatment of the cells expressing display cassette caused a significant decrease in whole cellular florescence. However, the whole cell fluorescence is not completely vanish after digestion reaction (Figure 10). It indicates that some of expressed sfGFP molecules are not cleavable for trypsin protease. As trypsin protease can't diffuse through cellular membrane, the inaccessible sfGFP molecules are trapped either in periplasm or in intracellular space. Although the expression of display cassette is carried out at low temperature, the sfGFP molecules might be prematurely folded prior to secretion and block the full maturation of Ag43 protein at cell surface. The his-tag labelling with conjugated antibodies reveals the same results with trypsin accessibility assay. Some of the expressed sfGFP molecules in cells can't display the protein on their surface. A heterogenic cell pool emerged after induction for recombinant protein display.

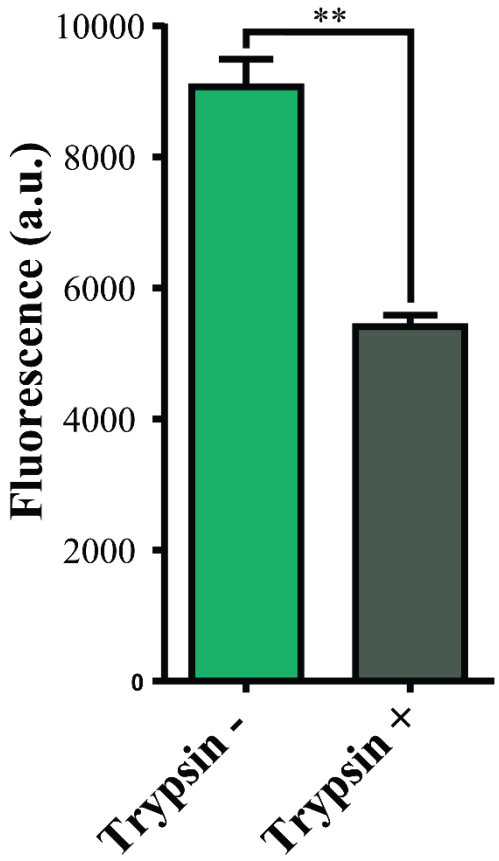

Figure 10: Whole cell fluorescence after trypsin protease accessibility assay of induced cells. The assay performed in triplicates, and statistical significance was determined with student's test. (**: $p < 0.01$)

3.1.3. Release of Surface Displayed Proteins with Heat Shock

The surface displayed proteins can be released to extracellular medium. The α-domain is cleaved passing through ß-barrel structure by internal protease motif and remains attached to the cell surface interacting with ß-domain.[91] The noncovalent interaction between ß- and α-domain can be disturbed with brief heat treatment. To release displayed sfGFP molecules from the cell surface, the induced cells were briefly heated, and release of cargo protein to extracellular medium is analysed with western blotting and fluorescence measurement.

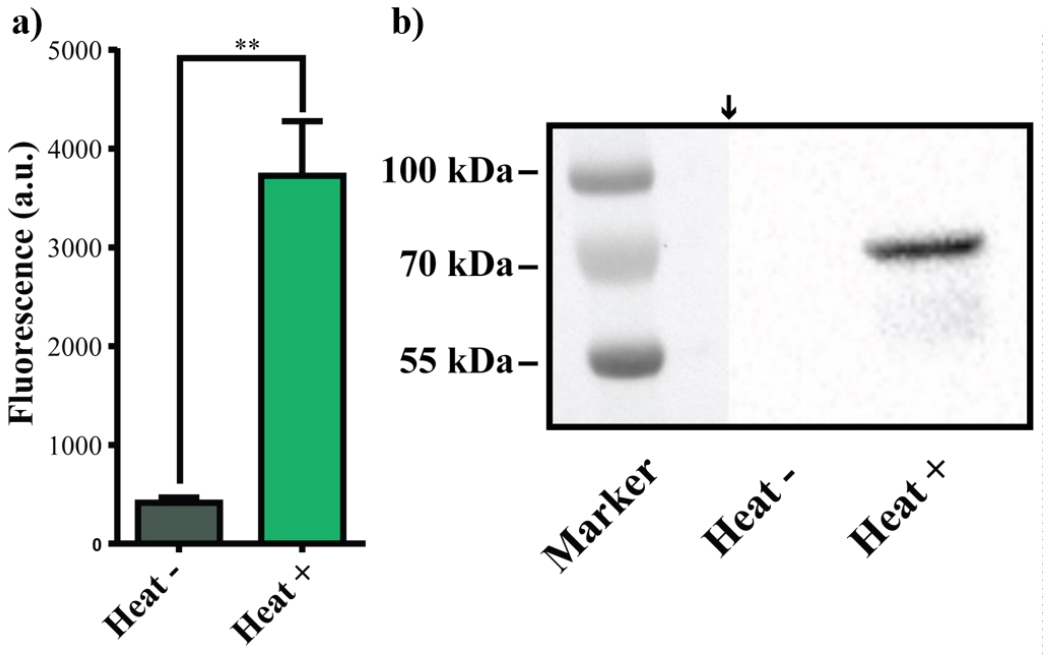

Figure 11: The heat shock is resulted in release of sfGFP molecules to extracellular medium. a) Fluorescence measurements from cell supernatants after heat shock. The experiments were performed in triplicates and statistical significance was determined with student's test. (**: $p < 0.01$). b) Western blotting analysis from supernatants after heat shock. To increase the protein concentration, the proteins were precipitated from supernatants with acetone. Expected band of sfGFP-truncated α-domain fusion protein is 63.4 kDa.

The supernatant fluorescence was increased after heat treatment compared to unheated cells (Figure 11a). The fluorescence increase indicates that sfGFP molecules are detached from surface upon heat shock. Furthermore, the presence of sfGFP-truncated α-domain fusion protein in supernatant after heat treatment was further verified with western blotting (Figure 11b). Based on the fluorescence measurements and western blotting, protein release from cell surface following the display can triggered on-demand with heat treatment. In addition, the

noncovalent interaction α- and ß-barrel domains can be broken with other physical parameters such as ionic strength.[92] In demand protein secretion can be used to facilitate reactions far away from the cells or to delivery proteins on site for targeted therapeutics delivery in body in which cells served as shuttles to increase the half-life of proteins. Although displayed proteins can be released with heating, the cargo protein is released attached to α-domain. Additional large protein domains fused with POI is undesirable because it might affect the correct folding and subsequently the activity of POI.[80-82]

Therefore, incorporated TEV protease recognition site between α-domain and POI aimed to be cleaved with TEV protease enzymes to release the displayed proteins from cell surface while α-domain remains attached cell surface. The accessibility of inserted recognition site was assessed with in vitro cleavage reactions.

3.1.4. Cloning, Expression and Purification of GST-TEV Protease

To test the cleavability of incorporated TEV recognition site, double GST- and His-tagged TEV protease was expressed and purified from *E. coli*. The GST tag is fused TEV protease to increase its solubility and to prevent formation of inclusion bodies at its high concentration in cells.

pET22b 6H GST-TEV vector was constructed to express recombinant GST- and His-tagged TEV protease in *E. coli* BL21 (DE3) strain. The GST gene amplified with Gibson overhangs and N-terminal His-tag via two rounds of PCR (Figure 12). The codon optimized TEV protease was synthesized from Genewiz and Gibson overhangs was added by PCR (Figure 13). The stop codon was included at 3’ to prevent the translation of C-terminal His-tag intrinsically found in pET22b.

pET22b vector was digested with XbaI and XhoI enzyme to linearize the vector (Figure 14). The DNA fragments was purified from agarose and assembled with Gibson Assembly reaction. The vector sequence was verified with Sanger sequencing technique (Appendix D).

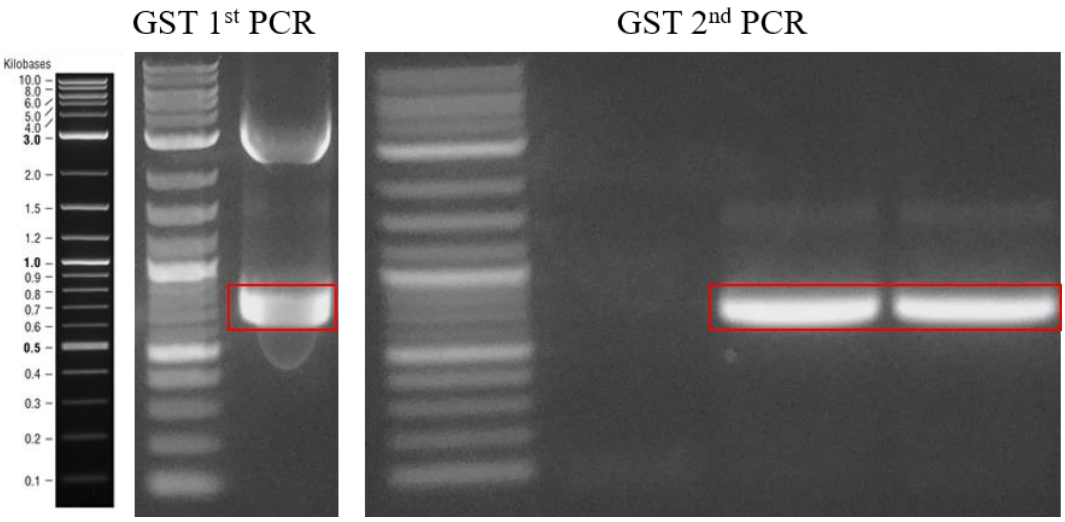

Figure 12: PCR products of GST amplifications to add Gibson overhangs and N-terminal His-tag coding region. Expected bands are 729 bp for first reaction, and 766 bp for second reaction.

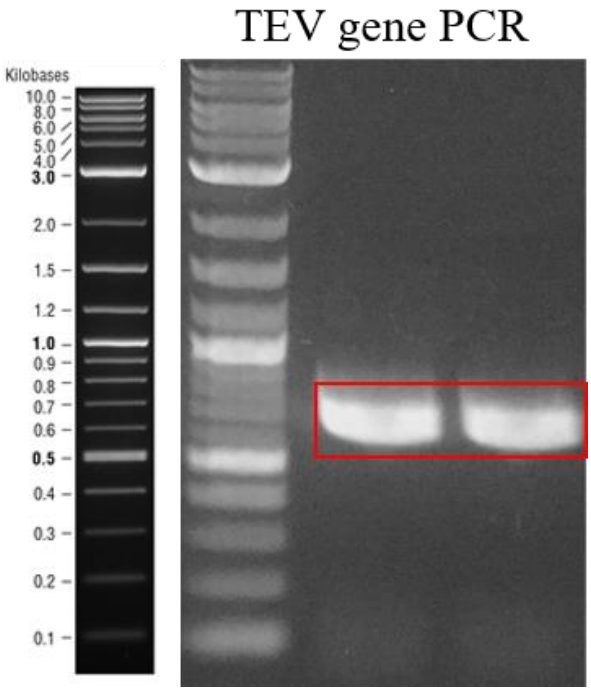

Figure 13: Amplification of codon optimized TEV protease coding region with Gibson Assembly overhangs. Expected bands are 777 bp.

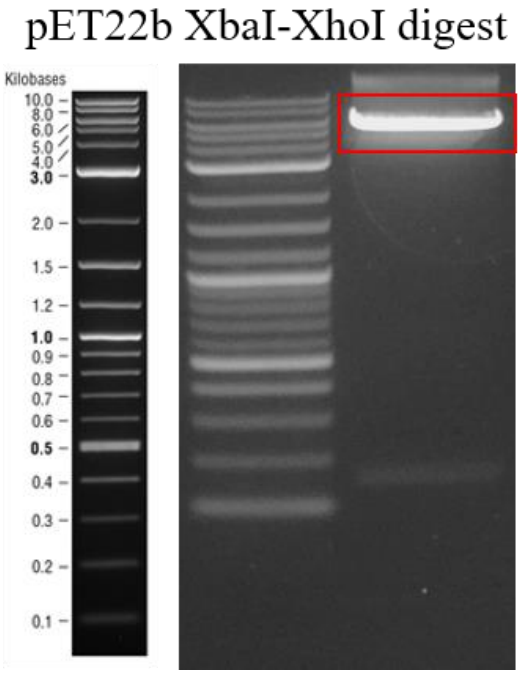

Figure 14: Digestion of pET22b vector with XbaI and XhoI restriction enzymes. Expected band is 5331 bp.

The sequence verified vector was transformed into *E. coli* BL21 (DE3) with chemical transformation. The protein expression was induced at mid-log phase with IPTG and expression was carried out at 30 ˚C to decrease formation of inclusion bodies. Collected cells after expression was resuspended in lysis buffer containing 10mM imidazole and was lysed with repeating freeze & thaw cycles. The GST- and His-tagged TEV proteases were purified by IMAC purification. The total lysate before and after binding to IMAC column, washing steps, and eluted proteins were loaded SDS-PAGE gel to verify the purification. Clear bands approximately at 55 kDa in elution lanes indicates that purification is successful (Figure 15).

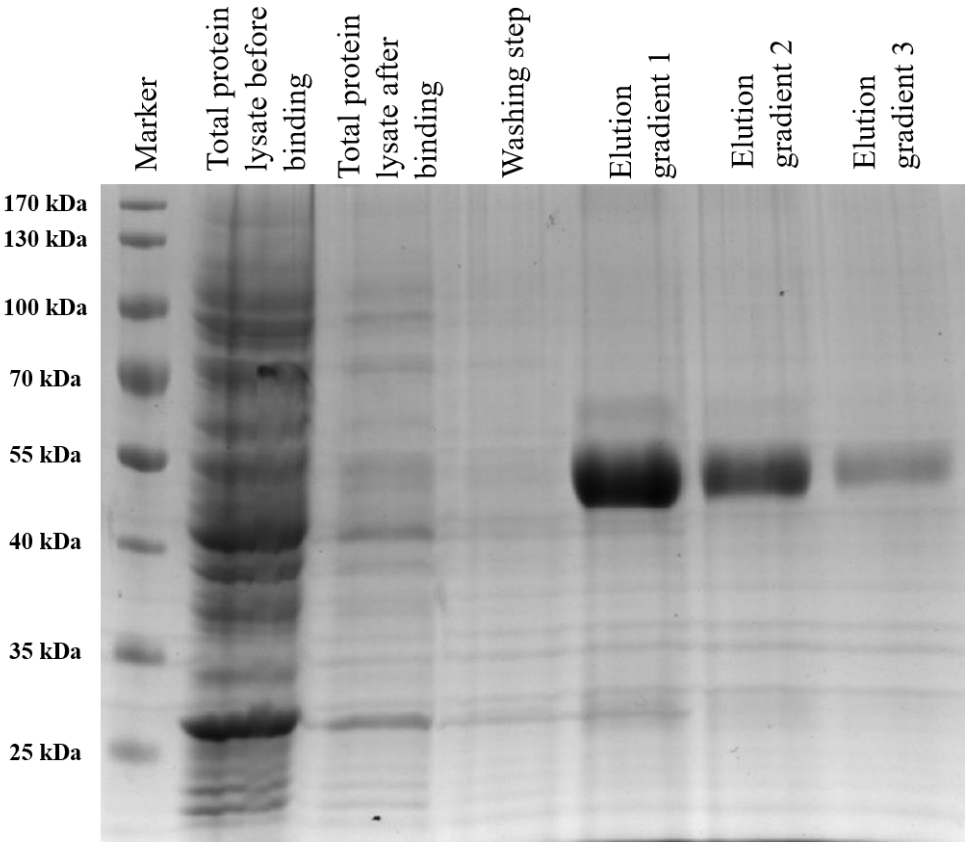

Figure 15: SDS-PAGE analysis after TEV purification. The lanes are annotated with corresponding sample taken in the different steps of IMAC purification.

The eluted proteins were dialyzed to storage buffer for long-term storage at -20 ˚C. The protein concentration was determined after the dialysis based on band intensity following the coomassie staining. The known concentration of BSA was loaded with dialyzed protein. The concentration was calculated with ImageLab analysis tools (Appendix F).

3.1.5. Cleavage of Displayed Protein with TEV Protease in Standart Reaction Buffer and Different Growth Media

The purified TEV protease was added to suspended cells in standard TEV reaction buffer, and incubated at 4 ˚C for overnight. Following the incubation, cells were centrifuged, and supernatants collected. The cell pellets were resuspended in 1x PBS. The resuspended cells were labelled with anti-his antibody. The Dylight550 signal wasn't be observed in the TEV treated cells confocal microscope while untreated cells were labelled same as previous labelling experiment (Figure 16). Moreover, the whole cell fluorescence was significantly decreased after TEV protease addition compared control group (Figure 17). The TEV protease treatments leads to loss of displayed sfGFP molecules from cell surface.

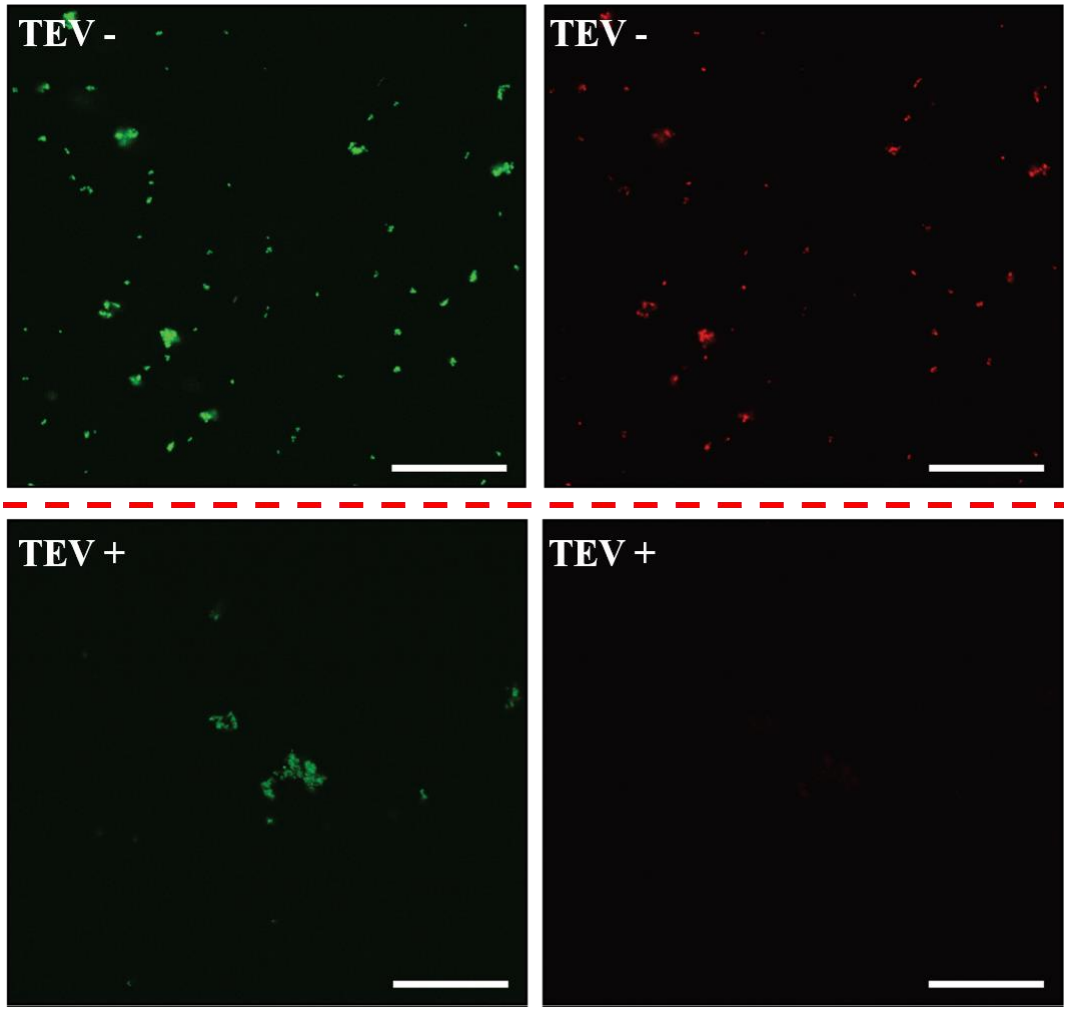

Figure 16: TEV protease is able to cleave the incorporated recognition site and to release displayed sfGFP molecules to extracellular medium in folded state. a) ICC staining of induced cells treated TEV protease in the absence of any membrane solubilizing agents. (white bars represent 40μm) b) The whole cell and supernatant fluorescence after TEV protease addition. The experiments were performed in triplicates and statistical significance was determined with student's t-test. (**: $p < 0.01$, and ***: $p < 0.001$) c) Western blotting analysis from precipitated supernatants obtained after TEV treatment.

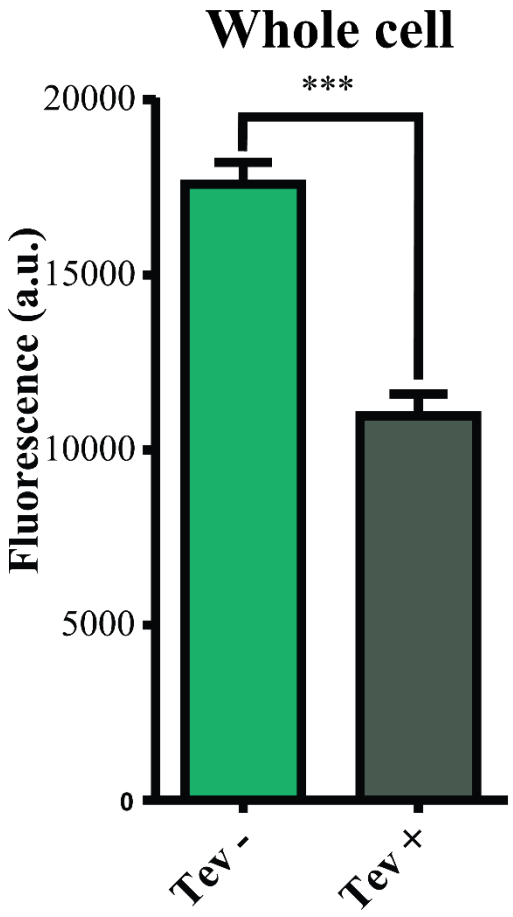

Figure 17: The whole cell after TEV protease addition. The experiments were performed in triplicates and statistical significance was determined with student's t-test. (***: $p < 0.001$)

To verify that loss of sfGFP signal isn't result of random degradation, the fluorescence emission of supernatants were measured. A significant increase was observed in fluorescence emission of the supernatant obtained from cells treated with TEV protease compared to control group. (Figure 18a). Furthermore, the cleaved sfGFP molecules were detected in the western blot from precipitated supernatants (Figure 18b). Based on the observations from fluorescence measurements, ICC, and western blotting, TEV protease is accessible to TEV recognition site between sfGFP and truncated α-domain. The addition of TEV

protease leads to cleavage of TEV recognition and results in release of displayed sfGFP molecules to extracellular medium in active state.

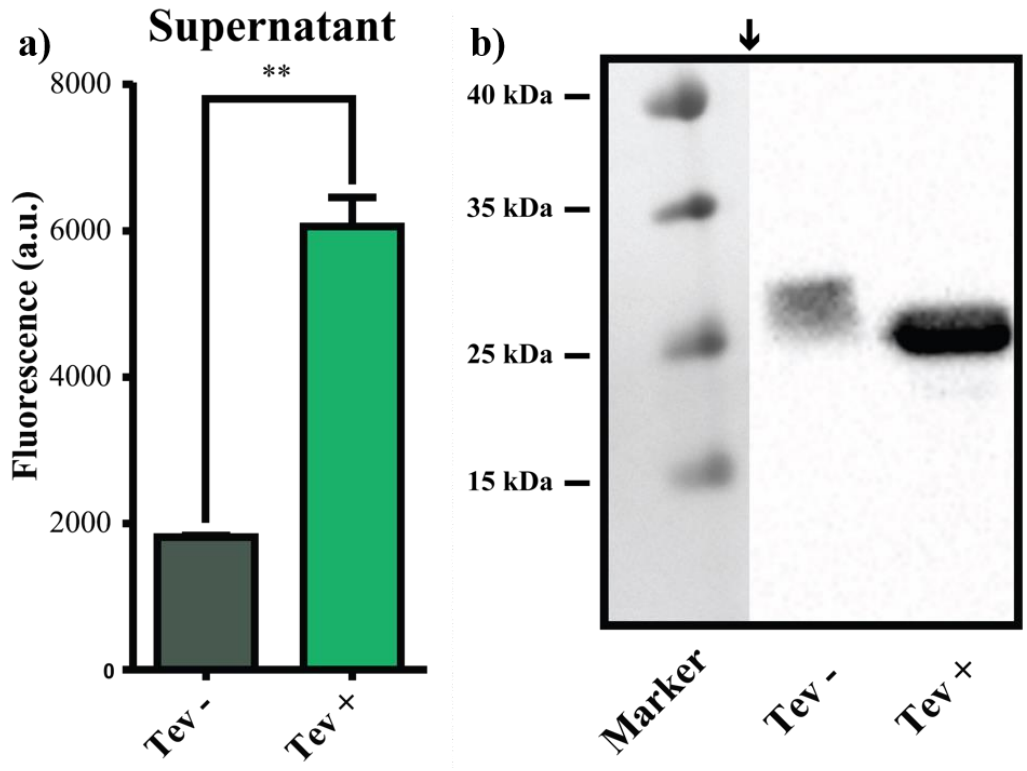

Figure 18: TEV protease addition leads to release of displayed sfGFP molecules to supernatant in folded states. a) Supernatant fluorescence after TEV protease addition. The experiments were performed in triplicates and statistical significance was determined with student's t-test. (**: $p < 0.01$) b) Westernblotting analysis from precipitated supernatants obtained after TEV treatment.

As the cleavage site is accessible, displayed sfGFP molecules can be released via secreting TEV protease that are expressed in cells. For proposed cell system, the external addition of purified TEV protease is not required. However, complex

mixture of growth medium might affect the TEV protease activity. Indeed, previous report showed that TEV protease can be inhibited by Zn^{+2} ions at the concentration greater than 5mM and agents causing oxidation of cysteine.[93] In addition, there is no information about effect of other divalent ions such as Mg^{+2}, which is required for cell wall integrity of *E. coli*.[94]Therefore, the activity of TEV protease was determined in different media at different pH.

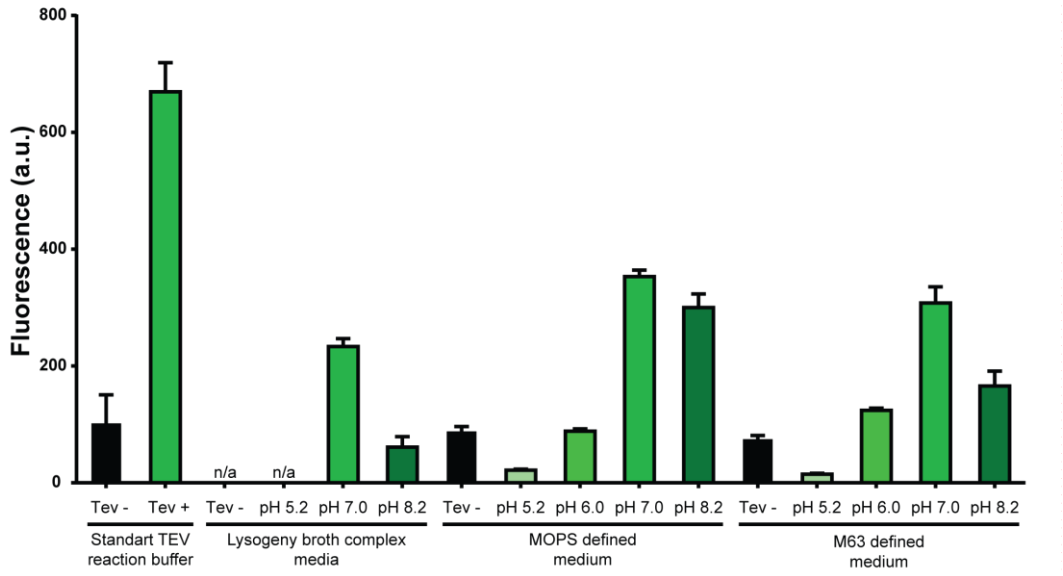

Figure 19: TEV protease activity in LB complex medium at pH equals to 5.2, 7 and 8.2, MOPS defined medium at pH equals to 5.2, 6.0, 7.0 and 8.2, and M63 defined medium at pH equals to 5.2, 6.0, 7.0 and 8.2.

To determine TEV protease activity, sfGFP displayed cells were suspended in different media including LB, MOPS defined medium and M63 defined medium at pH range between 5.2 to 8.2 (Figure 19). TEV protease was added in suspended cells, and cleavage reactions were incubated overnight at 4 ˚C. Following the incubation, cells were centrifuged and supernatants were collected to measure the fluorescence emission. Based on the comparison of supernatant fluorescence,

highest fluorescence signal was measured at pH 7 for all media. Nonetheless, TEV protease activity drastically affected by decrease or increase in pH of LB. As LB is an unbuffered complex media that includes yeast extract, TEV protease is inhibited quickly upon pH change. Reducing pH of M63 and MOPS defined medium similarly dramatically inhibited the cleavage activity of TEV protease however increase in pH for those defined medium has a modest effect on TEV protease activity. Highest fluorescence signal was observed from MOPS defined medium at pH 7. As pH is decreasing during *E. coli* growth due to acetate fermentation, the MOPS defined medium was selected for release experiments. Moreover, buffering capacity of MOPS defined medium was increase two-fold by increasing the concentration of MOPS to 80mM. The pH of modified MOPS defined medium was adjusted to 8.2.

Four different secretion strategies were employed to secrete TEV protease. 3D structure of TEV protease fusions were predicted to ensure that fused domain wasn't interfere with folding of the catalytic cleft of TEV protease. To ease the burden on cells, TEV protease molecules were expressed and secreted via different cells. The cells expressing display cassette and TEV protease were co-inoculated in same media to measure the release of displayed sfGFP expect for the autotransporter mediated surface display of TEV protease. The TEV protease molecules were co-displayed in same cells in this strategy.

3.2. Strategy 1: Secretion of TEV Protease with Type I Secretion System

C-terminal region of HlyA toxin is fused to TEV protease for secretion. The gene encoding the fusion protein was cloned under aTc inducible promoter. pVDL9.3 plasmid that encodes HlyB and HlyD transporter under IPTG inducible promoter proteins was obtained from [95].

3.2.1. 3D Structure Prediction of C-terminal HlyA tagged TEV protease

The 3D structure of TEV protease fused with C-terminal region of HlyA toxin was determined with I-Tasser server. One of the five predicted structure was selected manually based on the TEV protease folding accuracy to align with native TEV protease structure (PDB: 1lvm).[75] Overall structure and folding of TEV protease doesn't change with addition of C-terminal region of HlyA toxin to structure (Figure 20a and 20b). Although, the catalytic cleft of TEV protease is folded similar with native structure, the C-terminal region of HlyA isn't folded in any 2D structural motifs in the predicted structure (Figure 20b). Due to the random motions, it may temporarily block to cleft but it seems unlikely to inhibit activity completely. The alignment structure indicates that two proteins have nearly identical structure (Figure 20c). The root-mean-square deviation score which represent the how much matched atoms are distant from each other in angstrom is calculated as 0,465 for 195 matched atoms. The zoomed view of catalytic cleft reveals that the catalytic traid residues are found in similar location

but in different rotation. It is expected to find small difference in predicted structures as many algorithms try to calculate overall structure. The overall structure of TEV protease – C-terminal region of HlyA toxin fusion protein is similar with native TEV protease structure, and TEV protease is folded in its active form based on the predicted structure.

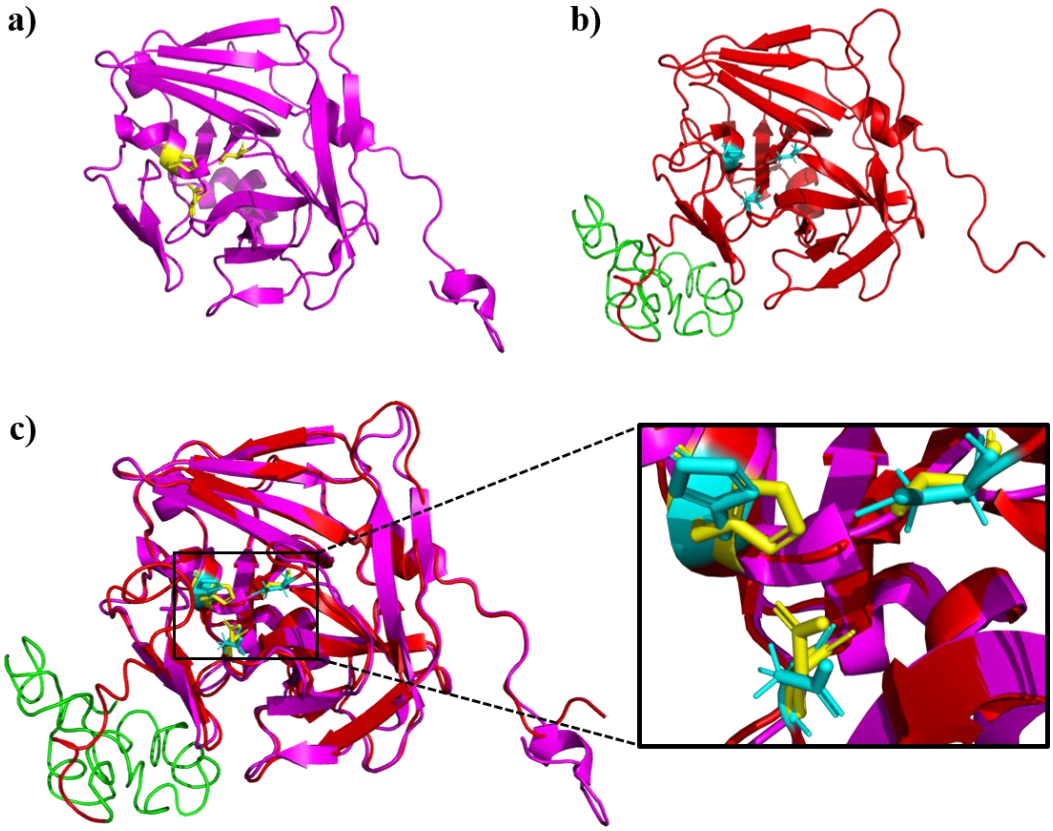

Figure 20: The predicted structure of TEV protease fused with HlyA shows that overall folding of TEV protease isn't affected. a) Native TEV protease structure (Protein Data Bank ID: 1lvm). b) Predicted structure of C-terminal region of HlyA fused with TEV protease. c) Alignment of predicted C-terminal HlyA-TEV protease fusion protein structure with native TEV protease structure.

3.2.2. Cloning and Expression of HlyA tagged TEV protease

The GST-TEV protease coding region was cloned downstream of aTc inducible promoter with C-terminal region of HlyA toxin into pET22b vector. The pVDL9.3 vector has p15A origin of replication; therefore, the vectors are compatible each other and it is possible to cotransform vector into same cell. The aTc promoter is used to express the protease protein as the display cassette and Hly transporter cassette were expressed with IPTG inducible promoter.

To construct the pET22b nTetO 6H HlyA tagged GST-TEV vector, the GST-TEV protease coding region was amplified with Gibson overhangs via PCR (Figure 21). The C-terminal region of HlyA toxin was amplified with PCR from BBa_K554002 vector (iGEM collection) (Figure 22). The pET22b nTetO vector was cut with XhoI and KpnI restriction digestion enzymes (Figure 23). The purified DNA fragments were assembled in Gibson Assembly reaction mix. The vector was sequenced with Sanger sequencing for verification (Appendix D).

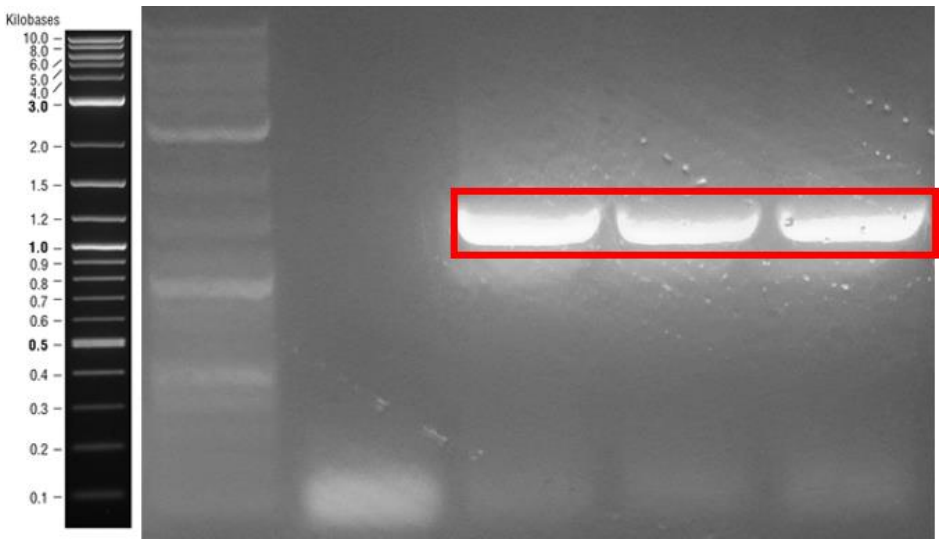

Figure 21: Amplification of GST-TEV protease coding region with Gibson Assembly overhangs. Expected bands are 1476 bp.

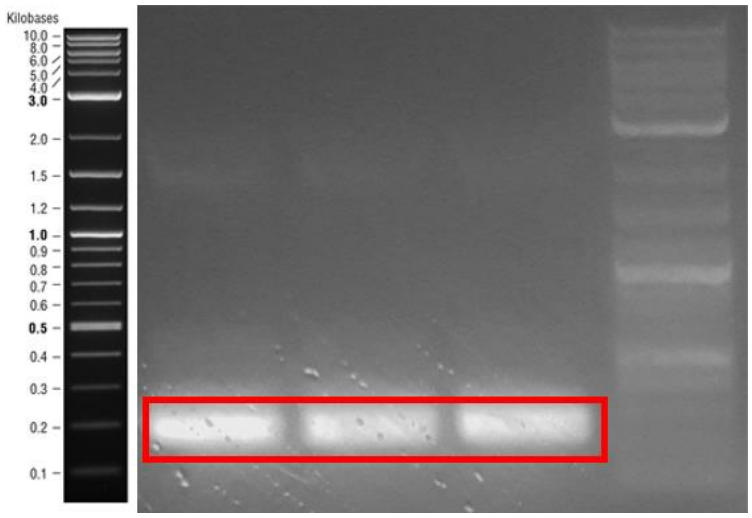

Figure 22: Amplification of C-terminal of HlyA toxin protease coding region with Gibson Assembly overhangs. Expected bands are 251 bp.

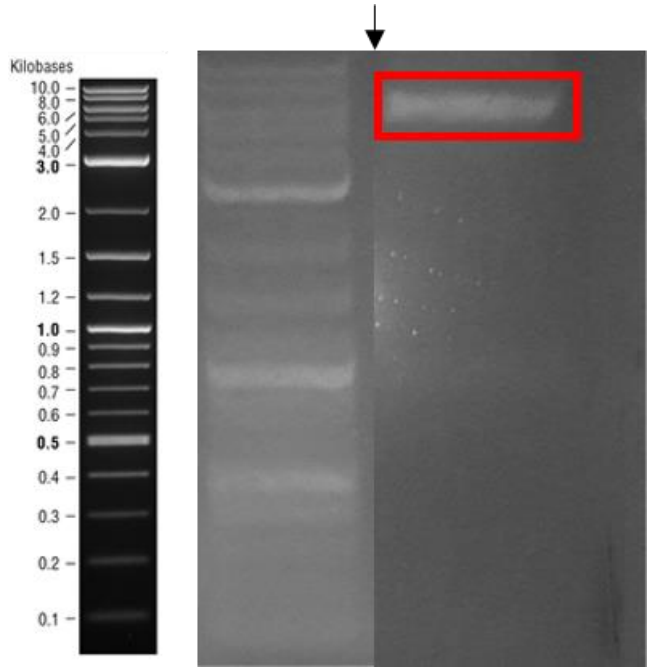

Figure 23: Digestion of pET22b nTetO vector with KpnI and XhoI restriction enzymes. Expected band is 5402 bp.

The sequence verified pET22b nTetO 6H HlyA tagged GST-TEV and pVDL9.3 vectors were sequentially co-transformed into BL21 (DE3) strain. The double transformant cells were inoculated in LB medium with proper antibiotics. The Hly transporter cassette was induced with IPTG and HlyA tagged GST-TEV protein was induced with aTc at mid-log phase. Following the induction, cells were centrifuged and supernatants were collected. The extracellular proteins were precipitated with acetone and analysed with westernblotting. Based on the western blot analysis, the HlyA tagged GST-TEV proteins aren't secreted to supernatant (Figure 24a). Whole cell proteins content was investigated with western blotting to assess expression of HlyA tagged GST-TEV proteins. There is no band observed on the gel run with whole cell content (Figure 24b). The cells either can't express the HlyA tagged GST-TEV proteins or degrade after translation.

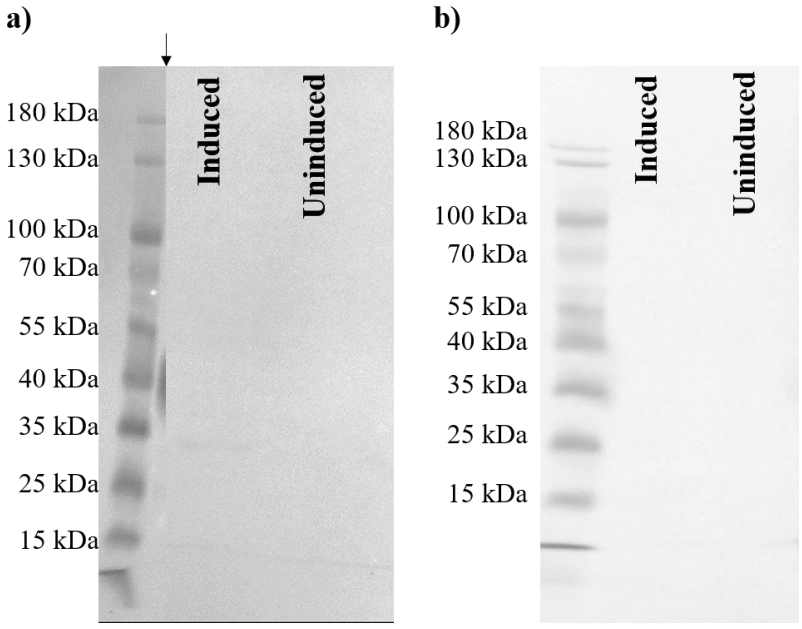

Figure 24: Western blot analysis of secreted and intracellular proteins from cells harboring the HlyA tagged GST-TEV protease expression cassette. a) Secreted proteins. b) Intracellular proteins.

3.3. Strategy 2: Secretion of TEV Protease Fused with YebF

TEV protease is fused with YebF carrier protein for secretion as HlyA tagged GST-TEV proteins can't be expressed in cells. The TEV protease was cloned to C-terminal of YebF protein. To ease burden on cells, the YebF-TEV protease expressing plasmids was transformed in different cells. The cells carrying display cassette and Yebf-TEV protease expression plasmid co-inoculated in same medium. The release of displayed sfGFP molecules was monitored with supernatant fluorescence measurements.

3.3.1. 3D Structure Prediction of YebF-TEV Protease Fusion Protein

YebF-TEV protease fusion protein structure was modelled using I-Tasser server. Among the five structure models, one that has highest similarity to native TEV protease folding (PDB: 1lvm) was selected manually. The folding and 2D structure motifs of TEV protease in fusion protein are almost identical to native TEV protease (25a and 25b). The overall structure of YebF protein in fusion seems to fold imperfectly. The disulphide in YebF structure can't be determined with I-Tasser.[89] Lack of the disulphide bridge, N-terminal signal peptide and disordered may iterate the structure to more disordered conformation. Two structure were aligned each other with PyMol to calculate RSM. The RSM score is found as 0.253 for 208 atoms. The vicinity of catalytic cleft and catalytic traid of TEV protease fold same as native TEV protease (25c).

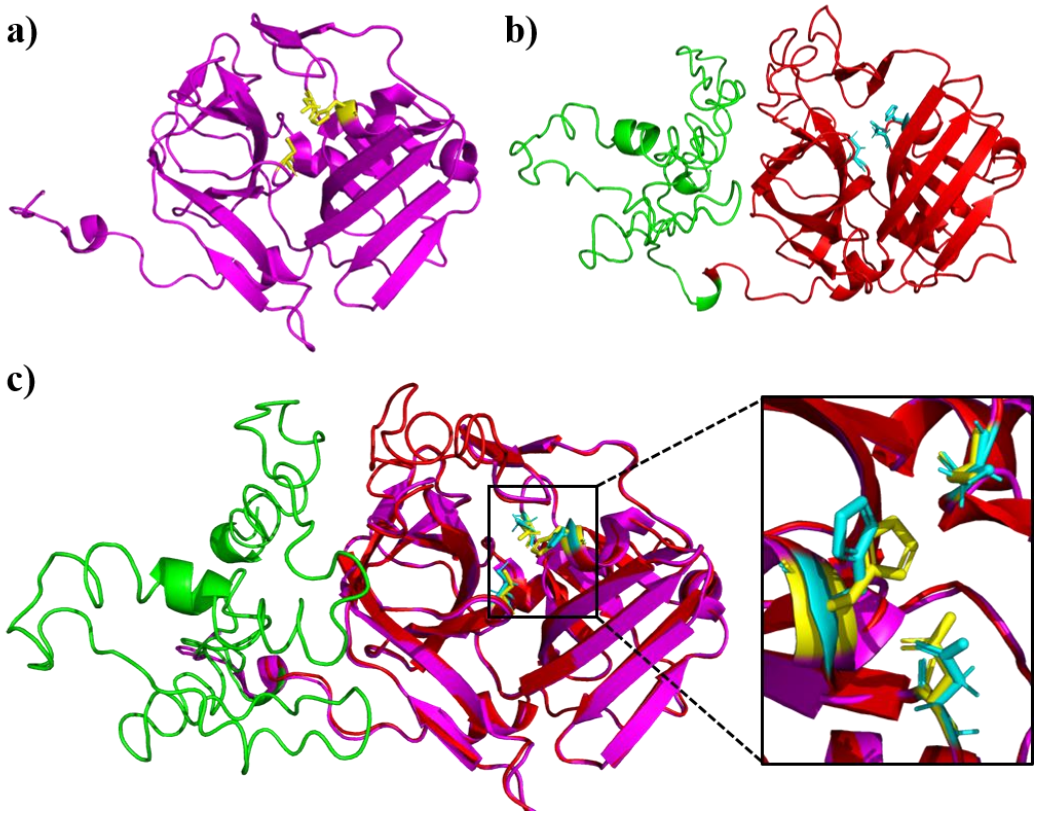

Figure 25: The predicted structure of TEV protease fused with YebF reveals similar structure with native TEV protease. a) Native TEV protease structure (Protein Data Bank ID: 1lvm). b) Predicted structure of TEV protease fused with YebF. c) Alignment of predicted C-terminal YebF-TEV fusion protein with native TEV protease structure.

3.3.2. Cloning and Expression of YebF-TEV Protease Fusion Protein

The YebF-TEV protease coding region was cloned downstream of TetO promoter in pZA vector as display cassette was expressed with IPTG-inducible promoter. pZA TetO YebF-TEV 6H vector was constructed. The YebF gene was amplified

with Gibson Assembly overhangs from *E. coli* DH5α genome. The pZA TEV protease vector was linearized with BamHI and KpnI digestion. The pZA TEV protease vector and YebF gene was assembled with Gibson Assembly. The sanger sequencing was utilized to verify the vector sequence after cloning (Appendix D).

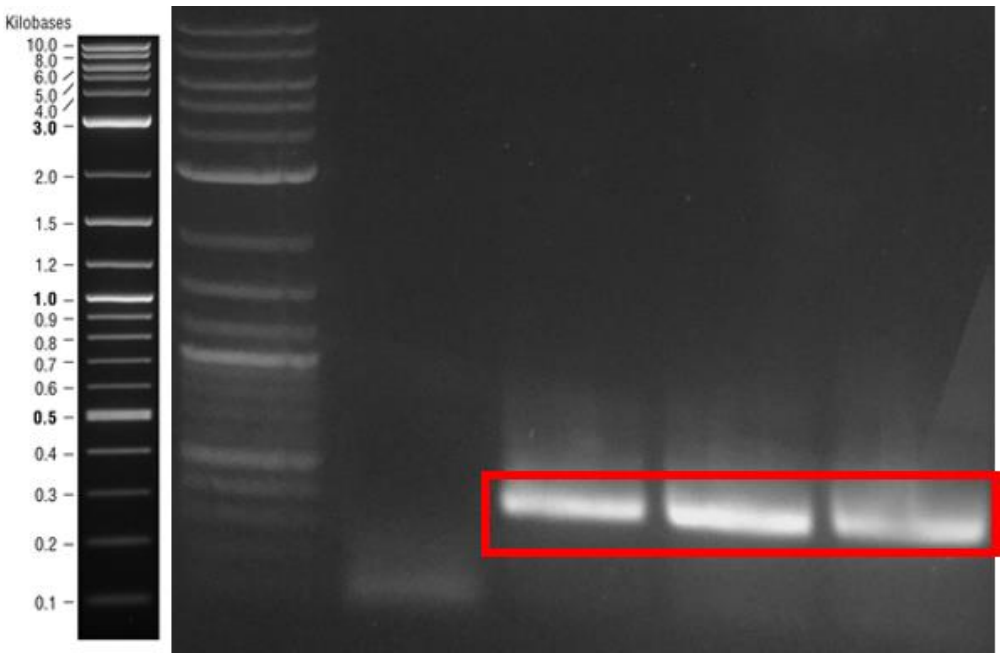

Figure 26: Amplification of YebF gene with Gibson Assembly overhangs. Expected bands are 423 bp.

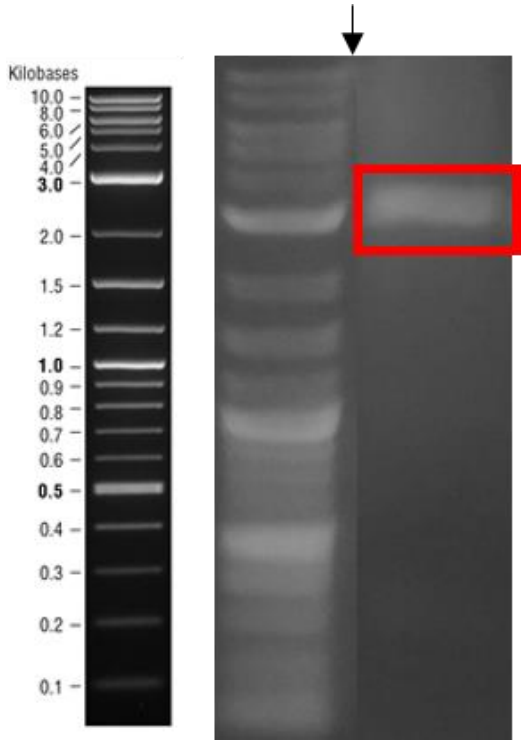

Figure 27: Digestion of pZA TEV vector with BamHI and KpnI restriction enzymes. Expected band is 3219 bp.

The sequence verified pZA TetO YebF-TEV vector was transformed into DH5α PRO cells as TetR repressor gene is required for repression of TetO promoter. Trasnformed cells were grown for overnight and reinoculated in fresh LB media with 1:100 dilution. The expression of YebF-TEV fusion protein was induced with aTc at mid-log phage. Subsequent to induction, the supernatants were collected and proteins were precipitated with acetone. The presence of YebF-TEV were investigated with western blotting. A clear band was observed between 40kDa and 35kDa bands. The YebF-TEV proteins are successfully secreted to extracellular medium.

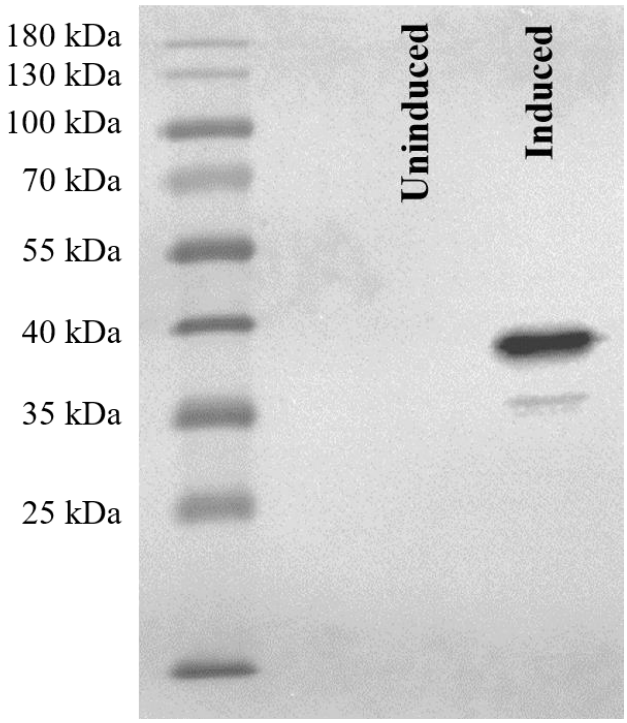

Figure 28: Western blot analysis of secreted YebF-TEV fusion proteins from cell supernatants.

3.3.3. Co-seeding of Cells Carrying Display, and YebF-TEV Protease Expression Cassette

To test the release of displayed sfGFP molecules upon secretion of YebF-TEV protease, cells harboring the plasmids for sfGFP display and YebF-TEV secretion were co-inoculated into same medium with 1:100 total cell dilution. Cells were mixed with ratio 1:1, 1:3, and 1:5 (cell carrying display cassette : cell carrying YebF-TEV secretion cassette) before dilution to investigate the effect of different cell populations on release of displayed sfGFP. The display cassette and TEV secretion cassette were induced with IPTG and aTc, respectively, at mid-log phase. The release of sfGFP molecules in different co-inoculated cell medium were assessed via fluorescence measurements from cell supernatants.

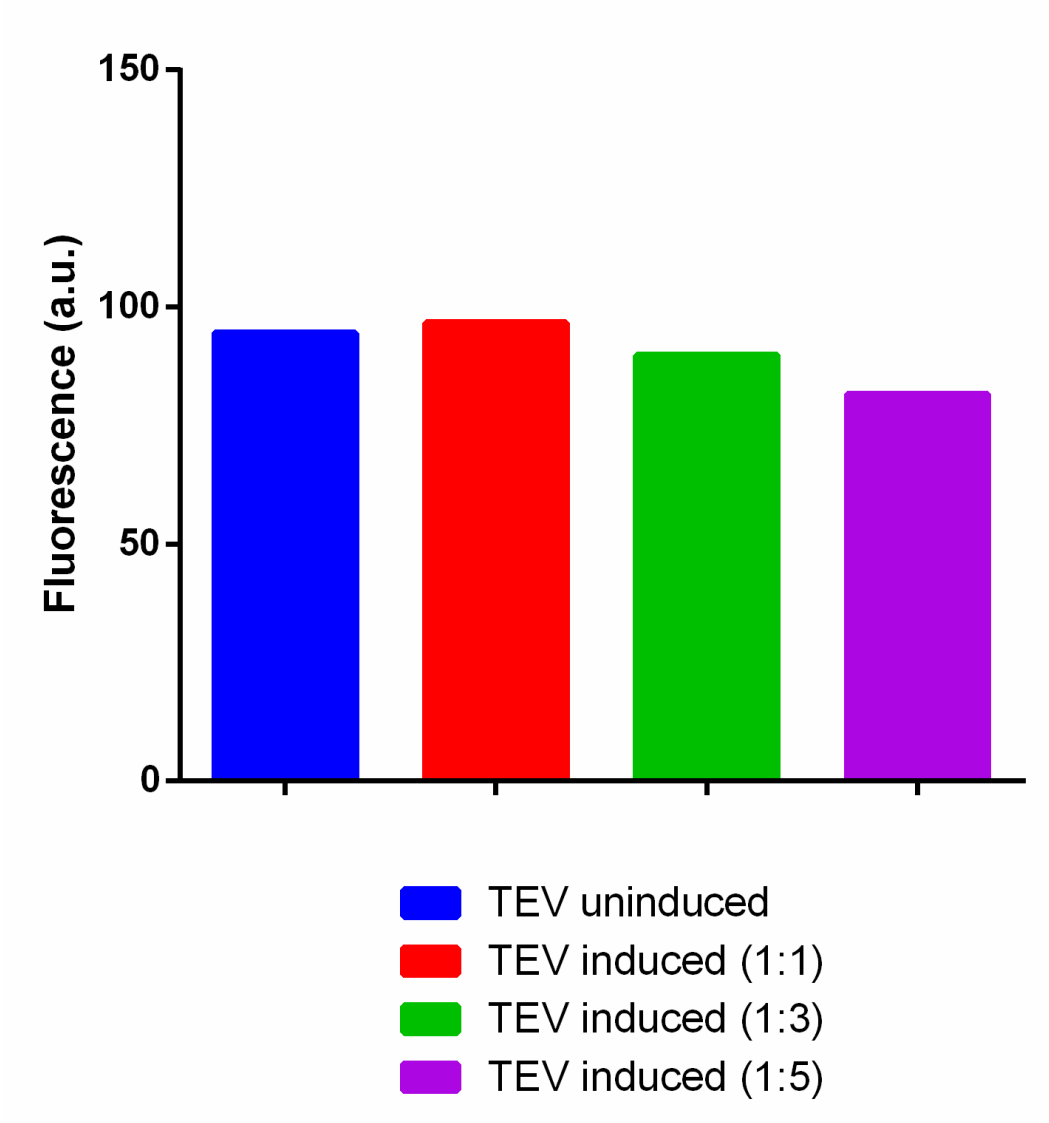

Figure 29: Cell supernatant fluorescence of co-inoculated medium with cells carrying display cassette and YebF-TEV secretion cassette after induction. Display cassette was induced in all conditions.

The displayed sfGFP molecules aren't released via secretion of YebF-TEV protease in any co-inoculation conditions. According to modelling studies, the YebF-TEV is folded in active state and catalytic cleft remains accessible to TEV recognition site. Moreover, the TEV protease can cleave the recognition in the cell medium according to our protease activity assays in different growth media. The

TEV protease might be inhibited as result of unspecific oxidation of cysteine residues during translocation of periplasmic space with YebF fusion protein because *E. coli* periplasm is an oxidizing environment that may lead to formation of disulphide bonds between cysteine. To check this hypothesis, dithiothreitol (DTT) which is a reducing agents, was added onto cells at 1mM, 5mM, and 10mM concentrations during the induction period. However, the addition of DTT don't have any effect on release of displayed sfGFP. Therefore, it is hypothesized that the amount of TEV protease secreted isn't high enough to cleave the recognition tag.

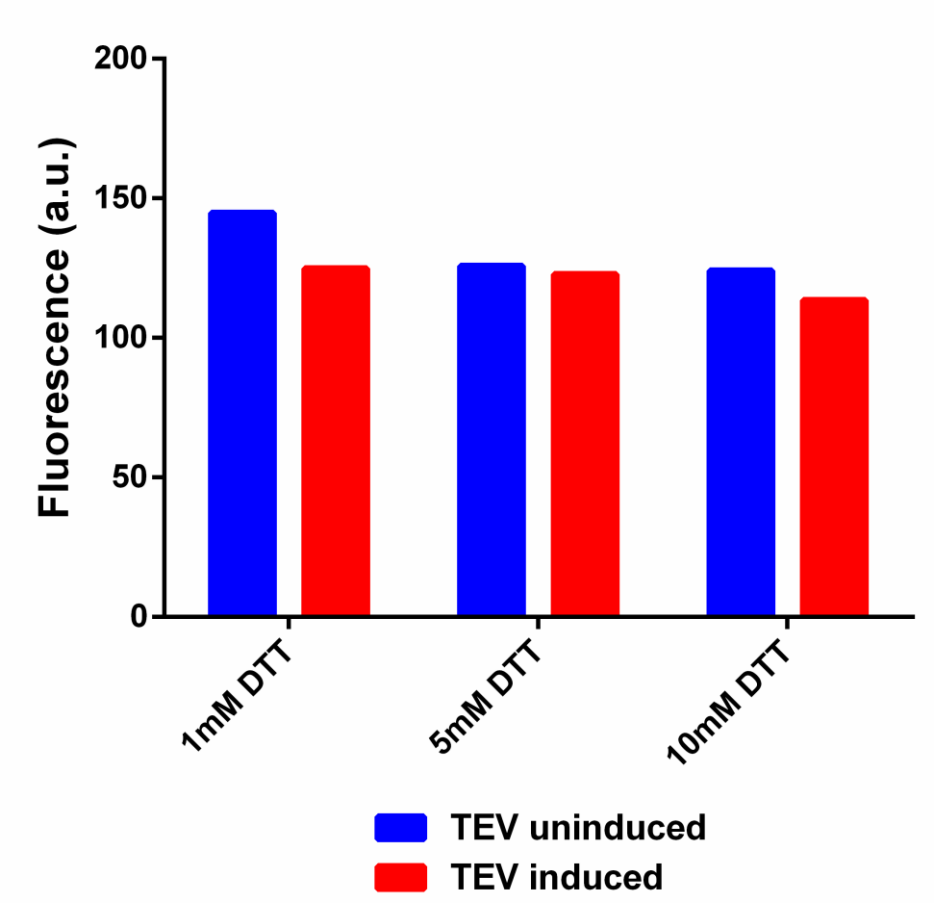

Figure 30: Cell supernatant fluorescence of co-inoculated cells in the presence of different concentrations of DTT

3.3.4. Cloning and Expression of YebF-TEV Protease Carrying DsbA and OmpA Signal Sequences

A previous report indicates that changing the sec translocon signal of YebF increases amount of secreted proteins.[96] Therefore, sec translocon signal of YebF protein was replaced with DsbA or OmpA sec translocon signal. The DsbA signal peptide (DsbAsp) recognized by signal recognition particle whereas SecB recognizes the OmpA signal peptide (OmpAsp) to target proteins the Sec translocation pathway.[97, 98] The DNA sequence of OmpA and DsbA signal peptides obtained from NCBI. The pZA TetO YebF-TEV vector was amplified with primers that have Gibson Assembly overhangs so that self-assembly product of PCR amplified vectors result in insertion of OmpA or DsbA signal peptide at the site of native sec translocon signal of YebF (Figure 31 and 32). The insertion of OmpA and DsbA signal peptides were verified with Sanger sequencing (Appendix D).

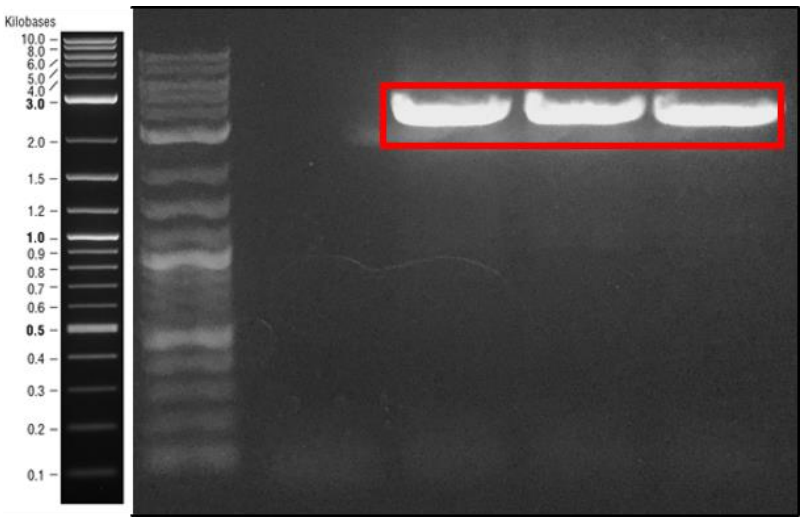

Figure 31: Amplification of pZA TetO YebF-TEV vector with Gibson overhangs to insert the DsbA signal peptide.

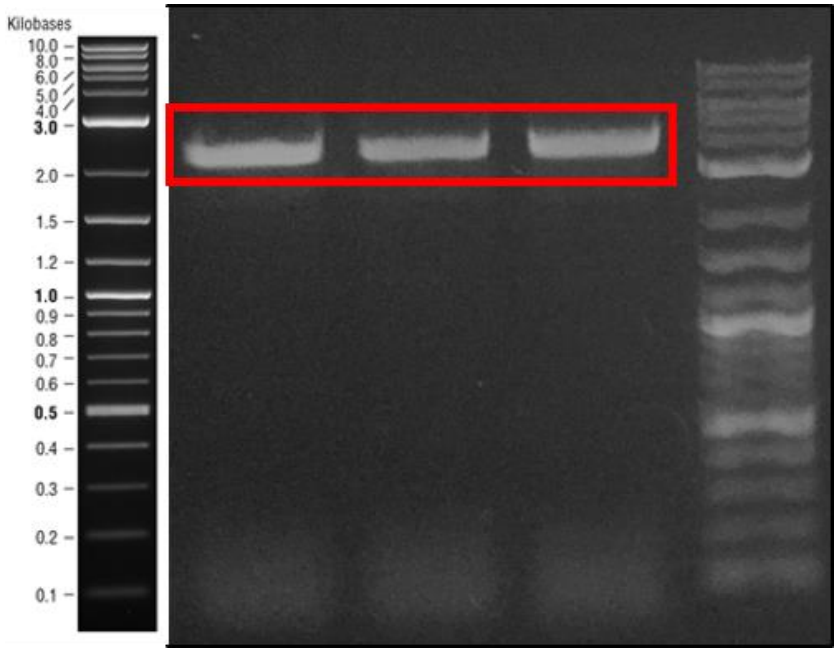

Figure 32: Amplification of pZA TetO YebF-TEV vector with Gibson overhangs to insert the OmpA signal peptide.

The expression of DsbAsp/YebF-TEV and OmpAsp/YebF-TEV fusion proteins were induced described same as above. The whole cell content and secreted proteins were analysed with western blotting. Based on analysis, OmpAsp/YebF-TEV is successfully expressed and secreted by cells whereas DsbAsp/YebF-TEV isn't expressed upon induction (Figure 33). Therefore, OmpAsp/YebF-TEV fusion protein was used in co-seeding experiments.

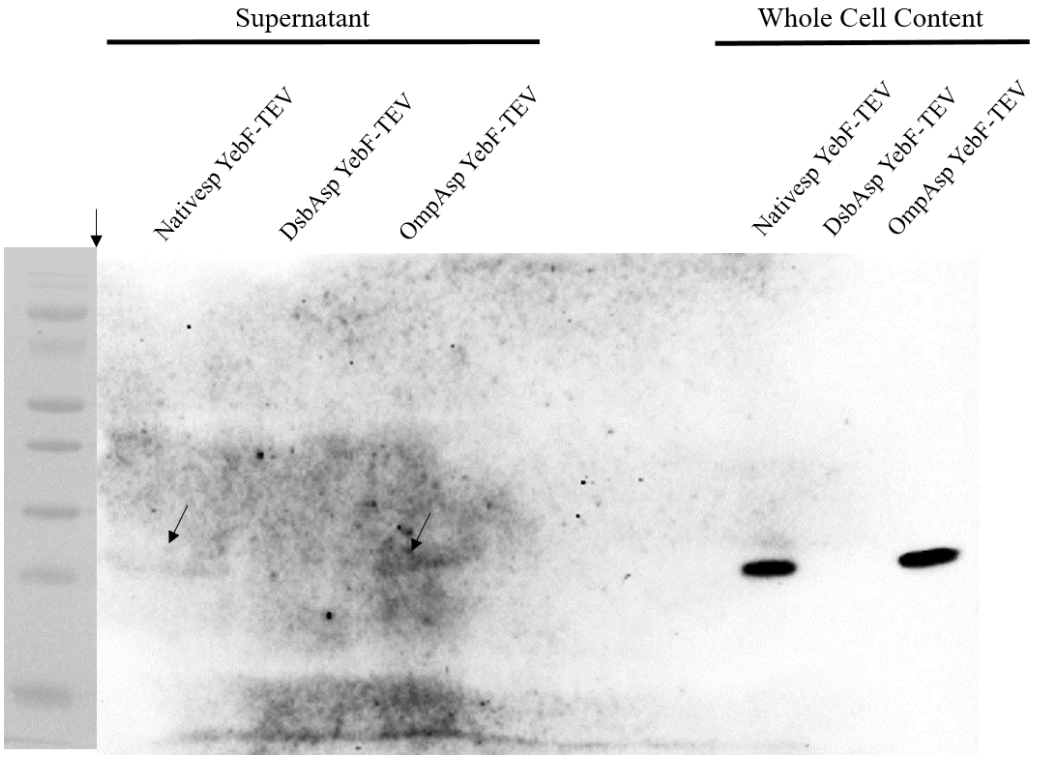

Figure 33: Western blotting analysis of OmpAsp/YebF and DsbA/YebF protein fusion from whole cell content and cell supernatant.

3.3.5. Co-seeding of Cells Carrying Display, and OmpAsp/YebF-TEV Protease Expression Cassette

Co-inoculation experiment was carried out same as described previously. Only 1:1 (display cassette carrying cells : OmpAsp/YebF-TEV expressing cells) cell mixing ratio was tried to release the sfGFP from cell surface. Following the induction, fluorescence of cell supernatants were measured. The displayed sfGFP molecules aren't released upon induction of YebF-TEV (Figure 34). Protein secretion by YebF fusions suffers from the low yield.[96] Even the change of sec translocon signal peptide doesn't increase the secretion efficiency high enough to cleave the recognition site. In literature, it was reported that some of *E. coli*

showed high secretory profile for YebF fusion protein however considering amount of time and money required for building those strain, the strategy switched to release through co-expressing lysis promoting genes.

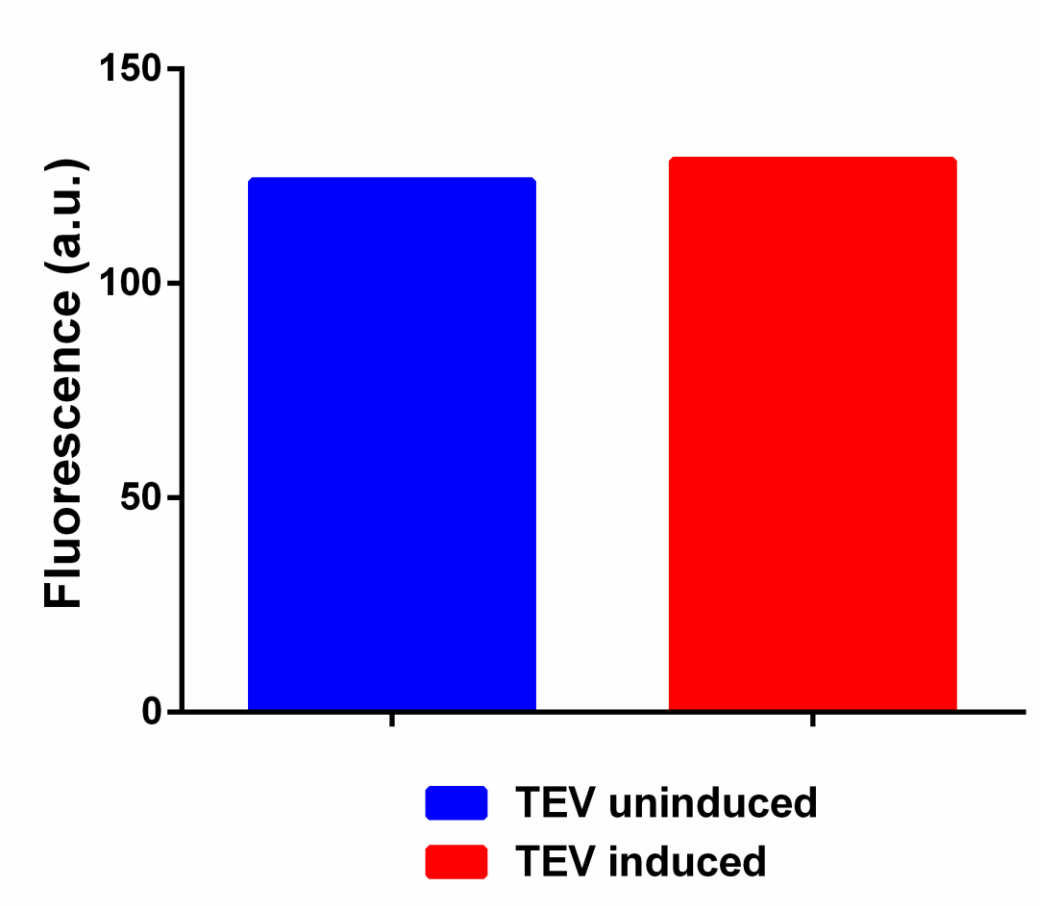

Figure 34: Cell supernatant fluorescence of co-inoculated cells carrying display cassette and OmpAsp/YebF-TEV protease expressing cassette after induction.

3.4. Strategy 3: Secretion of TEV Protease Through Co-Expressing E-Lysis Gene

Intracellularly expressed GST-TEV protease is aimed to be secreted to extracellular medium via co-expressing a lysis inducing gene called E-lysis.

Previous reports showed that co-induction of E-lysis resulted in release of all cytosolic on content to extracellular medium.[99] E-lysis gene is isolated from phi173 phage, and encoded protein interacts with MraY protein to lipid synthesis which cause formation of pore on membrane.[100] However, it is reported that dormant cells isn't lyse upon induction of E-lysis gene, cells need to be actively dividing for lysis.

3.4.1. Cloning and Expression of aTc Inducible E-lysis Gene

E-lysis gene was cloned in pZA nTetO E-lysis vector at upstream of aTc inducible vector. To clone the E-lysis gene, the DNA segments encoding the E-lysis gene was amplified with Gibson overhangs via PCR from pCSaE500.[86] pZA nTetO plasmid was linearized with digestion of KpnI and XhoI. The DNA fragments were assembled in Gibson Assembly reaction. The cloning was verified with sequencing.

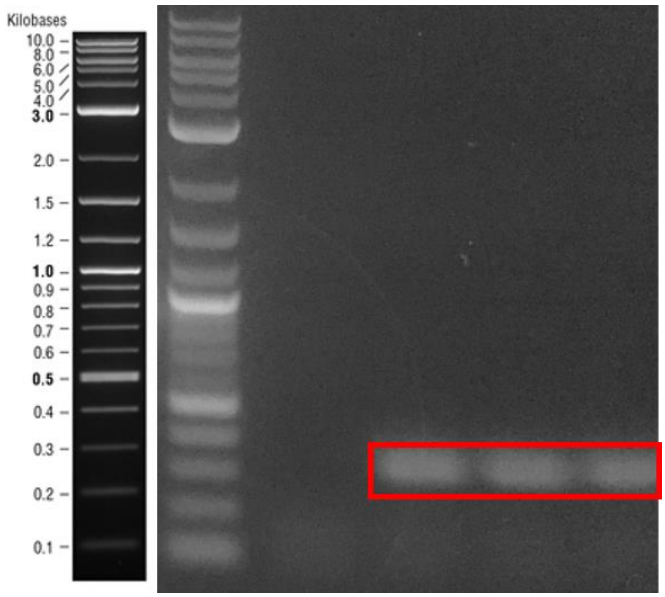

Figure 35: PCR amplification of E-lysis gene with Gibson overhangs. Expected bands are 348 bp.

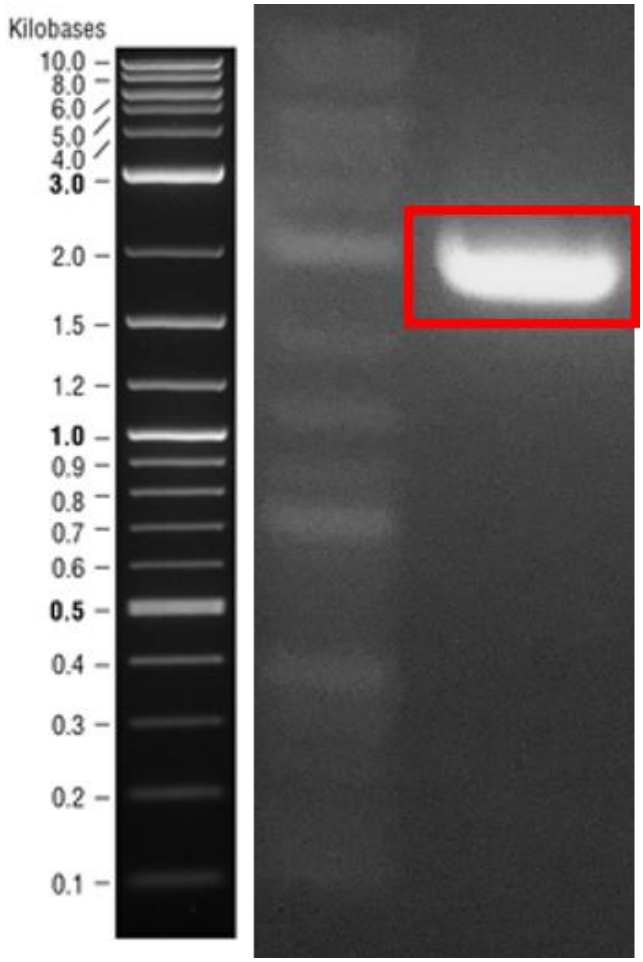

Figure 36: KpnI-XhoI digestion of pZA nTetO vector. Expected band is 1758 bp.

The sequence verified E-lysis expressing vector was transformed into *E. coli* DH5α PRO strain. The E-lysis gene was induced at mid-log phase and the OD_{600} was continuously monitored during induction. The optical density value of induced cells were sharply decreased whereas uninduced cells continue to grow (Figure 37).

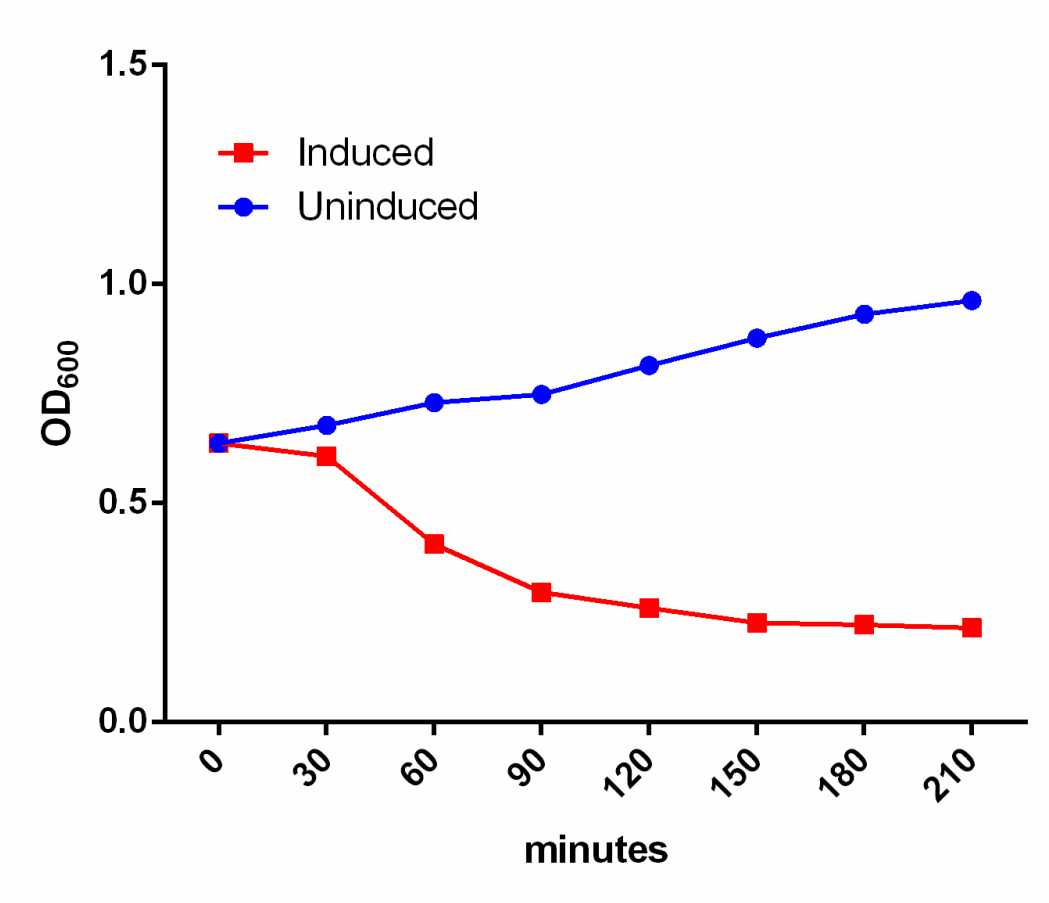

Figure 37: Growth curves of E-lysis induced and uninduced cells.

Following to the induction, cells were taken and spread onto agar plate. Next day, colony forming units were count on agar plate to find viable cells. The number of viable cells significantly decreased upon E-lysis induction (Figure 38). The cells were lysed subsequent to induction at mid-log phase.

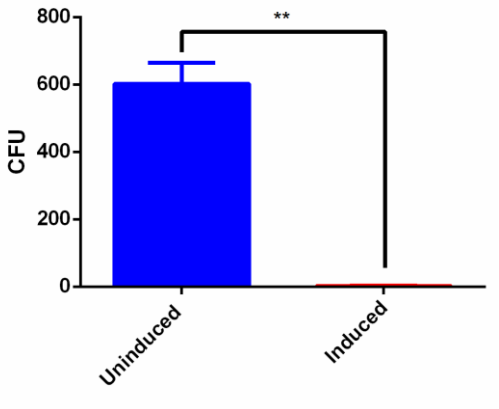

Figure 38: Viable cell count after E-lysis induction. The experiments were performed in triplicates and statistical significance was determined with student's t-test. (**: $p < 0.01$).

The cells were examined under ESEM to visualize the pores on cell membrane. Subsequent to induction, cells were taken and fixed in glutaraldehyde solution. The fixed cells were washed and dried in critical point dryer. Cells were coated with 8nm thick Au/Pd alloy and visualize under ESEM. The clear pore were observed in E-lysis expressing cells (Figure 39).

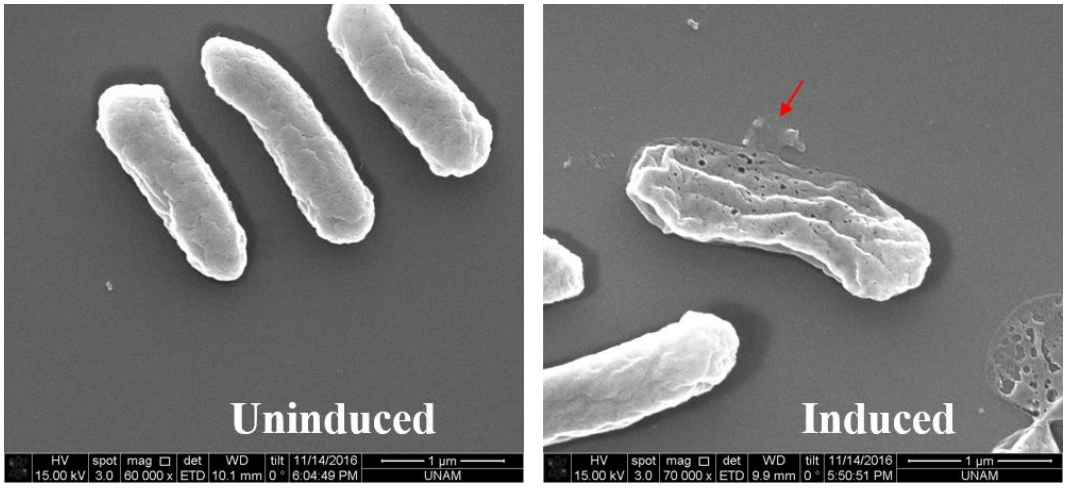

Figure 39: ESEM images of E-lysis expressing cells. The pore was indicated with red arrow.

3.4.2. Co-seeding of Cells Harboring E-lysis/GST-TEV plasmids and Display Cassette

The GST-TEV vector and E-lysis expressiong vector were sequentially transformed into BL21 (DE3) strain whereas the display cassette and mock chloramphenicol vector were transformed sequentially ito BL21 (DE3). The two different cells were co-inoculated in same media with 1:100 total dilution mixed 1:1 ratio. The display cassette and GST-TEV gene were induced with IPTG at early-log phase. The e-lysis gene was induced with aTc at mid-log phase. The OD_{600} values were monitored during growth and induction. Following to the induction, supernatants were collected, and supernatant fluorescence intensities were measured. The displayed sfGFP molecules aren't released following the lysis of the GST-TEV expressing cells (Figure 40). The intracellularly produced GST-TEV protein might be too diluted in media. Total concentration of GST-TEV protease might be too low for efficient cleavage reaction.

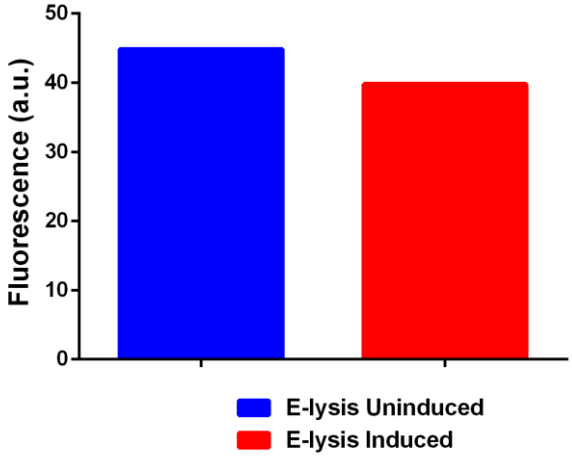

Figure 40: Fluorescence intensities of supernatants after lysis of GST-TEV expressing cells.

3.5. Strategy 4: Codisplay TEV protease on Cell Surface

As previous trails mainly fail due to the low concentration of TEV protease in culture medium after secretion, TEV protease is planned to be co-displayed with Ag43 transporter protein along with sfGFP molecules. The local concentration of TEV protease around sfGFP molecules will be much higher because diffusion of displayed TEV protease will be limited to bacterial surface area.

3.5.1. 3D Structure Prediction of TEV Protease-Truncated Ag43 α-Domain Fusion

Prior to clone the TEV protease in pET22b PelB 6H Ag43 160N vector, the 3D structure of TEV protease - truncated α-domain fusion protein was predicted using I-Tasser server. The best structure among five predicted structures was selected manually to align with native TEV protease protein (PDB: 1lvm). The primary analysis of predicted structure revealed that the fusion wasn't effect the overall folding of TEV protease (Figure 41a and 41b). The catalytic cleft folded similar with native structure as well as relative amino acid position of cysteine catalytic triad was conserved. Many of secondary structure of TEV protease in predicted fusion protein structure are good aligned to native TEV protease. The close-up view of catalytic triad indicates that the catalytic amino acid of TEV protease including histidine, aspartic acid, and cysteine have different rotation compared to native structure (Figure 41c). Small errors may occur in nature of computational modelling even with best algorithm but considering the overall structure, TEV protease is perfectly folded and seems to be active after folding.

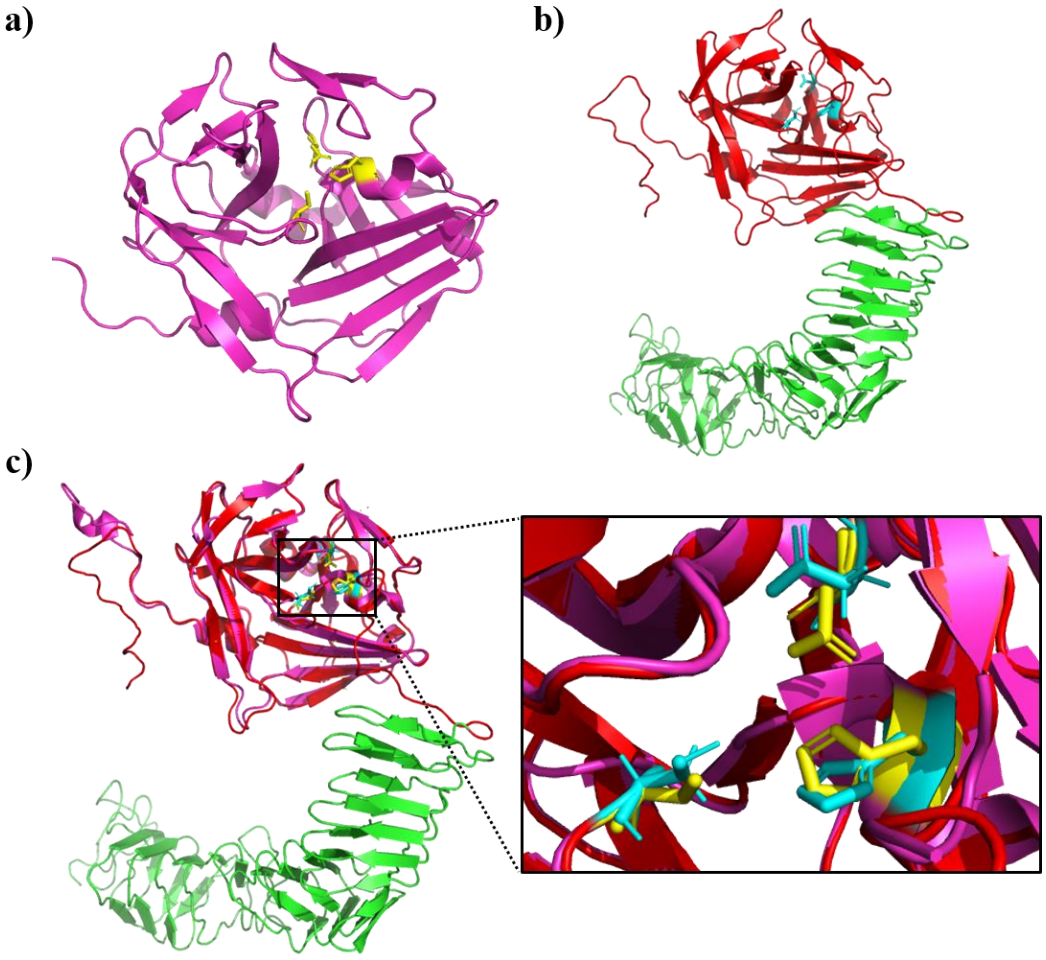

Figure 41: The predicted structure of TEV protease in fusion protein share similar global motifs with native TEV protease structure. a) Native TEV protease structure obtained from Protein Data Bank, 1lvm. b) The most accurate structure selected manually among five predicted structure by I-Tasser server. c) Alignment of TEV protease in predicted structure with native TEV protease structure. RSM=0.300 for 189 atoms.

3.5.2. Cloning, Expression and Labelling of PelB 6H Ag43 160N TEV Display Cassette

To clone the TEV protease coding in display cassette, TEV protease coding region was digested with BamHI and AflII enzymes from pZA yebF TEV vector. The sfGFP display cassette was cut with same to remove the sfGFP coding region. The DNA fragments were separated with agarose gel electrophoresis and purified (Figure 42). The TEV protease coding sequence was ligated to display cassette with T4 ligation. The constructed pET22b PelB 6H Ag43 160N TEV vector was verified with restriction digestion (data not shown).

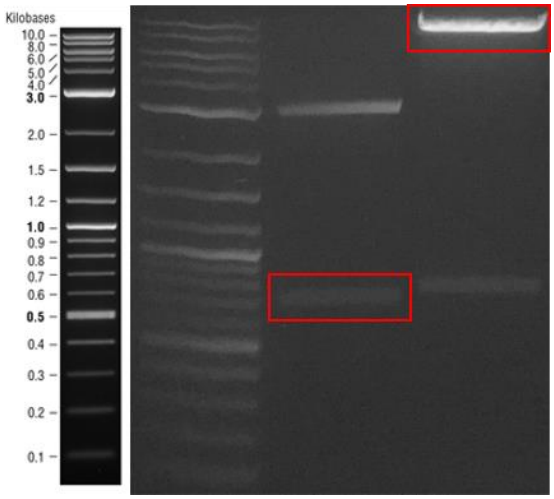

Figure 42: Restriction digestion of pZA YebF TEV (first lane) and pET22b PelB 6H Ag43 160N sfGFP plasmids (second lane). Expected bands for TEV coding region and mock display cassette are 720 bp and 7956 bp, respectively.

The sequence verified plasmids transformed in *E. coli* BL21 (DE3) strain and induced to express display cassette harboring the TEV protease gene same as previously described. The induced cells were labelled with Dylight550 conjugated anti-his antibody and visualized under epifluorescence microscope (Figure 43).

The labelling cells with anti-his antibody without any membrane solubilizing agents indicates that TEV protease is successfully displayed on cells surface. Furthmore, the TEV protease - α-domain fusion protein was released to extracellular medium with heat treatment and detected with westernblotting (Figure 44).

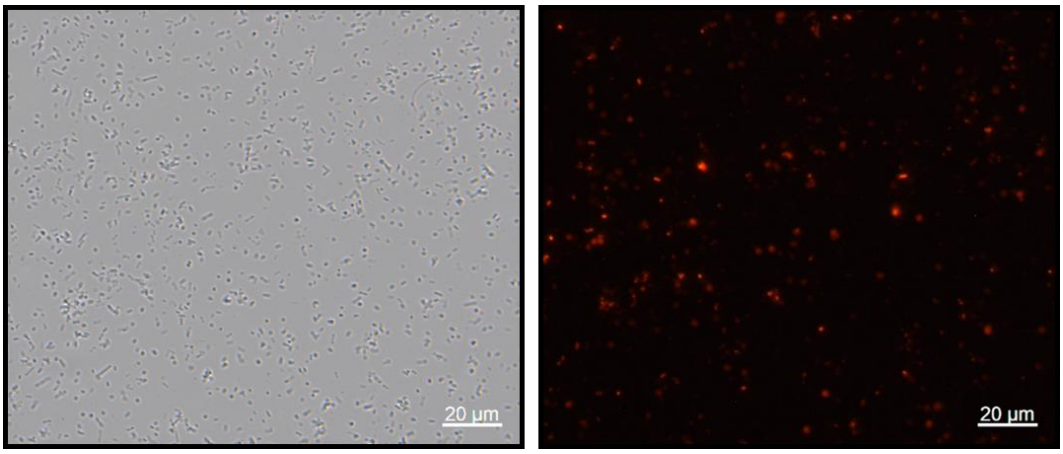

Figure 43: ICC staining of TEV protease displaying cells with Dylight550 attached anti-his antibody in the absence of any membrane solubilizing agents. (white bars represent 20µm).

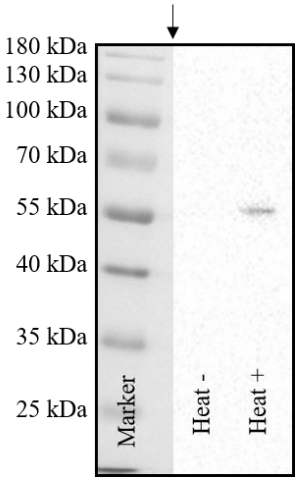

Figure 44: The western blotting analysis from acetone precipitated supernatants obtained following the heat treatment of TEV protease display cells.

3.5.3. Construction of pZA nTetO PelB 6H Ag43 160N TEV Plasmid

To test the release of sfGFP upon TEV protease display, genetic circuit that functions as an AND gate for input signals of sfGFP and TEV protease display cassette induction was constructed. The expression of sfGFP harboring display cassette was controlled under IPTG induction. Therefore, the TEV protease harboring display cassette was cloned into tetracycline inducible promoter. To construct the pZA nTetO PelB 6H Ag43 160N TEV plasmid, the TEV protease harboring display cassette was amplified from pET22b PelB 6H Ag43 160N TEV vector with Gibson overhangs (Figure 45). PCR was performed to amplify the region containing native tetracycline promoter and TetR repressor gene from the pdCas9-bacteria plasmid (Figure 46).

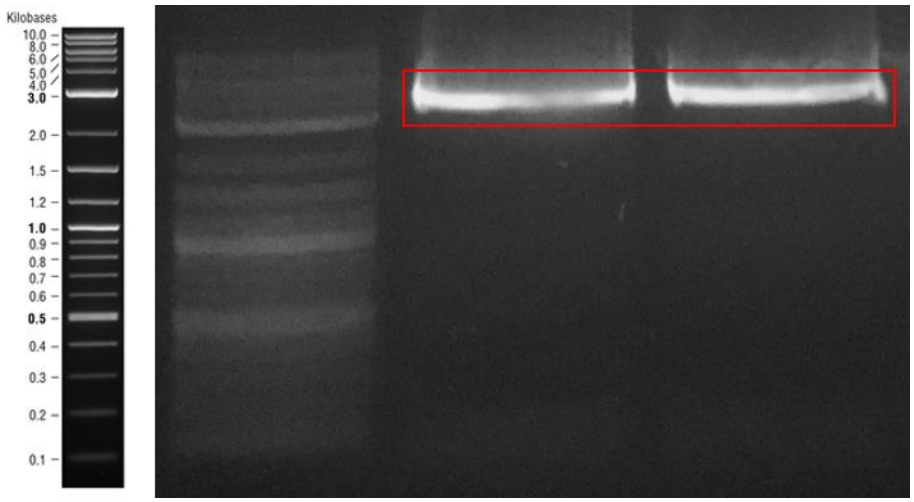

Figure 45: PCR amplification of TEV protease containing display casette. Expected band is 3364 bp.

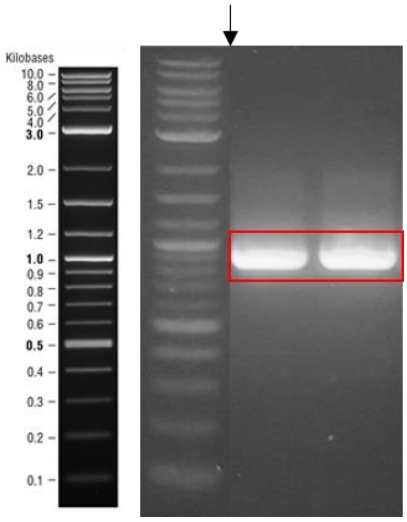

Figure 46: PCR product of region that includes native tetracycline promoter and TetR repressor gene. Expected band is 914 bp.

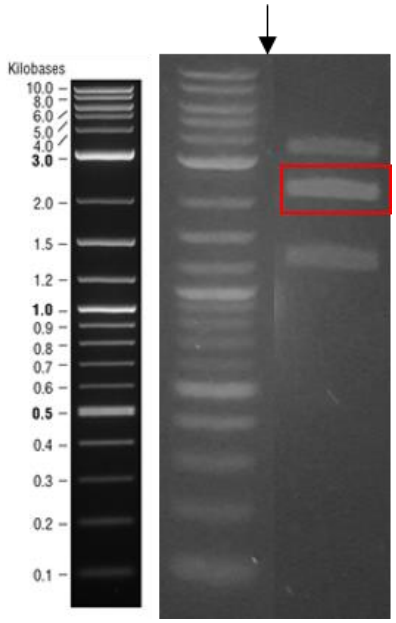

Figure 47: Digestion of pZA vector with NotI-MluI enzymes. Expected band is 1943 bp.

The pZA was linearized with digestion by NotI and MluI (figure 47). The DNA fragments purified from agarose gel were assembled with Gibson Assembly. The sequence of assembled plasmid with Sanger sequencing (Appendix D).

3.5.4. Co-display of TEV Protease and sfGFP on the Cell Surface

The pZA nTetO PelB 6H Ag43 160N TEV and pET22b PelB 6H Ag43 160N sfGFP plasmids were transformed sequentially into *E. coli* BL21 (DE3) strain. The overnight culture of the bacteria harboring the AND gate plasmids was re-inoculated into fresh modified MOPS media with %1 (w/v) glucose. The bacteria were induced with either IPTG or aTc or both of them at the early log phase (OD_{600}~0.4). The inductions were carried out at 18 ˚C for overnight. Following to the induction, cells were centrifuged and supernatants were collected to measure fluorescence emission. The output of constructed AND is the increase in fluorescence emission from supernatants as TEV protease and sfGFP molecules are needed to be displayed to release sfGFP molecules to extracellular medium (Figure 48a). The fluorescence emission of supernatant was increased by 3-fold for the condition that both of the display cassette was induced compared other conditions (Figure 48b). The fluorescence increase indicates that the autonomous TEV protease mediated protein secretion system is operating as expected.

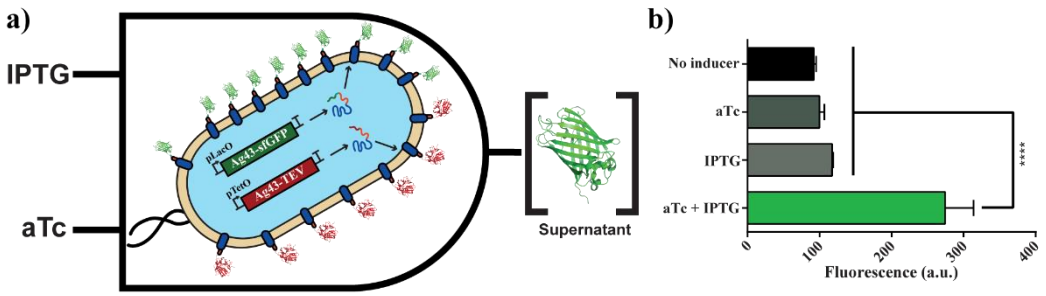

Figure 48: The co-induction of sfGFP and TEV protease carrying display cassette leads to secretion of displayed sfGFP molecules to extracellular environment. a) The constructed AND gate to test system. Output signal of AND is increased GFP fluorescence of cell supernatant. The induction of both TEV protease and sfGFP

is required to release the sfGFP molecules to extracellular environment. b) Supernatant fluorescence of cells induced with either aTc or IPTG or both of them. Fluorescence of supernatants obtained from uninduced cells were also measured. The experiments were performed in triplicates and statistical significance was determined with student's test (***: $p < 0.001$).

3.5.5. Release Kinetics of Autonomous TEV Protease Mediated Protein Secretion System

The secretion kinetics of the system was determined following the induction of both display cassette at different OD_{600} for hours. The genetic circuit transformed cells were grown until OD_{600} reached to 0.4 and 0.5. The OD_{600} values were selected near enough to see effect of induction at release. The cells were induced either with IPTG (labelled as TEV uninduced) or both IPTG and aTc (labelled as TEV induced) at same conditions described previous for induction of display cassette. Subsequent to the induction, cells were centrifuged and suspended in fresh media while induction parameters kept as same. The fluorescence emission of cell supernatants and whole cells were measured every for 4 hours.

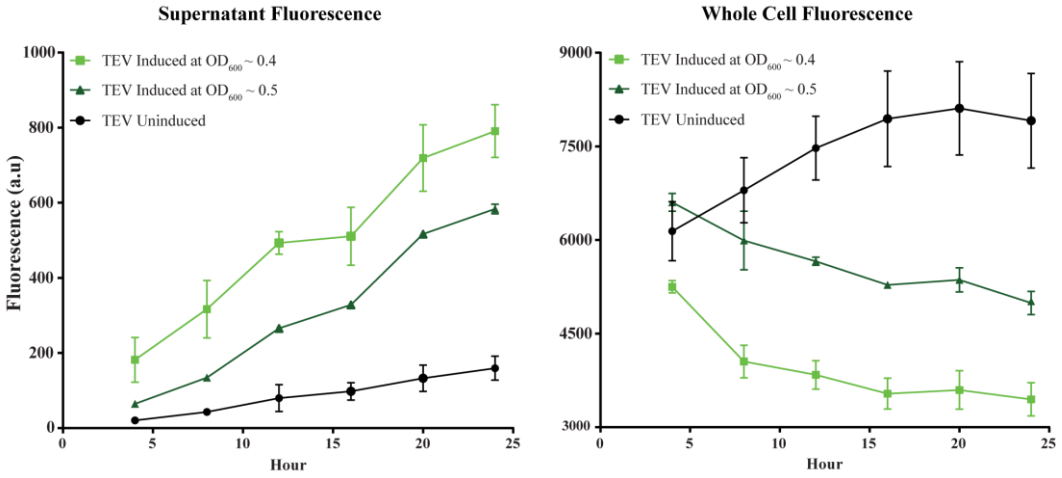

Figure 49: Release kinetics of genetic circuit for autonomous TEV protease mediated protein secretion induced at OD600 equals to 0.4 and 0.5

The less sfGFP molecules were released from the older induced cells (OD_{600} equals 0.5) compared younger induced cells (OD_{600} equals 0.4) through the number of sfGFP molecules expressed was fairly same for TEV uninduced cells (Figure 49).Considering finite space of cell surface, maximum number displayed proteins is constant. Co-induction of both display cassette creates a competition between sfGFP harbouring Ag43 proteins and TEV protease harbouring Ag43 proteins to translocate themselves to outer membrane. Due to the asymmetric distribution of cell membrane during cell division, the surface proteins may accumulate at the poles of membrane.[101] Our fluorescence microscope analysis revealed similar results which the displayed sfGFP proteins accumulated at certain location. The cleavage of recognition site probably is the result of increase TEV protease concentration around the sfGFP molecules on cell surface. Our constant trails were failed to cleave sfGFP molecules from cells surface with continuous secretion TEV protease molecules fused to YebF carrier protein. Therefore, the release of sfGFP molecules might be determined by the number of TEV protease molecules on surfaces. The co-induction at higher optical density may resulted less accumulation and display of TEV protease on cell surface which is resulted in less sfGFP release. Even if TEV protease display limiting the secretion of sfGFP molecules, almost one of third sfGFP molecules were released upon co-induction at 0.4 optical density.

CHAPTER 4

CONCLUSIONS

In conclusion, a cellular device that is able to display and secrete proteins on-demand was developed in this thesis. Ag43 autotransporter protein was engineered to display proteins on the cell surface. The displayed proteins can be released with both physical and biochemical inputs. To release the displayed proteins with signals recognized by genetically encoded parts, we sysmetically optimized biochemical release of displayed proteins with TEV protease in different conditions. Four different secretion strategy were employed to secrete TEV protease to extracellular medium. The TEV protease wasn't expressed fused with C-terminal region of HlyA toxin. The YebF-TEV fusion protein was expressed and secreted to extracellular medium. However, it was hypothesized that the amount of secreted proteases is too low to cleave the recognition site. In third strategy, lysis inducing gene E-lysis was co-expressed with TEV protease for secretion. However, the intracellular expressed TEV protease molecules were diluted to very low concentrations upon lysis for cleavage reaction. In the fourth strategy, codisplay of TEV protease and POI on cell surface led to release of POI to extracellular medium. Based on our observations, the release of POI is dependent on amount of TEV protease on the cell surface. Because the release of displayed proteins depends on genetically recognized signals, it is possible build simple logical operations which have output as release of the displayed proteins. Therefore, the proposed cellular device can be layered with additional genetic

circuits. The engineering effective plug-and-play secretory machines is crucial to develop better cellular machines that can be used for many different applications.

BIBLIOGRAPHY

[1] Moe-Behrens G, Davis R, Haynes K. Preparing synthetic biology for the world. Frontiers in Microbiology. 2013;4.

[2] Cao JC, Perez-Pinera P, Lowenhaupt K, Wu MR, Purcell O, de la Fuente-Nunez C, et al. Versatile and on-demand biologics co-production in yeast. Nature Communications. 2018;9.

[3] Tay PKR, Nguyen PQ, Joshi NS. A Synthetic Circuit for Mercury Bioremediation Using Self Assembling Functional Amyloids. Acs Synthetic Biology. 2017;6:1841-50.

[4] Chen AY, Deng ZT, Billings AN, Seker UOS, Lu MY, Citorik RJ, et al. Synthesis and patterning of tunable multiscale materials with engineered cells. Nature Materials. 2014;13:515-23.

[5] Bokinsky G, Peralta-Yahya PP, George A, Holmes BM, Steen EJ, Dietrich J, et al. Synthesis of three advanced biofuels from ionic liquid-pretreated switchgrass using engineered Escherichia coli. Proceedings of the National Academy of Sciences of the United States of America. 2011;108:19949-54.

[6] Fernandez LA, Berenguer J. Secretion and assembly of regular surface structures in Gram-negative bacteria. Fems Microbiology Reviews. 2000;24:21-44.

[7] Koebnik R, Locher KP, Van Gelder P. Structure and function of bacterial outer membrane proteins: barrels in a nutshell. Molecular Microbiology. 2000;37:239-53.

[8] Schneewind O, Missiakas DM. Protein secretion and surface display in Gram-positive bacteria. Philosophical Transactions of the Royal Society B-Biological Sciences. 2012;367:1123-39.

[9] Costa TRD, Felisberto-Rodrigues C, Meir A, Prevost MS, Redzej A, Trokter M, et al. Secretion systems in Gram-negative bacteria: structural and mechanistic insights. Nature Reviews Microbiology. 2015;13:343-59.

[10] Mergulhao FJM, Summers DK, Monteiro GA. Recombinant protein secretion in Escherichia coli. Biotechnology Advances. 2005;23:177-202.

[11] Sung Ho Y, Seong Keun K, Jihyun FK. Secretory Production of Recombinant Proteins in Escherichia coli. Recent Patents on Biotechnology. 2010;4:23-9.

[12] Joshi H, Jain V. Novel method to rapidly and efficiently lyse Escherichia coli for the isolation of recombinant protein. Analytical Biochemistry. 2017;528:1-6.

[13] Choi JH, Lee SY. Secretory and extracellular production of recombinant proteins using Escherichia coli. Applied Microbiology and Biotechnology. 2004;64:625-35.

[14] Le HV, Trotta PP. Purification of secreted recombinant proteins from Escherichia coli. Bioprocess Technol. 1991;12:163-81.

[15] Angkawidjaja C, Kuwahara K, Omori K, Koga Y, Takano K, Kanaya S. Extracellular secretion of Escherichia coli alkaline phosphatase with a C-terminal tag by type I secretion system: purification and biochemical characterization. Protein Engineering Design & Selection. 2006;19:337-43.

[16] Gottschalk U, Brorson K, Shukla AA. The need for innovation in biomanufacturing. Nature Biotechnology. 2012;30:489-92.

[17] Mohr BP, Retterer ST, Doktycz MJ. While-you-wait proteins? Producing biomolecules at the point of need. Taylor & Francis; 2016.

[18] Perez-Pinera P, Han NR, Cleto S, Cao JC, Purcell O, Shah KA, et al. Synthetic biology and microbioreactor platforms for programmable production of biologics at the point-of-care. Nature Communications. 2016;7.

[19] Natarajan A, Haitjema CH, Lee R, Boock JT, DeLisa MP. An Engineered Survival-Selection Assay for Extracellular Protein Expression Uncovers Hypersecretory Phenotypes in Escherichia coli. Acs Synthetic Biology. 2017;6:875-83.

[20] Steen EJ, Kang YS, Bokinsky G, Hu ZH, Schirmer A, McClure A, et al. Microbial production of fatty-acid-derived fuels and chemicals from plant biomass. Nature. 2010;463:559-U182.

[21] Yang C, Song CJ, Freudl R, Mulchandani A, Qiao CL. Twin-Arginine Translocation of Methyl Parathion Hydrolase in Bacillus subtilis. Environmental Science & Technology. 2010;44:7607-12.

[22] Silva N, Vilela C, Marrucho IM, Freire CSR, Neto CP, Silvestre AJD. Protein-based materials: from sources to innovative sustainable materials for biomedical applications. Journal of Materials Chemistry B. 2014;2:3715-40.

[23] Heidebrecht A, Scheibel T. Recombinant production of spider silk proteins. Advances in applied microbiology: Elsevier; 2013. p. 115-53.

[24] Baneyx F, Mujacic M. Recombinant protein folding and misfolding in Escherichia coli. Nature Biotechnology. 2004;22:1399-408.

[25] Kalyoncu E, Ahan RE, Olmez TT, Seker UOS. Genetically encoded conductive protein nanofibers secreted by engineered cells. Rsc Advances. 2017;7:32543-51.

[26] Wang X, Zhou YZ, Ren JJ, Hammer ND, Chapman MR. Gatekeeper residues in the major curlin subunit modulate bacterial amyloid fiber biogenesis. Proceedings of the National Academy of Sciences of the United States of America. 2010;107:163-8.

[27] Claesen J, Fischbach MA. Synthetic Microbes As Drug Delivery Systems. ACS Synthetic Biology. 2015;4:358-64.

[28] Hamady ZZR, Scott N, Farrar MD, Lodge JPA, Holland KT, Whitehead T, et al. Xylan-regulated delivery of human keratinocyte growth factor-2 to the inflamed colon by the human anaerobic commensal bacterium Bacteroides ovatus. Gut. 2010;59:461-9.

[29] Steidler L, Hans W, Schotte L, Neirynck S, Obermeier F, Falk W, et al. Treatment of murine colitis by Lactococcus lactis secreting interleukin-10. Science. 2000;289:1352-5.

[30] Vandenbroucke K, de Haard H, Beirnaert E, Dreier T, Lauwereys M, Huyck L, et al. Orally administered L. lactis secreting an anti-TNF Nanobody demonstrate efficacy in chronic colitis. Mucosal Immunology. 2010;3:49-56.

[31] Duan FP, Curtis KL, March JC. Secretion of Insulinotropic Proteins by Commensal Bacteria: Rewiring the Gut To Treat Diabetes. Applied and Environmental Microbiology. 2008;74:7437-8.

[32] Teixeira AP, Fussenegger M. Synthetic biology-inspired therapies for metabolic diseases. Current Opinion in Biotechnology. 2017;47:59-66.

[33] Kleiner-Grote GR, Risse JM, Friehs K. Secretion of recombinant proteins from E. coli. Engineering in Life Sciences.

[34] Mergulhão FJ, Monteiro GA. Periplasmic targeting of recombinant proteins in Escherichia coli. Protein Targeting Protocols: Springer; 2007. p. 47-61.

[35] Koster M, Bitter W, Tommassen J. Protein secretion mechanisms in Gram-negative bacteria. International Journal of Medical Microbiology. 2000;290:325-31.

[36] Ni Y, Chen R. Extracellular recombinant protein production from Escherichia coli. Biotechnology Letters. 2009;31:1661-70.

[37] Gentschev I, Mollenkopf H, Sokolovic Z, Hess J, Kaufmann SHE, Goebel W. Development of antigen-delivery systems, based on the Escherichia coli hemolysin secretion pathway. Gene. 1996;179:133-40.

[38] Zhang GJ, Brokx S, Weiner JH. Extracellular accumulation of recombinant proteins fused to the carrier protein YebF in Escherichia coli. Nature Biotechnology. 2006;24:100-4.

[39] Qian ZG, Xia XX, Choi JH, Lee SY. Proteome-based identification of fusion partner for high-level extracellular production of recombinant proteins in Escherichia coli. Biotechnology and Bioengineering. 2008;101:587-601.

[40] Ignatova Z, Mahsunah A, Georgieva M, Kasche V. Improvement of posttranslational bottlenecks in the production of penicillin amidase in recombinant Escherichia coli strains. Applied and Environmental Microbiology. 2003;69:1237-45.

[41] Ni Y, Reye J, Chen RR. Lpp deletion as a permeabilization method. Biotechnology and bioengineering. 2007;97:1347-56.

[42] Leo JC, Grin I, Linke D. Type V secretion: mechanism(s) of autotransport through the bacterial outer membrane. Philosophical Transactions of the Royal Society B-Biological Sciences. 2012;367:1088-101.

[43] Sichwart S, Tozakidis IEP, Teese M, Jose J. Maximized Autotransporter-Mediated Expression (MATE) for Surface Display and Secretion of Recombinant Proteins in Escherichia coli. Food Technology and Biotechnology. 2015;53:251-60.

[44] Fernandez LA, de Lorenzo V. Formation of disulphide bonds during secretion of proteins through the periplasmic-independent type I pathway. Molecular Microbiology. 2001;40:332-46.

[45] Binet R, Letoffe S, Ghigo JM, Delepelaire P, Wandersman C. Protein secretion by Gram-negative bacterial ABC exporters - A review. Gene. 1997;192:7-11.

[46] Gentschev I, Dietrich G, Goebel W. The E-coli alpha-hemolysin secretion system and its use in vaccine development. Trends in Microbiology. 2002;10:39-45.

[47] Jarchau T, Chakraborty T, Garcia F, Goebel W. SELECTION FOR TRANSPORT COMPETENCE OF C-TERMINAL POLYPEPTIDES DERIVED FROM ESCHERICHIA-COLI HEMOLYSIN - THE SHORTEST PEPTIDE CAPABLE OF AUTONOMOUS HLYB/HLYD-DEPENDENT SECRETION COMPRISES THE C-TERMINAL-62 AMINO-ACIDS OF HLYA. Molecular and General Genetics. 1994;245:53-60.

[48] Blight MA, Holland IB. HETEROLOGOUS PROTEIN SECRETION AND THE VERSATILE ESCHERICHIA-COLI HEMOLYSIN TRANSLOCATOR. Trends in Biotechnology. 1994;12:450-5.

[49] Sapriel G, Wandersman C, Delepelaire P. The SecB chaperone is bifunctional in Serratia marcescens: SecB is involved in the Sec pathway and required for HasA secretion by the ABC transporter. Journal of Bacteriology. 2003;185:80-8.

[50] Fernandez LA, Sola I, Enjuanes L, de Lorenzo V. Specific secretion of active single-chain Fv antibodies into the supernatants of Escherichia coli cultures by use of the hemolysin system. Applied and Environmental Microbiology. 2000;66:5024-+.

[51] Li YY, Chen CX, von Specht BU, Hahn HP. Cloning and hemolysin-mediated secretory expression of a codon-optimized synthetic human interleukin-6 gene in Escherichia coli. Protein Expression and Purification. 2002;25:437-47.

[52] Lee PS, Lee KH. Engineering HlyA hypersecretion in Escherichia coli based on proteomic and microarray analyses. Biotechnology and Bioengineering. 2005;89:195-205.

[53] Sugamata Y, Shiba T. Improved secretory production of recombinant proteins by random mutagenesis of hlyB, an alpha-hemolysin transporter from Escherichia coli. Applied and Environmental Microbiology. 2005;71:656-62.

[54] Portaliou AG, Tsolis KC, Loos MS, Zorzini V, Economou A. Type III Secretion: Building and Operating a Remarkable Nanomachine. Trends in Biochemical Sciences. 2016;41:175-89.

[55] Galan JE, Lara-Tejero M, Marlovits TC, Wagner S. Bacterial Type III Secretion Systems: Specialized Nanomachines for Protein Delivery into Target Cells. In: Gottesman S, editor. Annual Review of Microbiology, Vol 682014. p. 415-38.

[56] Diepold A, Wagner S. Assembly of the bacterial type III secretion machinery. Fems Microbiology Reviews. 2014;38:802-22.

[57] Majander K, Anton L, Antikainen J, Lång H, Brummer M, Korhonen TK, et al. Extracellular secretion of polypeptides using a modified Escherichia coli flagellar secretion apparatus. Nature biotechnology. 2005;23:475.

[58] Reeves AZ, Spears WE, Du J, Tan KY, Wagers AJ, Lesser CF. Engineering Escherichia coli into a Protein Delivery System for Mammalian Cells. Acs Synthetic Biology. 2015;4:644-54.

[59] Widmaier DM, Tullman-Ercek D, Mirsky EA, Hill R, Govindarajan S, Minshull J, et al. Engineering the Salmonella type III secretion system to export spider silk monomers. Molecular Systems Biology. 2009;5.

[60] Kotzsch A, Vernet E, Hammarstrom M, Berthelsen J, Weigelt J, Graslund S, et al. A secretory system for bacterial production of high-profile protein targets. Protein Science. 2011;20:597-609.

[61] Dresler K, van den Heuvel J, Muller RJ, Deckwer WD. Production of a recombinant polyester-cleaving hydrolase from Thermobifida fusca in Escherichia coli. Bioprocess and Biosystems Engineering. 2006;29:169-83.

[62] Tanaka T, Horio T, Matuo Y. Secretory production of recombinant human C-reactive protein in Escherichia coli, capable of binding with phosphorylcholine,

and its characterization. Biochemical and Biophysical Research Communications. 2002;295:163-6.

[63] Durrani FG, Gul R, Sadaf S, Akhtar MW. Expression and rapid purification of recombinant biologically active ovine growth hormone with DsbA targeting to Escherichia coli inner membrane. Applied Microbiology and Biotechnology. 2015;99:6791-801.

[64] Shin HD, Chen RR. Extracellular Recombinant Protein Production From an Escherichia coli lpp Deletion Mutant. Biotechnology and Bioengineering. 2008;101:1288-96.

[65] Gumpert J, Hoischen C. Use of cell wall-less bacteria (L-forms) for efficient expression and secretion of heterologous gene products. Current opinion in biotechnology. 1998;9:506-9.

[66] Haeusser DP, Hoashi M, Weaver A, Brown N, Pan J, Sawitzke JA, et al. The Kil peptide of bacteriophage λ blocks Escherichia coli cytokinesis via ZipA-dependent inhibition of FtsZ assembly. PLoS genetics. 2014;10:e1004217.

[67] Hsiung HM, Cantrell A, Luirink J, Oudega B, Veros AJ, Becker GW. USE OF BACTERIOCIN RELEASE PROTEIN IN E. COLI FOR EXCRETION OF HUMAN GROWTH-HORMONE INTO THE CULTURE-MEDIUM. Bio-Technology. 1989;7:267-71.

[68] van Ulsen P, Rahman SU, Jong WSP, Daleke-Schermerhom MH, Luirink J. Type V secretion: From biogenesis to biotechnology. Biochimica Et Biophysica Acta-Molecular Cell Research. 2014;1843:1592-611.

[69] Babu M, Bundalovic-Torma C, Calmettes C, Phanse S, Zhang QZ, Jiang Y, et al. Global landscape of cell envelope protein complexes in Escherichia coli. Nature Biotechnology. 2018;36:103-+.

[70] Jong WSP, Sauri A, Luirink J. Extracellular production of recombinant proteins using bacterial autotransporters. Current Opinion in Biotechnology. 2010;21:646-52.

[71] Rutherford N, Mourez M. Surface display of proteins by Gram-negative bacterial autotransporters. Microbial Cell Factories. 2006;5.

[72] Wargacki AJ, Leonard E, Win MN, Regitsky DD, Santos CNS, Kim PB, et al. An Engineered Microbial Platform for Direct Biofuel Production from Brown Macroalgae. Science. 2012;335:308-13.

[73] Zhou CD, Yan YP, Fang J, Cheng BJ, Fan J. A new fusion protein platform for quantitatively measuring activity of multiple proteases. Microbial Cell Factories. 2014;13.

[74] Cesaratto F, Burrone OR, Petris G. Tobacco Etch Virus protease: A shortcut across biotechnologies. Journal of Biotechnology. 2016;231:239-49.

[75] Phan J, Zdanov A, Evdokimov AG, Tropea JE, Peters HK, Kapust RB, et al. Structural basis for the substrate specificity of tobacco etch virus protease. Journal of Biological Chemistry. 2002;277:50564-72.

[76] Mort J, Barrett A, Rawlings N, Woessner J. Handbook of proteolytic enzymes. 2004.

[77] Mótyán JA, Tóth F, Tőzsér J. Research applications of proteolytic enzymes in molecular biology. Biomolecules. 2013;3:923-42.

[78] Waugh DS. An overview of enzymatic reagents for the removal of affinity tags. Protein Expression and Purification. 2011;80:283-93.

[79] Fernandez-Rodriguez J, Voigt CA. Post-translational control of genetic circuits using Potyvirus proteases. Nucleic Acids Research. 2016;44:6493-502.

[80] Kapust RB, Waugh DS. Controlled intracellular processing of fusion proteins by TEV protease. Protein Expression and Purification. 2000;19:312-8.

[81] Costa S, Almeida A, Castro A, Domingues L. Fusion tags for protein solubility, purification, and immunogenicity in Escherichia coli: the novel Fh8 system. Frontiers in Microbiology. 2014;5.

[82] Waugh DS. Making the most of affinity tags. Trends in Biotechnology. 2005;23:316-20.

[83] Goh HC, Sobota RM, Ghadessy FJ, Nirantar S. Going native: Complete removal of protein purification affinity tags by simple modification of existing tags and proteases. Protein Expression and Purification. 2017;129:18-24.

[84] Olson EJ, Hartsough LA, Landry BP, Shroff R, Tabor JJ. Characterizing bacterial gene circuit dynamics with optically programmed gene expression signals. Nature Methods. 2014;11:449-+.

[85] Qi LS, Larson MH, Gilbert LA, Doudna JA, Weissman JS, Arkin AP, et al. Repurposing CRISPR as an RNA-Guided Platform for Sequence-Specific Control of Gene Expression. Cell. 2013;152:1173-83.

[86] Tanouchi Y, Pai A, Buchler NE, You LC. Programming stress-induced altruistic death in engineered bacteria. Molecular Systems Biology. 2012;8.

[87] Zhang Y. I-TASSER server for protein 3D structure prediction. Bmc Bioinformatics. 2008;9.

[88] Yang JY, Yan RX, Roy A, Xu D, Poisson J, Zhang Y. The I-TASSER Suite: protein structure and function prediction. Nature Methods. 2015;12:7-8.

[89] Roy A, Kucukural A, Zhang Y. I-TASSER: a unified platform for automated protein structure and function prediction. Nature Protocols. 2010;5:725-38.

[90] van der Woude MW, Henderson IR. Regulation and Function of Ag43 (Flu). Annual Review of Microbiology2008. p. 153-69.

[91] Kjaergaard K, Hasman H, Schembri MA, Klemm P. Antigen 43-mediated autotransporter display, a versatile bacterial cell surface presentation system. Journal of Bacteriology. 2002;184:4197-204.

[92] Girard V, Cote JP, Charbonneau ME, Campos M, Berthiaume F, Hancock MA, et al. Conformation Change in a Self-recognizing Autotransporter Modulates Bacterial Cell-Cell Interaction. Journal of Biological Chemistry. 2010;285:10616-26.

[93] Waugh DS. TEV Protease FAQ. Macromolecular Crystallography Laboratory; 2010.

[94] Clifton LA, Skoda MWA, Le Brun AP, Ciesielski F, Kuzmenko I, Holt SA, et al. Effect of Divalent Cation Removal on the Structure of Gram-Negative Bacterial Outer Membrane Models. Langmuir. 2015;31:404-12.

[95] Tzschaschel BD, Guzman CA, Timmis KN, deLorenzo V. An Escherichia coli hemolysin transport system-based vector for the export of polypeptides: Export of Shiga-like toxin IIeB subunit by Salmonella typhimurium aroA. Nature Biotechnology. 1996;14:765-9.

[96] Broedel Jr SE, Papciak SM. Technical Support. ACES2007.

[97] Reusch RN. Insights into the structure and assembly of Escherichia coli outer membrane protein A. Febs Journal. 2012;279:894-909.

[98] Schierle CF, Berkmen M, Huber D, Kumamoto C, Boyd D, Beckwith J. The DsbA signal sequence directs efficient, cotranslational export of passenger proteins to the Escherichia coli periplasm via the signal recognition particle pathway. Journal of Bacteriology. 2003;185:5706-13.

[99] Din MO, Danino T, Prindle A, Skalak M, Selimkhanov J, Allen K, et al. Synchronized cycles of bacterial lysis for in vivo delivery. Nature. 2016;536:81-+.

[100] Tanaka S, Clemons Jr WM. Minimal requirements for inhibition of MraY by lysis protein E from bacteriophage ΦX174. Molecular microbiology. 2012;85:975-85.

[101] Bergmiller T, Andersson AMC, Tomasek K, Balleza E, Kiviet DJ, Hauschild R, et al. Biased partitioning of the multidrug efflux pump AcrAB-TolC underlies long-lived phenotypic heterogeneity. Science. 2017;356:309-11.

APPENDIX A

DNA sequences of constructs used in this study

Table A.1: Gene sequences used in this study

Gene Name	Sequence
Ag43 Protein	ATGAAACGACATCTGAATACCTGCTACAGGCTGGTATGG AATCACATGACGGGCGCTTTCGTGGTTGCCTCCGAACTGG CCCGCGCACGGGGTAAACGTGGCGGTGTGGCGGTTGCAC TGTCTCTTGCCGCAGTCACGTCACTCCCGGTGCTGGCTGC TGACATCGTTGTGCACCCGGGAGAAACCGTGAACGGCGG AACACTGGCAAATCATGACAACCAGATTGTCTTCGGTACG ACCAACGGAATGACCATCAGTACCGGGCTGGAGTATGGG CCGGATAACGAGGCCAATACCGGCGGGCAATGGGTACAG GATGGCGGAACAGCCAACAAAACGACTGTCACCAGTGGT GGTCTTCAGAGAGTGAACCCCGGTGGAAGTGTCTCAGAC ACGGTTATCAGTGCCGGAGGCGGACAGAGCCTTCAGGGA CGGGCTGTGAACACCACGCTGAATGGTGGCGAACAGTGG ATGCATGAGGGGGCGATAGCCACAGGAACCGTCATTAAT GATAAGGGCTGGCAGGTCGTCAAGCCCGGTACAGTGGCA ACGGATACCGTTGTTAATACCGGGGCGGAAGGGGGACCG GATGCAGAAAACGGTGATACCGGGCAGTTTGTTCGCGGG GATGCCGTACGCACAACCATCAATAAAAACGGTCGCCAG ATTGTGAGAGCTGAAGGAACGGCAAATACCACTGTGGTT TATGCCGGCGGCGACCAGACTGTACATGGTCACGCACTG GATACCACGCTGAATGGGGGATACCAGTATGTGCACAAC GGCGGTACAGCGTCTGACACTGTTGTGAACAGTGACGGCT GGCAGATTGTCAAAAACGGGGGTGTGGCCGGGAATACCA CCGTTAATCAGAAGGGCAGACTGCAGGTGGACGCCGGTG GTACAGCCACGAATGTCACCCTGAAGCAGGGCGGCGCAC TGGTTACCAGTACGGCTGCAACCGTTACCGGCATAAACCG CCTGGGAGCATTCTCTGTTGTGGAGGGTAAAGCTGATAAT GTCGTACTGGAAAATGGCGGACGCCTGGATGTGCTGACC GGACACACAGCCACTAATACCCGCGTGGATGATGGCGGA ACGCTGGATGTCCGCAACGGTGGCACCGCCACCACCGTAT CCATGGGAAATGGCGGTGTACTGCTGGCCGATTCCGGTGC CGCTGTCAGTGGTACCCGGAGCGACGGAAAGGCATTCAG TATCGGAGGCGGTCAGGCGGATGCCCTGATGCTGGAAAA AGGCAGTTCATTCACGCTGAACGCCGGTGATACGGCCAC GGATACCACGGTAAATGGCGGACTGTTCACCGCCAGGGG CGGCACACTGGCGGGCACCACCACGCTGAATAACGGCGC

	CATACTTACCCTTTCCGGGAAGACGGTGAACAACGATACC CTGACCATCCGTGAAGGCGATGCACTCCTGCAGGGAGGC TCTCTCACCGGTAACGGCAGCGTGGAAAAATCAGGAAGT GGCACACTCACTGTCAGCAACACCACACTCACCCAGAAA GCCGTCAACCTGAATGAAGGCACGCTGACGCTGAACGAC AGTACCGTCACCACGGATGTCATTGCTCAGCGCGGTACAG CCCTGAAGCTGACCGGCAGCACTGTGCTGAACGGTGCCAT TGACCCCACGAATGTCACTCTCGCCTCCGGTGCCACCTGG AATATCCCCGATAACGCCACGGTGCAGTCGGTGGTGGAT GACCTCAGCCATGCCGGACAGATTCATTTCACCTCCACCC GCACAGGGAAGTTCGTACCGGCAACCCTGAAAGTGAAAA ACCTGAACGGACAGAATGGCACCATCAGCCTGCGTGTAC GCCCGGATATGGCACAGAACAATGCTGACAGACTGGTCA TTGACGGCGGCAGGGCAACCGGAAAAACCATCCTGAACC TGGTGAACGCCGGCAACAGTGCGTCGGGGCTGGCGACCA GCGGTAAGGGTATTCAGGTGGTGGAAGCCATTAACGGTG CCACCACGGAGGAAGGGGCCTTTGTCCAGGGGAACAGGC TGCAGGCCGGTGCCTTTAACTACTCCCTCAACCGGGACAG TGATGAGAGCTGGTATCTGCGCAGTGAAAATGCTTATCGT GCAGAAGTCCCCCTGTATGCCTCCATGCTGACACAGGCAA TGGACTATGACCGGATTGTGGCAGGCTCCCGCAGCCATCA GACCGGTGTAAATGGTGAAAACAACAGCGTCCGTCTCAG CATTCAGGGCGGTCATCTCGGTCACGATAACAATGGCGGT ATTGCCCGTGGGGCCACGCCGGAAAGCAGCGGCAGCTAT GGATTCGTCCGTCTGGAGGGTGACCTGATGAGAACAGAG GTTGCCGGTATGTCTGTGACCGCGGGGGTATATGGTGCTG CTGGCCATTCTTCCGTTGATGTTAAGGATGATGACGGCTC CCGTGCCGGCACGGTCCGGGATGATGCCGGCAGCCTGGG CGGATACCTGAATCTGGTACACACGTCCTCCGGCCTGTGG GCTGACATTGTGGCACAGGGAACCCGCCACAGCATGAAA GCGTCATCGGACAATAACGACTTCCGCGCCCGGGGCTGG GGCTGGCTGGGCTCACTGGAAACCGGTCTGCCCTTCAGTA TCACTGACAACCTGATGCTGGAGCCACAACTGCAGTATAC CTGGCAGGGACTTTCCCTGGATGACGGTAAGGACAACGC CGGTTATGTGAAGTTCGGGCATGGCAGTGCACAACATGTG CGTGCCGGTTTCCGTCTGGGCAGCCACAACGATATGACCT TTGGCGAAGGCACCTCATCCCGTGCCCCCCTGCGTGACAG TGCAAAACACAGTGTGAGTGAATTACCGGTGAACTGGTG GGTACAGCCTTCTGTTATCCGCACCTTCAGCTCCCGGGGA GATATGCGTGTGGGGACTTCCACTGCAGGCAGCGGGATG ACGTTCTCTCCCTCACAGAATGGCACATCACTGGACCTGC AGGCCGGACTGGAAGCCCGTGTCCGGGAAAATATCACCC TGGGCGTTCAGGCCGGTTATGCCCACAGCGTCAGCGGCA GCAGCGCTGAAGGGTATAACGGTCAGGCCACACTGAATG TGACCTTCTGA
sfGFP	ATGCGTAAAGGCGAAGAGCTGTTCACTGGTGTCGTCCCTA TTCTGGTGGAACTGGATGGTGATGTCAACGGTCATAAGTT TTCCGTGCGTGGCGAGGGTGAAGGTGACGCAACTAATGG

	TAAACTGACGCTGAAGTTCATCTGTACTACTGGTAAACTG CCGGTACCTTGGCCGACTCTGGTAACGACGCTGACTTATG GTGTTCAGTGCTTTGCTCGTTATCCGGACCATATGAAGCA GCATGACTTCTTCAAGTCCGCCATGCCGGAAGGCTATGTG CAGGAACGCACGATTTCCTTTAAGGATGACGGCACGTAC AAAACGCGTGCGGAAGTGAAATTTGAAGGCGATACCCTG GTAAACCGCATTGAGCTGAAAGGCATTGACTTTAAAGAA GACGGCAATATCCTGGGCCATAAGCTGGAATACAATTTTA ACAGCCACAATGTTTACATCACCGCCGATAAACAAAAAA ATGGCATTAAAGCGAATTTTAAAATTCGCCACAACGTGGA GGATGGCAGCGTGCAGCTGGCTGATCACTACCAGCAAAA CACTCCAATCGGTGATGGTCCTGTTCTGCTGCCAGACAAT CACTATCTGAGCACGCAAAGCGTTCTGTCTAAAGATCCGA ACGAGAAACGCGATCATATGGTTCTGCTGGAGTTCGTAAC CGCAGCGGGCATCACGCATGGTATGGATGAACTGTACAA ATGATGA
TEV protease	GGTGAGAGCCTGTTTAAGGGTCCTCGCGATTACAACCCGA TCAGCAGTACCATCTGCCACCTGACCAACGAGAGTGATG GCCATACCACCAGCCTGTATGGCATCGGCTTCGGCCCGTT TATCATCACCAACAAACACCTGTTTCGCCGCAACAATGGC ACCCTGCTGGTGCAGAGCCTGCATGGCGTGTTCAAAGTGA AGAACACCACCACCCTGCAGCAGCACCTGATCGATGGCC GCGACATGATTATCATCCGCATGCCGAAAGACTTCCCGCC GTTTCCGCAGAAACTGAAATTCCGCGAACCGCAGCGCGA AGAACGCATTTGTCTGGTGACCACCAATTTTCAGACCAAA AGCATGAGCAGCATGGTGAGCGATACCAGTTGCACCTTTC CGAGCAGCGATGGCATCTTCTGGAAACACTGGATTCAAA CCAAAGATGGCCAGTGTGGCAGCCCGCTGGTGAGTACCC GCGATGGCTTTATCGTGGGCATTCATAGTGCCAGTAATTT TACCAACACCAATAATTACTTTACCAGCGTGCCGAAGAAC TTCATGGAACTGCTGACCAACCAGGAAGCACAGCAGTGG GTGAGCGGTTGGCGCCTGAATGCAGATAGCGTGCTGTGG GGCGGCCATAAAGTGTTCATGGTGAAACCGGAAGAACCG TTCCAGCCGGTGAAAGAAGCCACCCAGCTGATGAAT
GST-Tag	ATGTCCCCTATACTAGGTTATTGGAAAATTAAGGGCCTTG TGCAACCCACTCGACTTCTTTTGGAATATCTTGAAGAAAA ATATGAAGAGCATTTGTATGAGCGCGATGAAGGTGATAA ATGGCGAAACAAAAAGTTTGAATTGGGTTTGGAGTTTCCC AATCTTCCTTATTATATTGATGGTGATGTTAAATTAACAC AGTCTATGGCCATCATACGTTATATAGCTGACAAGCACAA CATGTTGGGTGGTTGTCCAAAAGAGCGTGCAGAGATTTCA ATGCTTGAAGGAGCGGTTTTGGATATTAGATACGGTGTTT CGAGAATTGCATATAGTAAAGACTTTGAAACTCTCAAAGT TGATTTTCTTAGCAAGCTACCTGAAATGCTGAAAATGTTC GAAGATCGTTTATGTCATAAAACATATTTAAATGGTGATC ATGTAACCCATCCTGACTTCATGTTGTATGACGCTCTTGAT GTTGTTTTATACATGGACCCAATGTGCCTGGATGCGTTCC CAAAATTAGTTTGTTTTAAAAAACGTATTGAAGCTATCCC

	ACAAATTGATAAGTACTTGAAATCCAGCAAGTATATAGC ATGGCCTTTGCAGGGCTGGCAAGCCACGTTTGGTGGTGGC GACCATCCTCCAAAA
HlyA-tag	TTAGCCTATGGAAGTCAGGGTGATCTTAATCCATTAATTA ATGAAATCAGCAAAATCATTTCAGCAGCAGGTAGCTTCG ATGTTAAAGAGGAAAGAACCGCAGCTTCTTTATTGCAGTT GTCCGGTAATGCCAGTGATTTTTCATATGGACGGAACTCA ATAACCCTGACCACATCAGCA
YebF	ATGAAAAAAAGAGGGGCGTTTTTAGGGCTGTTGTTGGTTT CTGCCTGCGCATCAGTTTTCGCTGCCAATAATGAAACCAG CAAGTCGGTCACTTTCCCAAAGTGTGAAGATCTGGATGCT GCCGGAATTGCCGCGAGCGTAAAACGTGATTATCAACAA AATCGCGTGGCGCGTTGGGCAGATGATCAAAAAATTGTC GGTCAGGCCGATCCCGTGGCTTGGGTCAGTTTGCAGGACA TTCAGGGTAAAGATGATAAATGGTCAGTACCGCTAACCGT GCGTGGTAAAAGTGCCGATATTCATTACCAGGTCAGCGTG GACTGCAAAGCGGGAATGGCGGAATATCAGCGGCGT
Serine mutant TEV	GGAAAGAGCTTGTTTAATGGGCCGCGTGATTACAACCCG ATATCGAGCACCATATGTCATTTGACGAATGAATCTGATG GGCTCACAACAACGTTGTATGGTCTCGGATTTGGCCCCTT CATCATTACAAACAAGCACTTGTTTAGAGGAAATAATGG AACACTGTTGGTCCAATCACTACATGGTGTATTCAAGGTC AAAAACACCACGACTTTGCAACAACACCTCATTGATGGG AGGGACATGATAATTATTCGCATGCCTAAGGATTTCCCGC CATTTCCTCAAAAGTTGAAATTTAGAGAGCCACAAAGAG AAGAGCGCATATGTCTTGTGTCAACCAACTTCCAAACTAA GAGCATGTCCAGCATGGTGTCAGACACTAGTTGCACATTC CCTTCATCTGATGGCATATTCTGGAAGCATTGGATTCAAA CCAAGGATGGGCAGAGTGGATCCCCAGTAGTATCAACTA GAGATGGGTTCATTGTTGGCATACACTCAGCATCGAATTT CACCAAGACAAACAATTATTTCACTAGCGTGCCGAAAAA CTTCATGGAATTGTTGACAAATCAGGATGCGCAGCAGTGG GTTAGTGGTTGGCGATTAAATACTGACTCAGTAATGTGGG GGGGCCATAGAGTTTTCATGGTGAAACCTGAAGGGCCTTT TCAGCCAGTTAGGAAG
E-lysis	ATGGTACGCTGGACTTTGTGGGATACCCTCGCTTTCCTGC TCCTGTTGAGTTTATTGCTGCCGTCATTGCTTATTATGTTC ATCCCGTCAACATTCAAACGGCCTGTCTCATCATGGAAGG CGCTGAATTTACGGAAAACATTATTAATGGCGTCGAGCGT CCGGTTAAAGCCGCTGAATTGTTCGCGTTTACCTTGCGTG TACGCGCAGGAAACACTGACGTTCTTACTGACGCAGAAG AAAACGTGCGTCAAAAATTACGTGCGGAAGGAGTGA

Table A.2: Regulatory and miscellaneous DNA elements used in this study

DNA Element	**Sequence**
T7-LacO promoter	TAATACGACTCACTATAGGGGAATTGTGAGCGGATAACA ATTCC
Epsilon and ribosome binding site	TTAACTTTAAGAAGGAG
Native TetO promoter with TetR	TCACACTGGCTCACCTTCGGGTGGGCCTTTCTGCGTTTATA TACTAGAGAGAGAATATAAAAAGCCAGATTATTAATCCG GCTTTTTTATTATTTCCTGCAGGGCGGCCGCTTTAGCTTCC TTAGCTCCTGAAAATCTCGATAACTCAAAAAATACGCCCG GTAGTGATCTTATTTCATTATGGTGAAAGTTGGAACCTCTT ACGTGCCGATCAACGTCTCATTTTCGCCAGATATCGACGT CTTAAGACCCACTTTCACATTTAAGTTGTTTTTCTAATCCG CATATGATCAATTCAAGGCCGAATAAGAAGGCTGGCTCTG CACCTTGGTGATCAAATAATTCGATAGCTTGTCGTAATAA TGGCGGCATACTATCAGTAGTAGGTGTTTCCCTTTCTTCTT TAGCGACTTGATGCTCTTGATCTTCCAATACGCAACCTAA AGTAAAATGCCCCACAGCGCTGAGTGCATATAATGCATTC TCTAGTGAAAAACCTTGTTGGCATAAAAAGGCTAATTGAT TTTCGAGAGTTTCATACTGTTTTTCTGTAGGCCGTGTACCT AAATGTACTTTTGCTCCATCGCGATGACTTAGTAAAGCAC ATCTAAAACTTTTAGCGTTATTACGTAAAAAATCTTGCCA GCTTTCCCCTTCTAAAGGGCAAAAGTGAGTATGGTGCCTA TCTAACATCTCAATGGCTAAGGCGTCGAGCAAAGCCCGCT TATTTTTTACATGCCAATACAATGTAGGCTGCTCTACACCT AGCTTCTGGGCGAGTTTACGGGTTGTTAAACCTTCGATTC CGACCTCATTAAGCAGCTCTAATGCGCTGTTAATCACTTT ACTTTTATCTAATCTAGACATCATTAATTCCTAATTTTTGT TGACACTCTATCGTTGATAGAGTTATTTTACCACTCCCTAT CAGTGATAGAGAAAAGAATTCAAAAGATCT
PelB tag coding sequence	ATGAAATACCTGCTGCCGACCGCTGCTGCTGGTCTGCTGC TCCTCGCTGCCCAGCCGGCGATGGCC
TEV protease site coding sequence	GAAAACCTGTACTTTCAGGGC
His-tag coding sequence	CACCACCACCACCACCAC

DsbA signal sequence	ATGAAAAAGATTTGGCTGGCGCTGGCTGGTTTAGTTTTAGCGTTTAGCGCATCGGCG
OmpA signal sequence	ATGAAAAAGACAGCTATCGCGATTGCAGTGGCACTGGCTGGTTTCGCTACCGTAGCGCAGGCC

APPENDIX B

List of primers used in this study

Table B.1: Primers utilized in PCR.

Cloning of pET22b PelB 6H Ag43 160N sfGFP vector	Ag43 gene	R1	5’ TCAGTGGTGGTGGTGGTGGTGCTCGAGTC ATCAGAAGGTCACATTCAGTG 3’
		R2	5’ TTTCAGGGCGGTGGCGGTGGTAGCCTT AAGCGCACAACCATCAATAAAAACG 3’
	sfGFP gene	R3	5’ GCCCTGAAAGTACAGGTTTTCGCTACCA CGCCACCTTTGTACAGTTCATCCATACCATG CG 3’
		R4	5’ TTTATTGATGGTTGTGCGCTTAAGGCTAC CACCGCCACCGCCCTGAAAGTACAGGTTTT C 3’
		R5	5’ GCCGGCGATGGCCATGGGCCACCACCAC CACCACCACGGTGGCGGTGGATCCATGCGT AAAGGCGAAGAG 3’
Cloning of pZA nTetO PelB 6H Ag43 160N TEV vector	Gene	R6	5’ AAGAATTCAAAAGATCTGAAGGAGGGTA CCATGAAATACCTGCTGCCGA 3’
		R7	5’ TGAGCCTTTCGTTTTATTTGATGCCACGC GTTCAGAAGGTCACATTCAGTGTG 3’
	TetO	R8	5’ CTTTTTTATTATTTCCTGCAGGGCGGCCG CTTTAGCTTCCTTAGCTCCTGAA 3’
		R9	5’ CTCCTTCAGATCTTTTGAATTCTTTTC 3’
Cloning of pET22b 6H GST-TEV vector	TEV gene	R10	5’ ATCTCAGTGGTGGTGGTGGTGGTGCTCGA GTCATCATTCATTCATCAGCTGGGTGGC 3’
		R11	5’ GACCATCCTCCAAAAGGATCCAAAGGCC CGGGTGAGAGCCTGTTTAAGGG 3’
	GST gene	R12	5’ AAACAGGCTCTCACCCGGGCCTTTGGATC CTTTTGGAGGATGGTCGCC 3’
		R13	5’ GGTACCATGAACACCATTCATCACCATCA CCATCACAACACTAGTATGTCCCCTATACT AGGTTATTGG 3’
		R14	5’ ATTGTGAGCGGATAACAATTCCCCTCTAG ATTAACTTTAAGAAGGAGGGTACCATGAAC ACCATTCATC 3’
Cloning of pET22b	GST-	R15	5' AGTGATAGAGAAAAGAATTCAAAAGATC

nTetO 6H HlyA tagged GST-TEV vector	TEV gene		TGAAGGAGGGTACCATGAACACC 3’
		R16	5' AAGCTTACCGCCACCTTCATTCATCAGCT GGGTGGCTTC 3'
	HlyA tag	R17	5' CCACCCAGCTGATGAATGAAGGTGGCGG TAAGCTTTTAGCCTATGGAAGTCAGGGTG 3'
		R18	5' ATCTCAGTGGTGGTGGTGGTGGTGCTCGA GTTATTATGCTGATGTGGTCAGG 3'
Cloning of pZA TetO YebF-TEV 6H vector	YebF	R19	5' GATTTGGGTATTAAAGAGGAGAAAGGTA CCATGAAAAAAAGAGGGGCGTTTTTAGGGC 3'
		R20	5' CGGCCCCTTAAACAAGCTTTCTCCGGATC CACCGCCACCACGCCGCTGATATTCCGCC 3'
Cloning of pZA TetO DsbA Secsig YebF-TEV 6H vector	*	R21	5' AAAACTAAACCAGCCAGCGCCAGCCAAA TCTTTTTCATGGTACCTTTCTCCTCTTTAATA CCC 3'
		R22	5' GCGCTGGCTGGTTTAGTTTTAGCGTTTAG CGCATCGGCGGCCAATAATGAAACCAGCAA GTCG 3'
Cloning of pZA TetO OmpA Secsig YebF-TEV 6H vector	*	R23	5' CAGCCAGTGCCACTGCAATCGCGATAGCT GTCTTTTTCATGGTACCTTTCTCCTCTTTAAT ACCC 3'
		R24	5' TTGCAGTGGCACTGGCTGGTTTCGCTACC GTAGCGCAGGCCGCCAATAATGAAACCAGC AAGTCG 3'
Cloning of pZA nTetO E-lysis vector	E-lysis gene	R25	5' AAGAATTCAAAAGATCTGAAGGAGGGTA CCATGGTACGCTGGACTTTGTG 3'
		R26	5' AGCCTTTCGTTTTATTTGATGCCACGCGT CTCGAGTCACTCCTTCCGCACGTAATTTTTG 3'

APPENDIX C

Plasmid maps used in this study

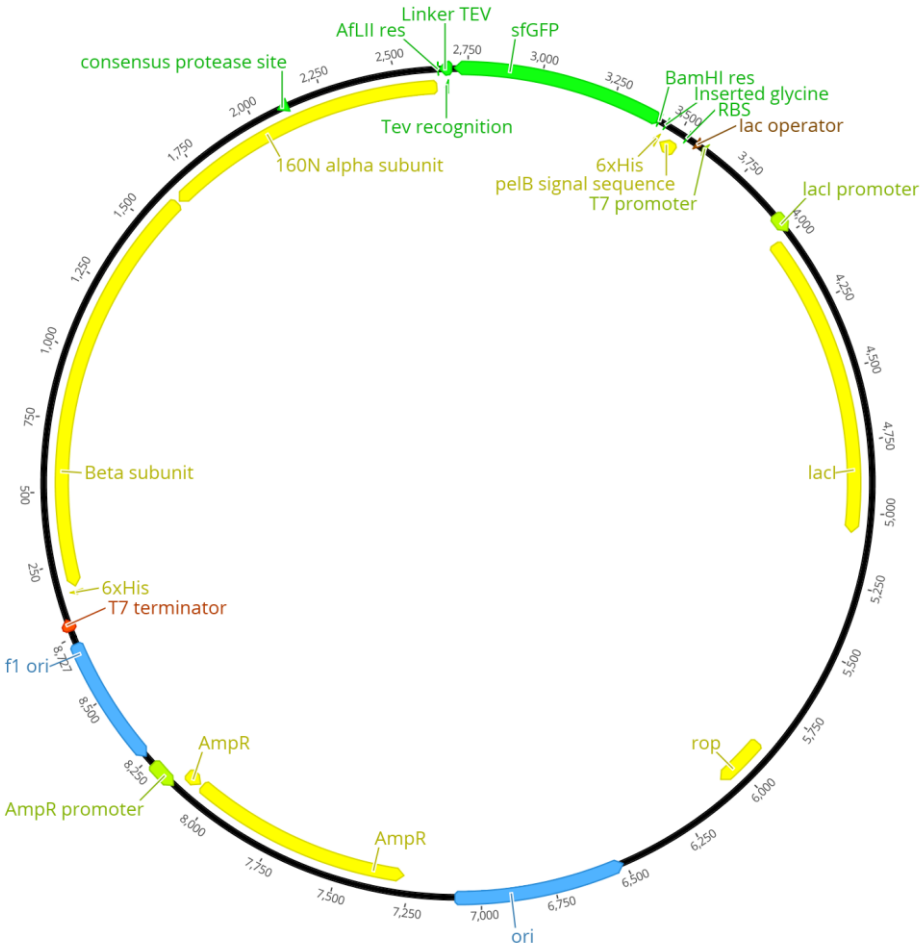

Figure C1: Schematic representation of pET22b PelB 6H Ag43 160N sfGFP vector

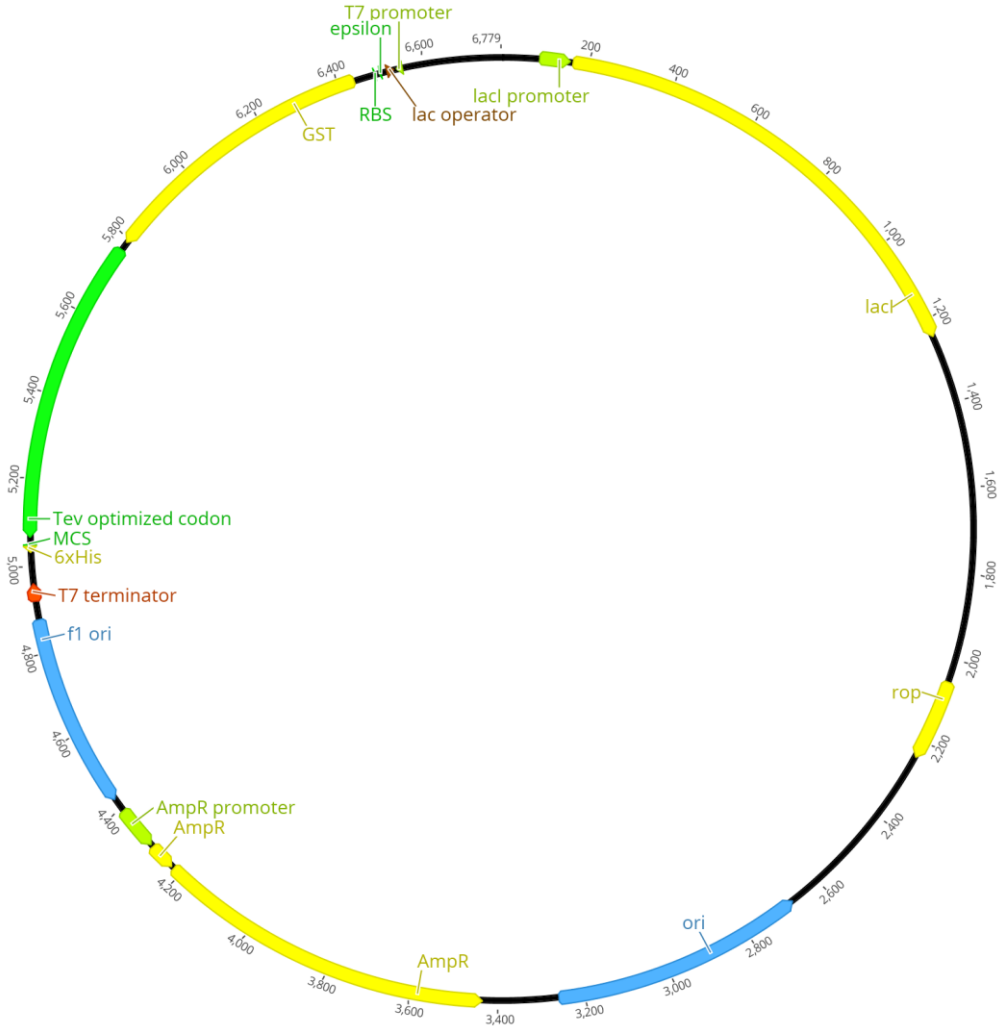

Figure C2: Schematic representation of pET22b 6H GST-TEV vector

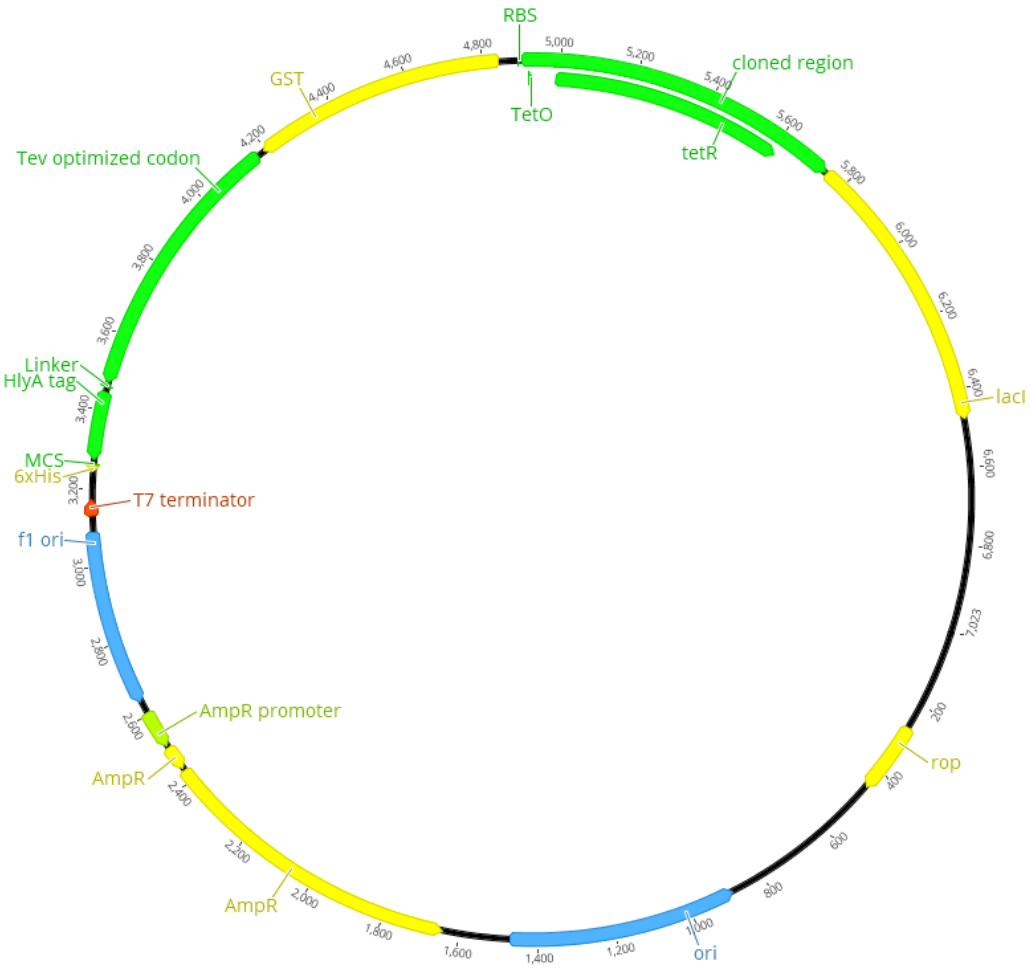

Figure C3: Schematic representation of pET22b GST-TEV HlyA vector.

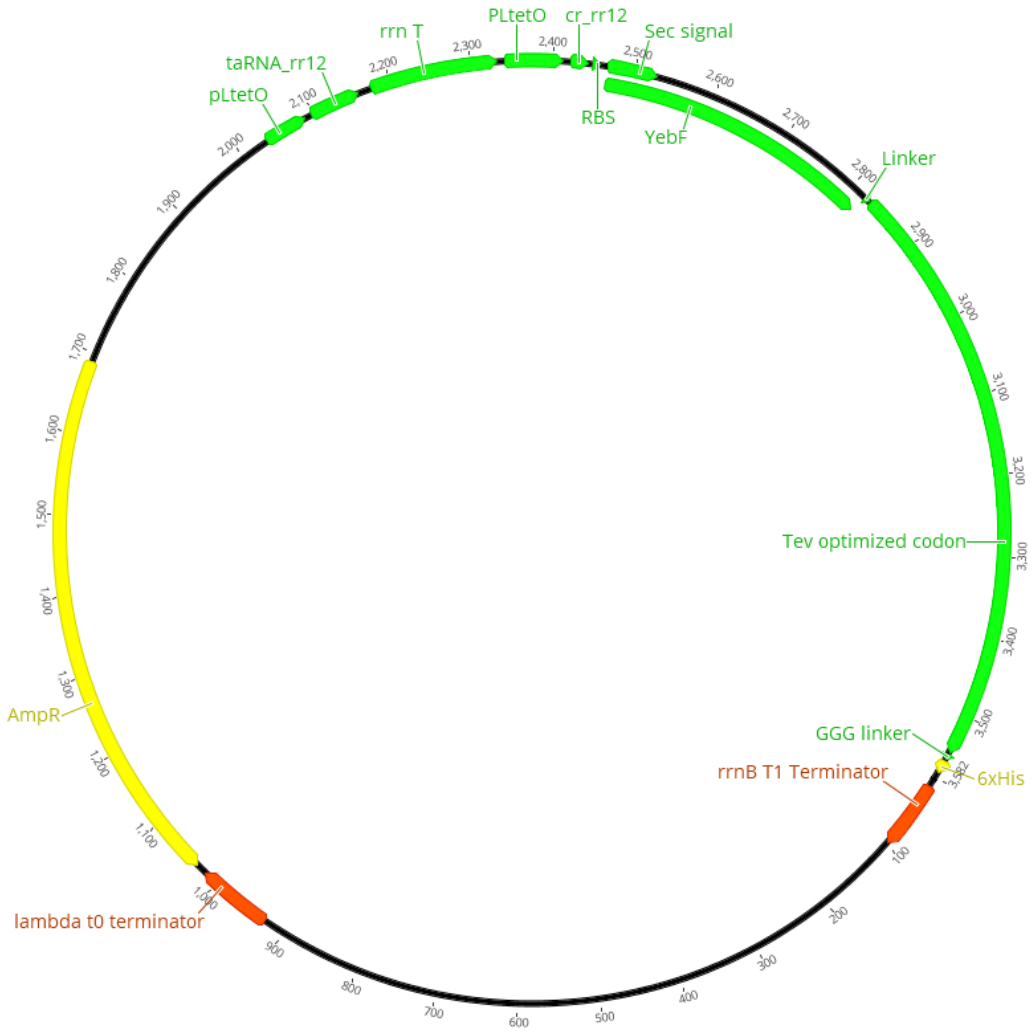

Figure C4: Schematic representation of pZA TetO YebF TEV protease vector.

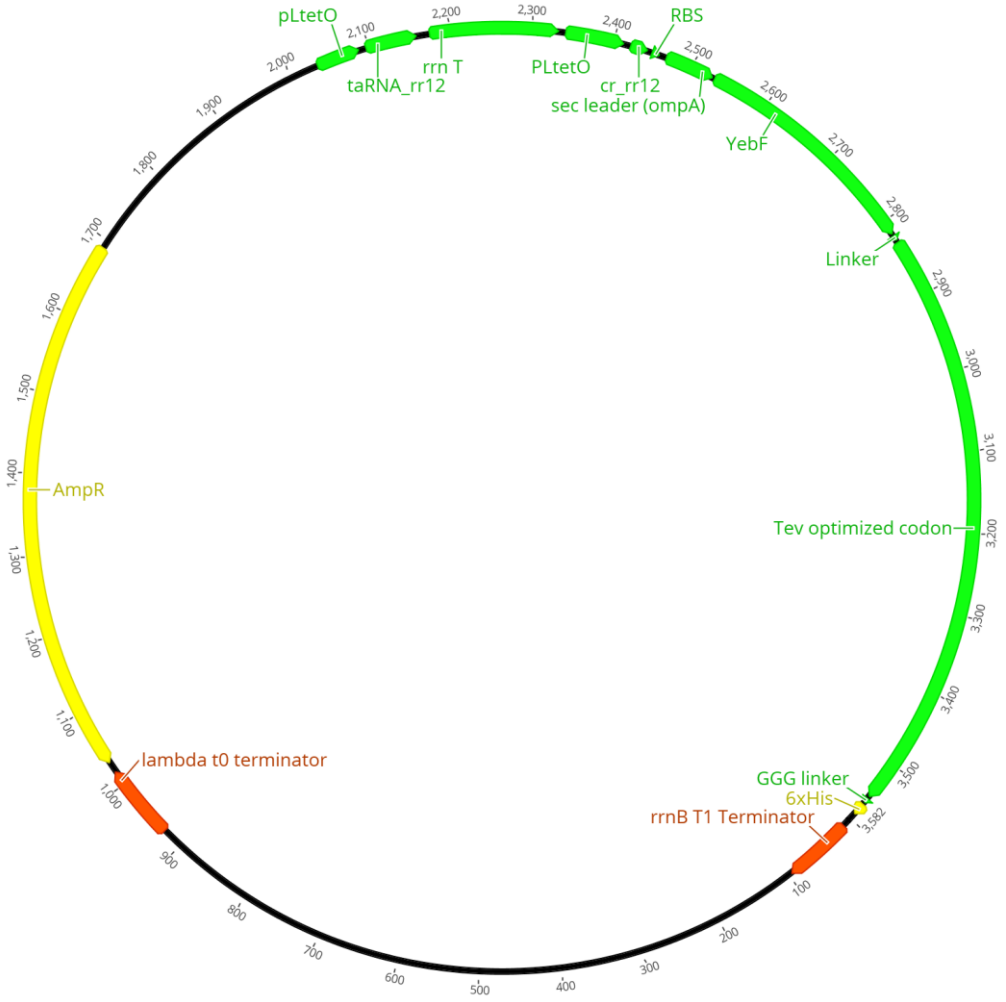

Figure C5: Schematic representation of pZA TetO OmpA YebF TEV protease vector

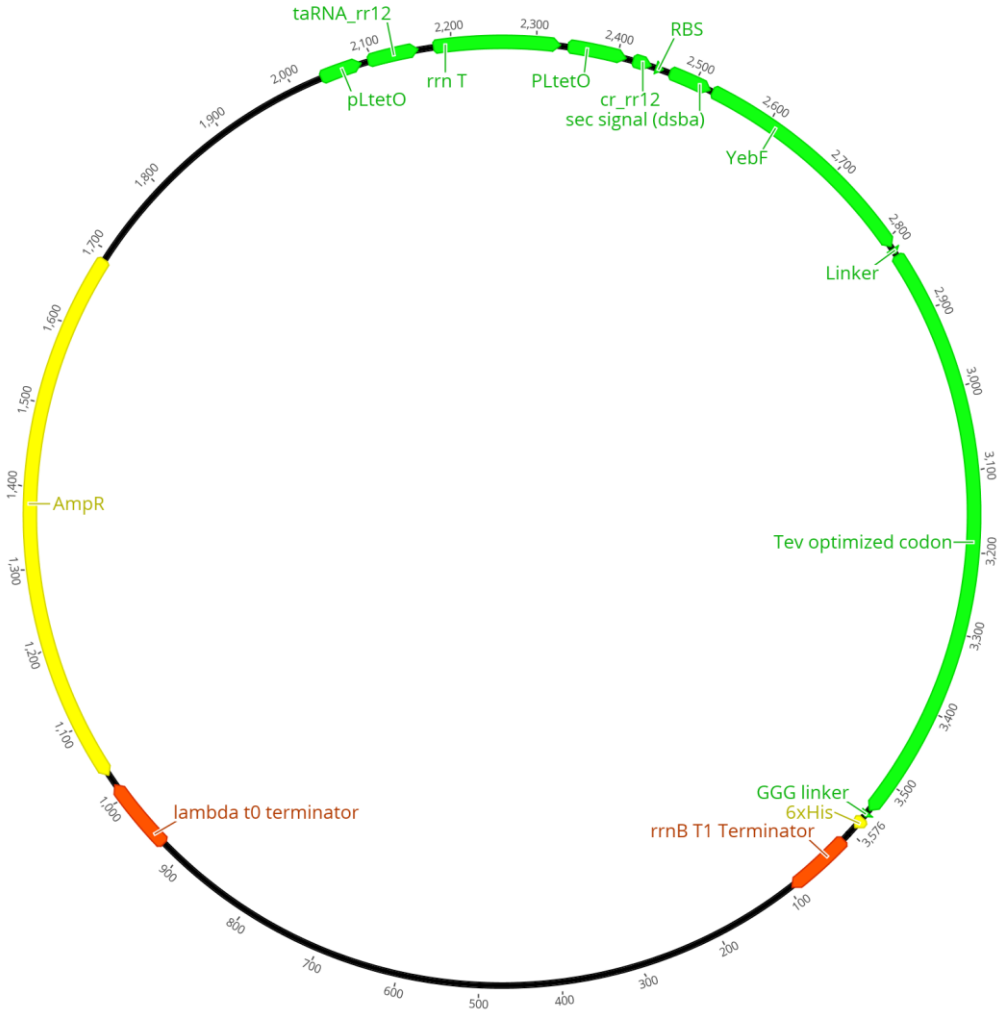

Figure C6: Schematic representation of pZA DsbA TetO YebF TEV protease vector

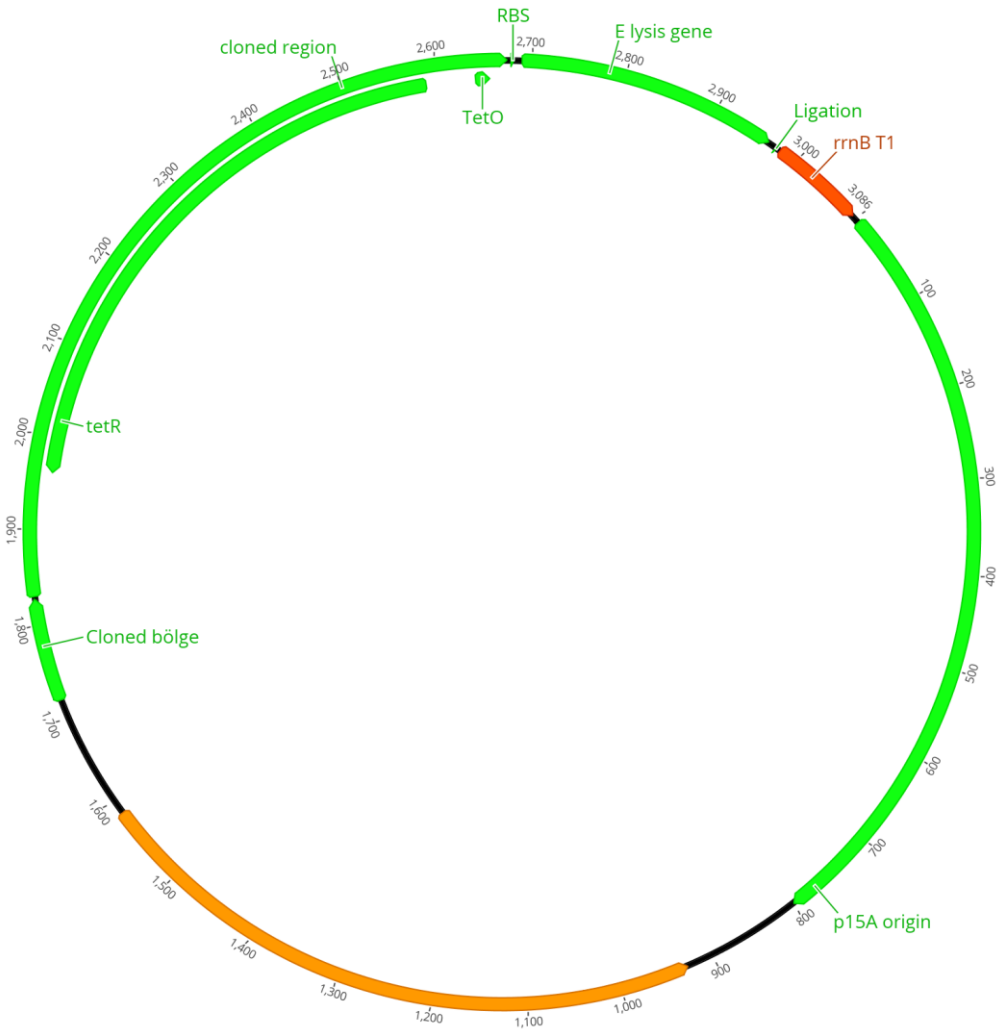

Figure C7: Schematic representation of pZA TetO E-Lysis vector

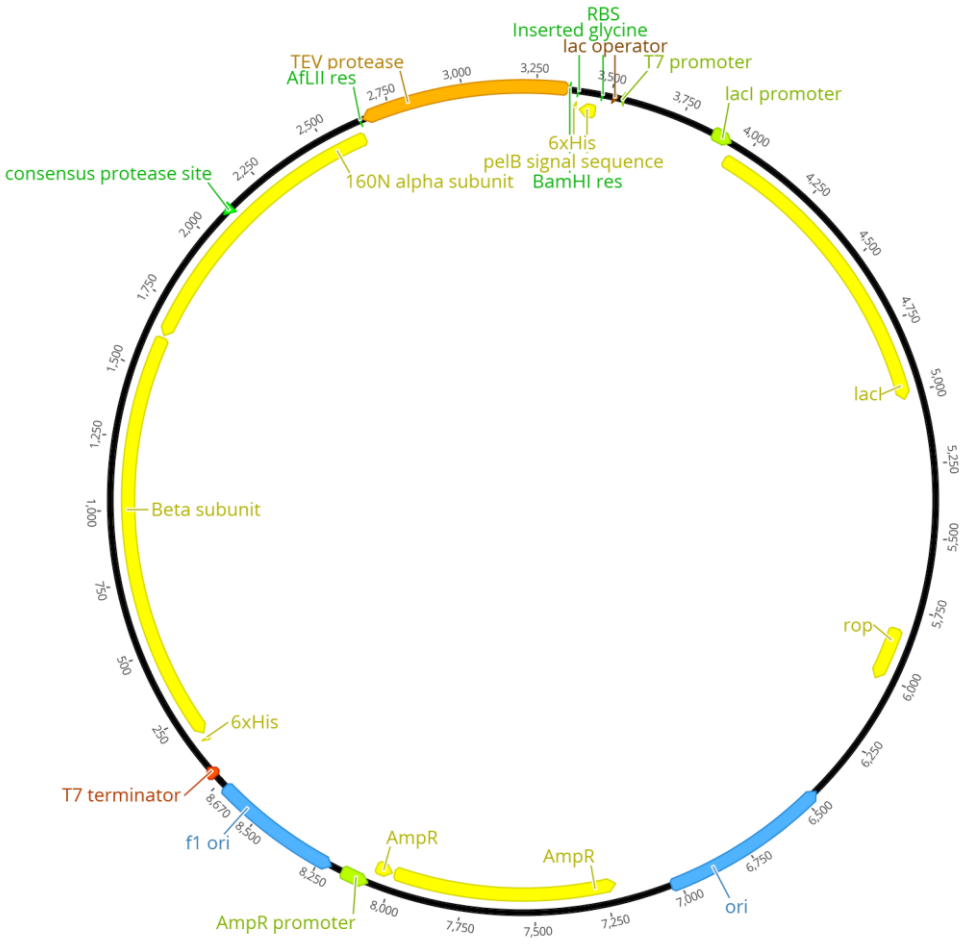

Figure C8: Schematic representation of pET22b PelB 6H Ag43 160N TEV vector.

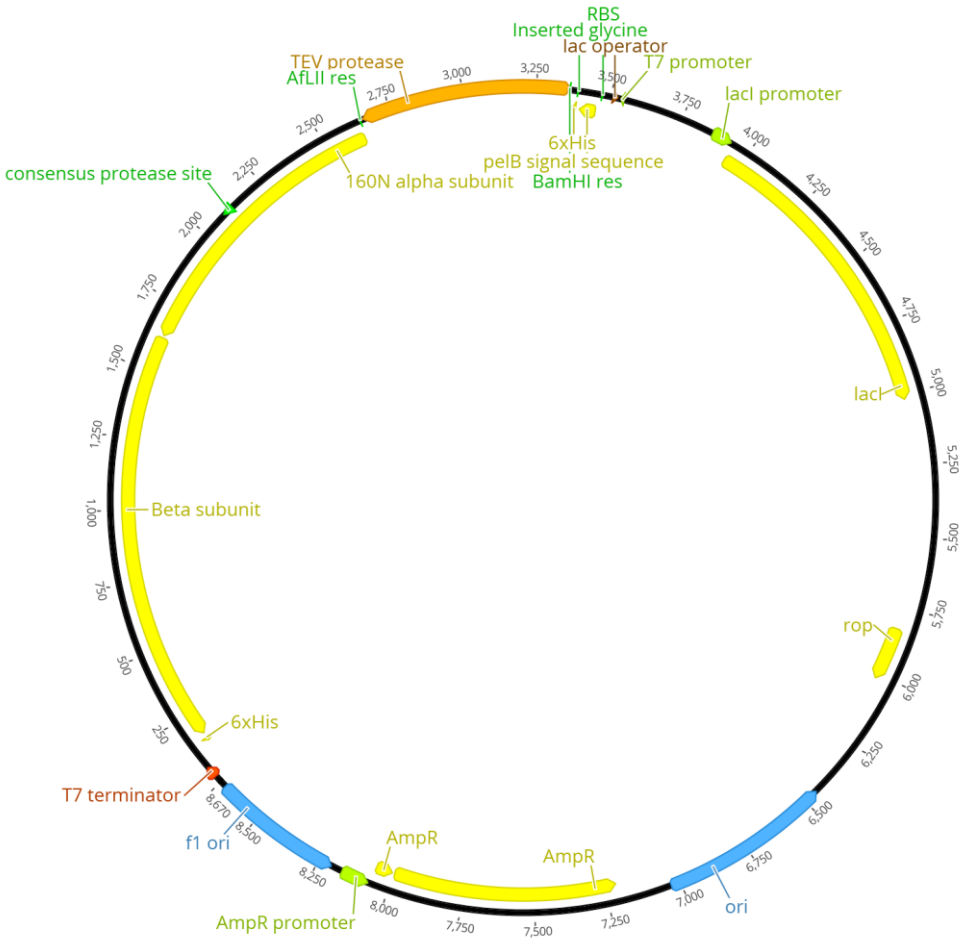

Figure C9: Schematic representation of pZA nTetO PelB 6H Ag43 160N TEV vector

APPENDIX D

Sanger sequencing results of the plasmids in this thesis

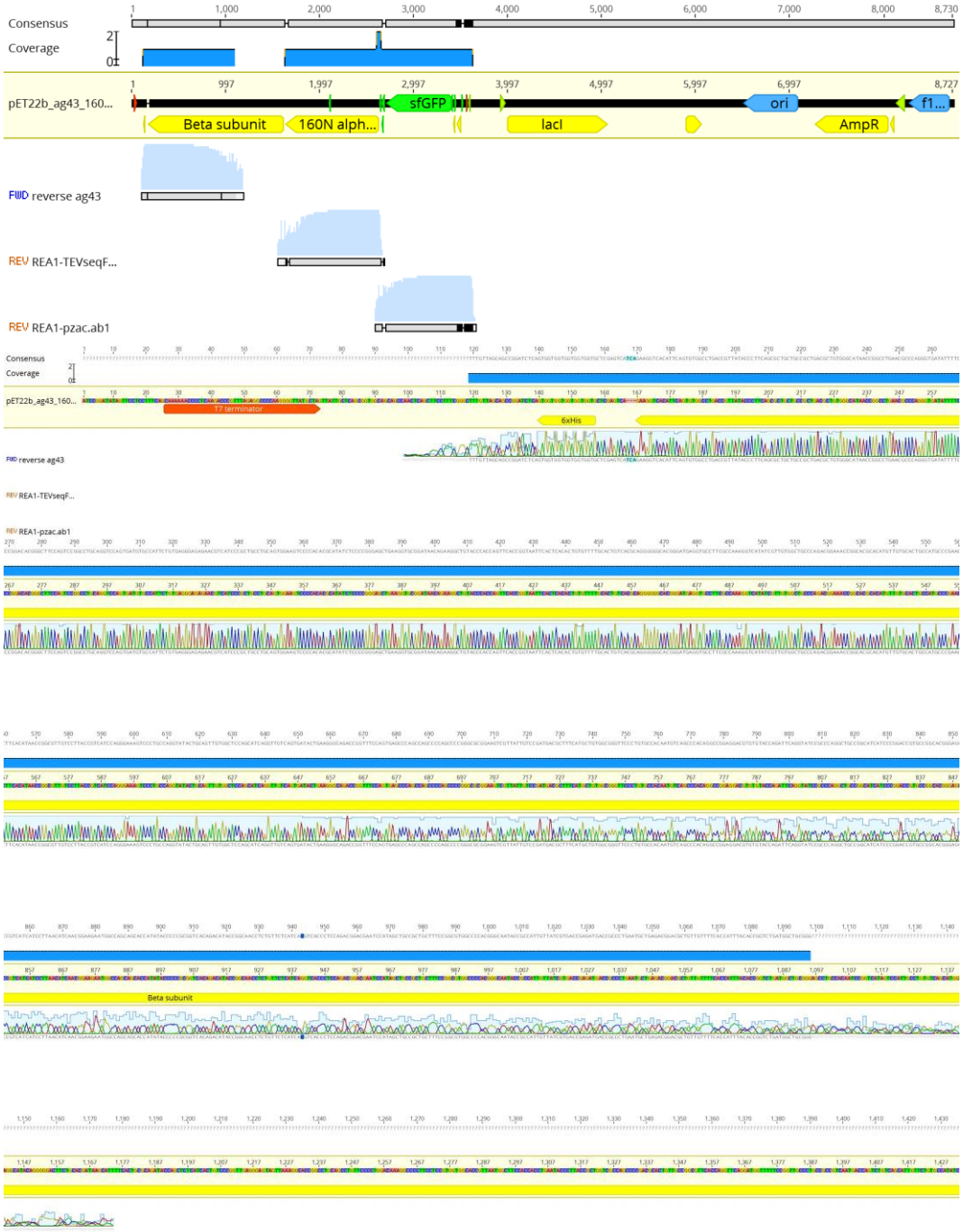

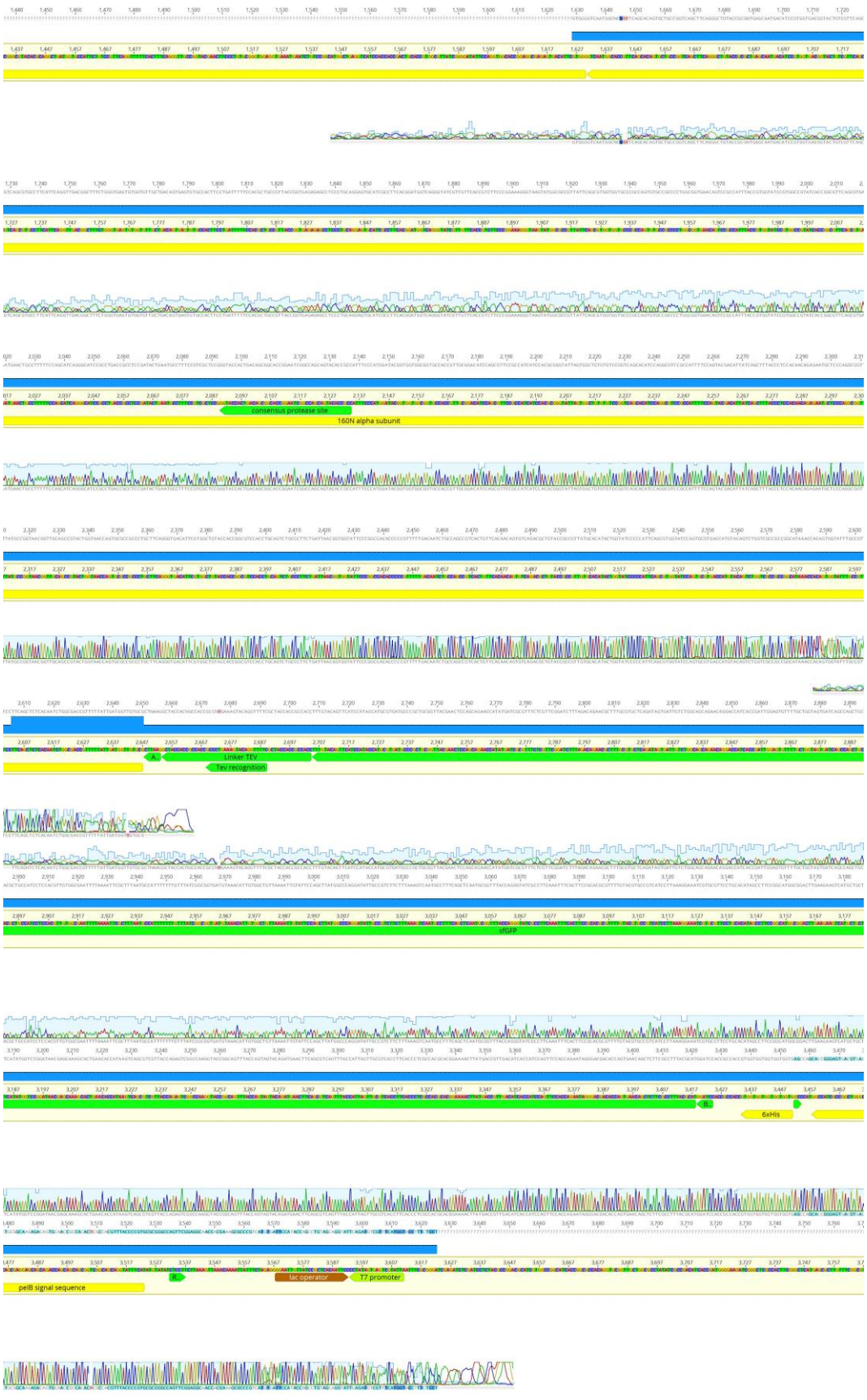
consensus protease site
160N alpha subunit
Linker TEV
Tev recognition
sfGFP
6xHis
pelB signal sequence
lac operator
T7 promoter

Figure D1: Sequence alignment of cloned of truncated Ag43 gene fused with sfGFP and His tag in pET22b vector. First alignment is broader view of alignment result in Geneious software. The following pictures shows the zoom in view in order.

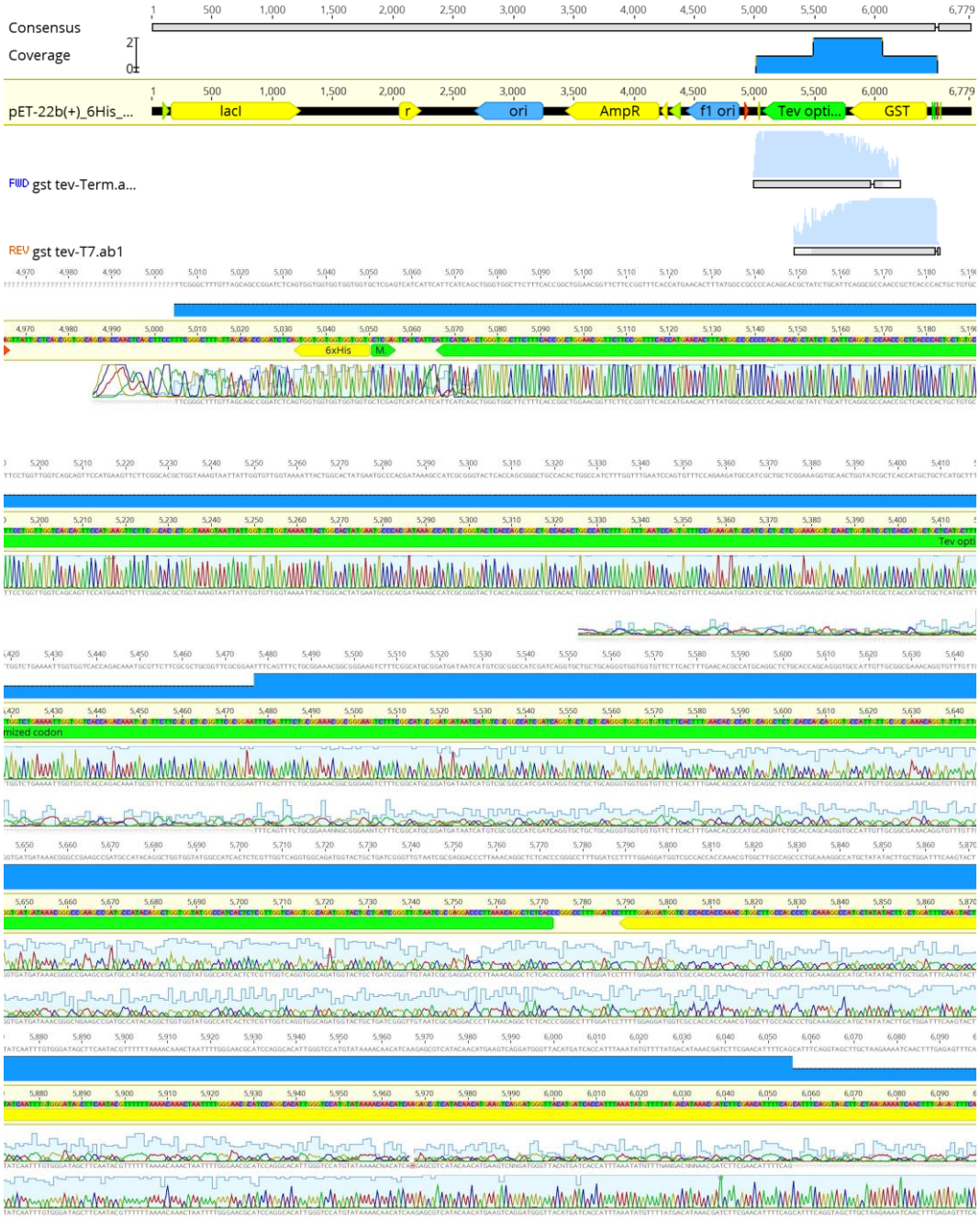

Figure D2: Sequence alignment of cloned GST gene fused with TEV protease coding sequence and N-terimal His tag in pET22b vector. First alignment is broader view of alignment result in Geneious software. The following pictures shows the zoom in view in order.

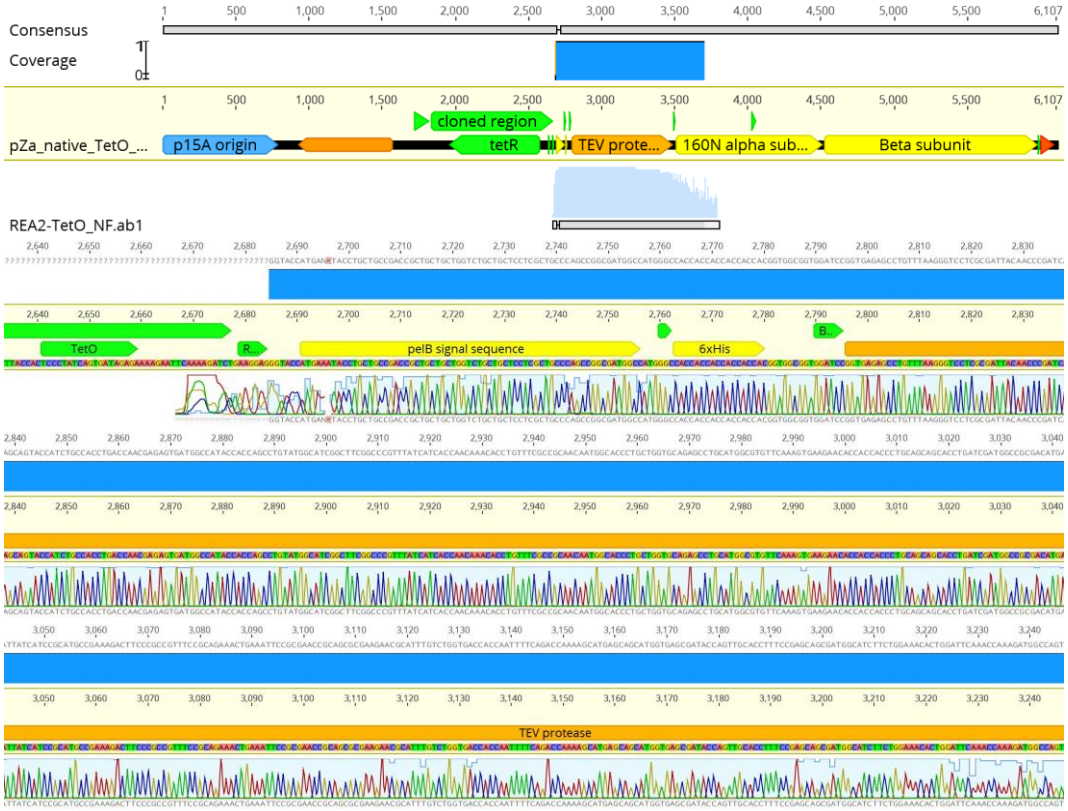

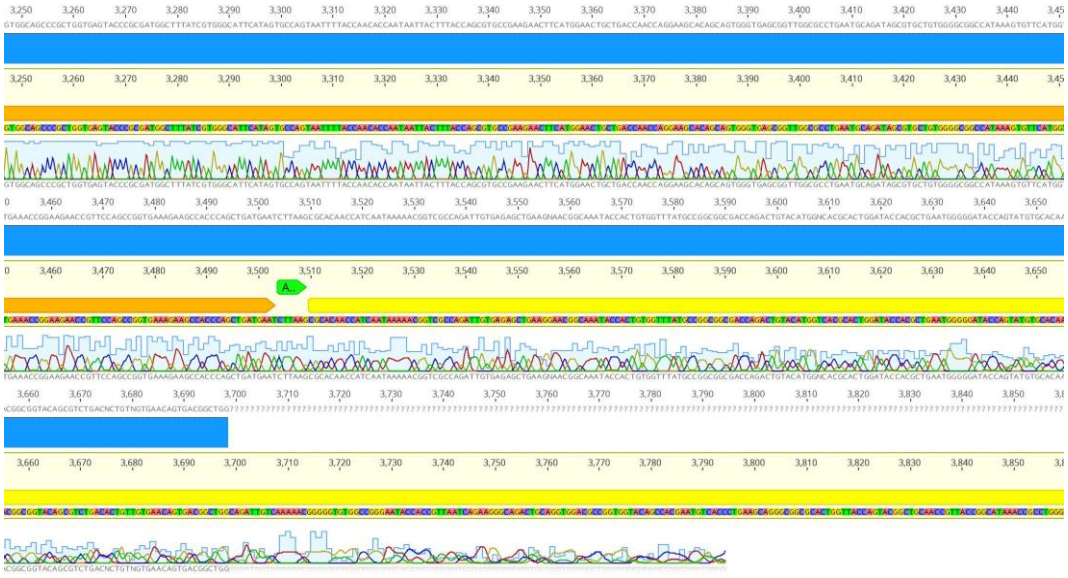

Figure D3: Sequence alignment of cloned truncated Ag43 gene fused with TEV protease coding sequence and His tag in pET22b vector. First alignment is broader view of alignment result in Geneious software. The following pictures shows the zoom in view in order.

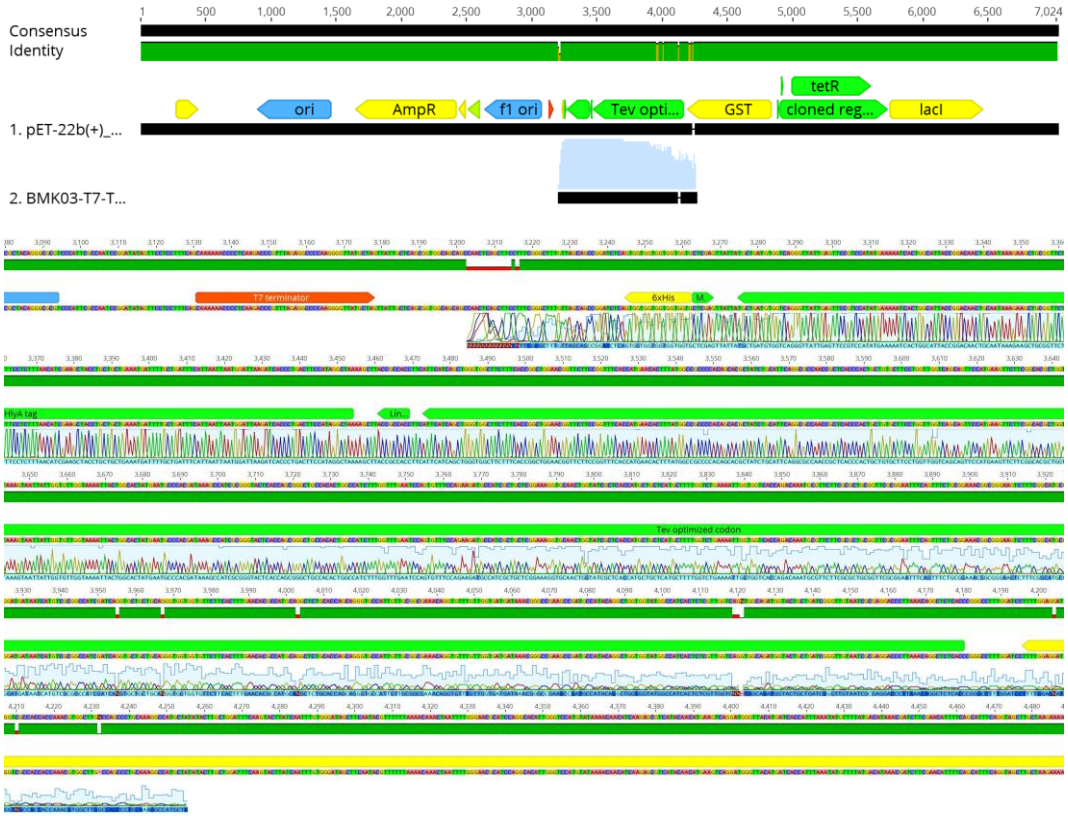

Figure D4: Sequence alignment of pET22b nTetO 6H HlyA tagged GST-TEV vector and sequencing results. First alignment is broader view of alignment result in Geneious software. The following pictures shows the zoom in view in order.

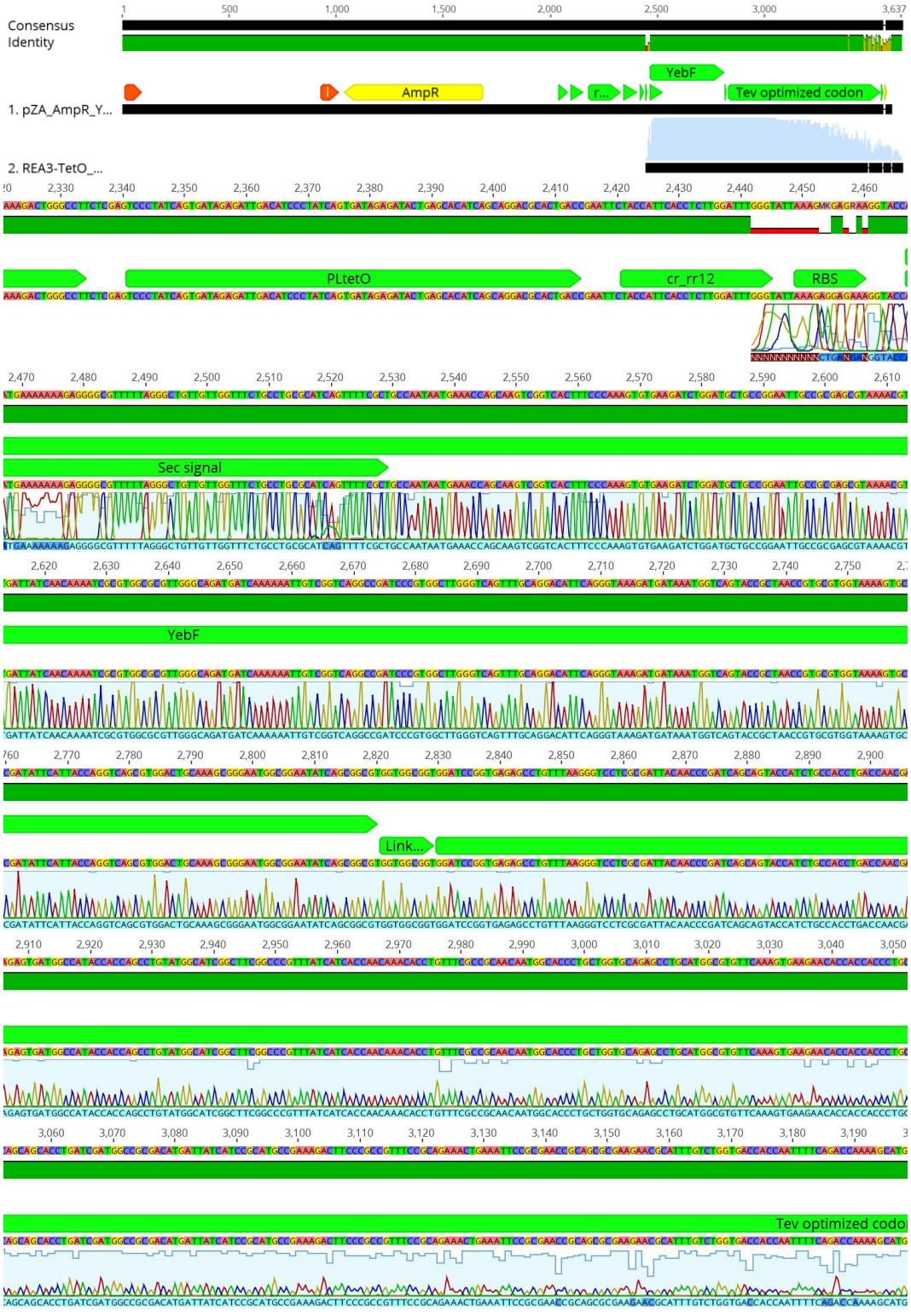

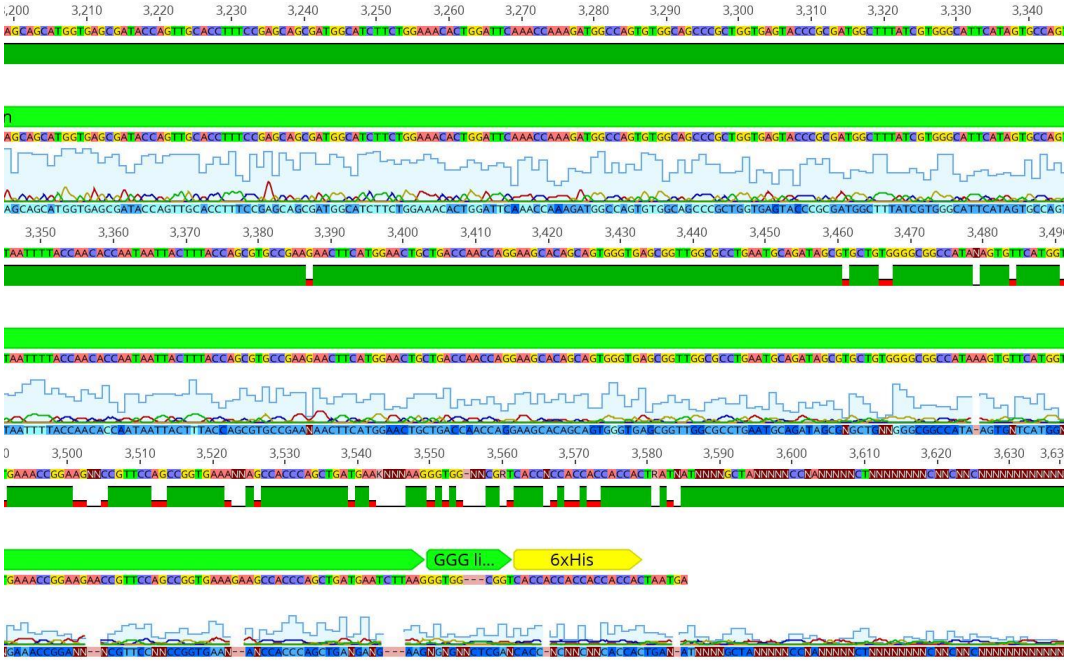

Figure D5: Sequence alignment of pZA TetO YebF-TEV vector and sequencing results. First alignment is broader view of alignment result in Geneious software. The following pictures shows the zoom in view in order.

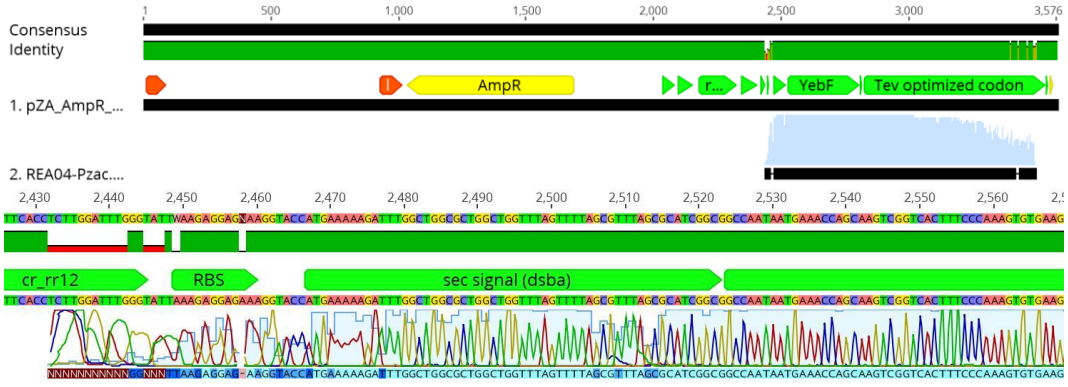

Figure D6: Sequence alignment of pZA DsbAsp/TetO YebF-TEV vector and sequencing results. First alignment is broader view of alignment result in Geneious software. The following pictures shows the zoom in view in order.

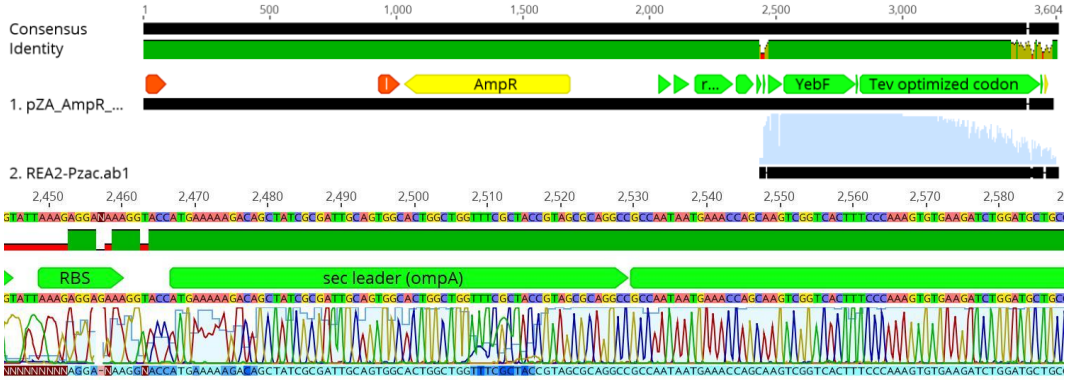

Figure D7: Sequence alignment of pZA OmpAsp/TetO YebF-TEV vector and sequencing results. First alignment is broader view of alignment result in Geneious software. The following pictures shows the zoom in view in order.

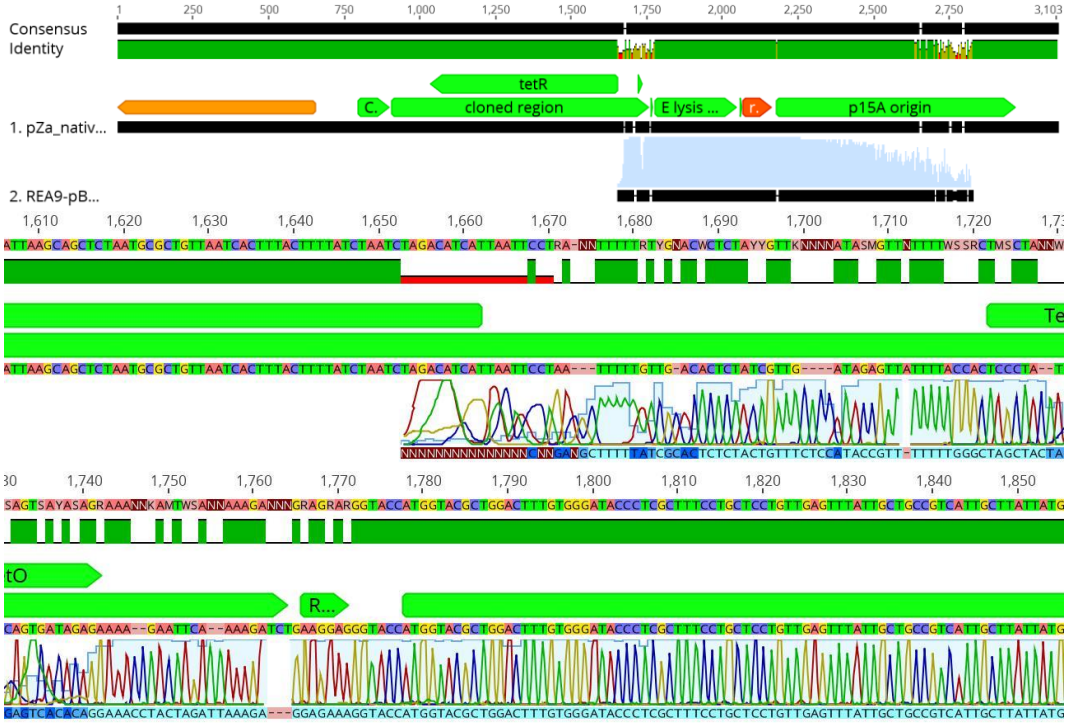

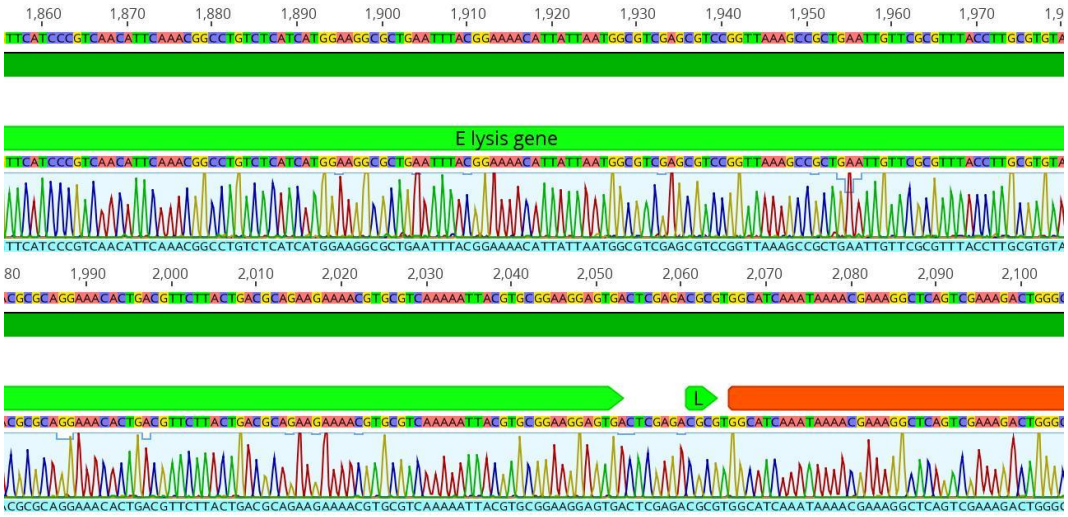

Figure D8: Sequence alignment of pZA nTetO E-lysis vector and sequencing results. First alignment is broader view of alignment result in Geneious software. The following pictures shows the zoom in view in order.

APPENDIX E

Additional reaction recipes and methods

Table E.1: Q5 polymerase PCR conditions

STEP	TEMPERATURE	TIME
Initial Denaturation	98°C	30 seconds
Polymerization	98°C	5–10 seconds
25–35 Cycles	50–72°C	10–30 seconds
	72°C	20–30 seconds/kb
Final Extension	72°C	2 minutes
Hold	4–10°C	

Table E.2: Gibson Assembly mix recipe (1.33x)

Substance	Amount
Taq ligase (40u/µl)	50µl
*5x isothermal buffer**	100µl
T5 exonuclease (1u/µl)	2µl

Phusion polymerase (2u/µl)	6.25µl
Nuclease-free water	216.75µl

Table E.3: 5x isothermal buffer recipe

Substance	**Amount**
PEG-8000	25%
Tris-HCl	500mM, pH 7.5
$MgCl_2$	50mM
DTT	50mM
NAD	5mM
dNTPs	1mM each

Table E.4: T4 ligation reaction recipe

COMPONENT	**20µl REACTION**
T4 DNA Ligase Buffer (10X)	2µl
Vector DNA	50ng
Insert DNA	equal molar to vector DNA

Nuclease-free water	to 20µl
T4 DNA Ligase	1µl

APPENDIX F

Additional results

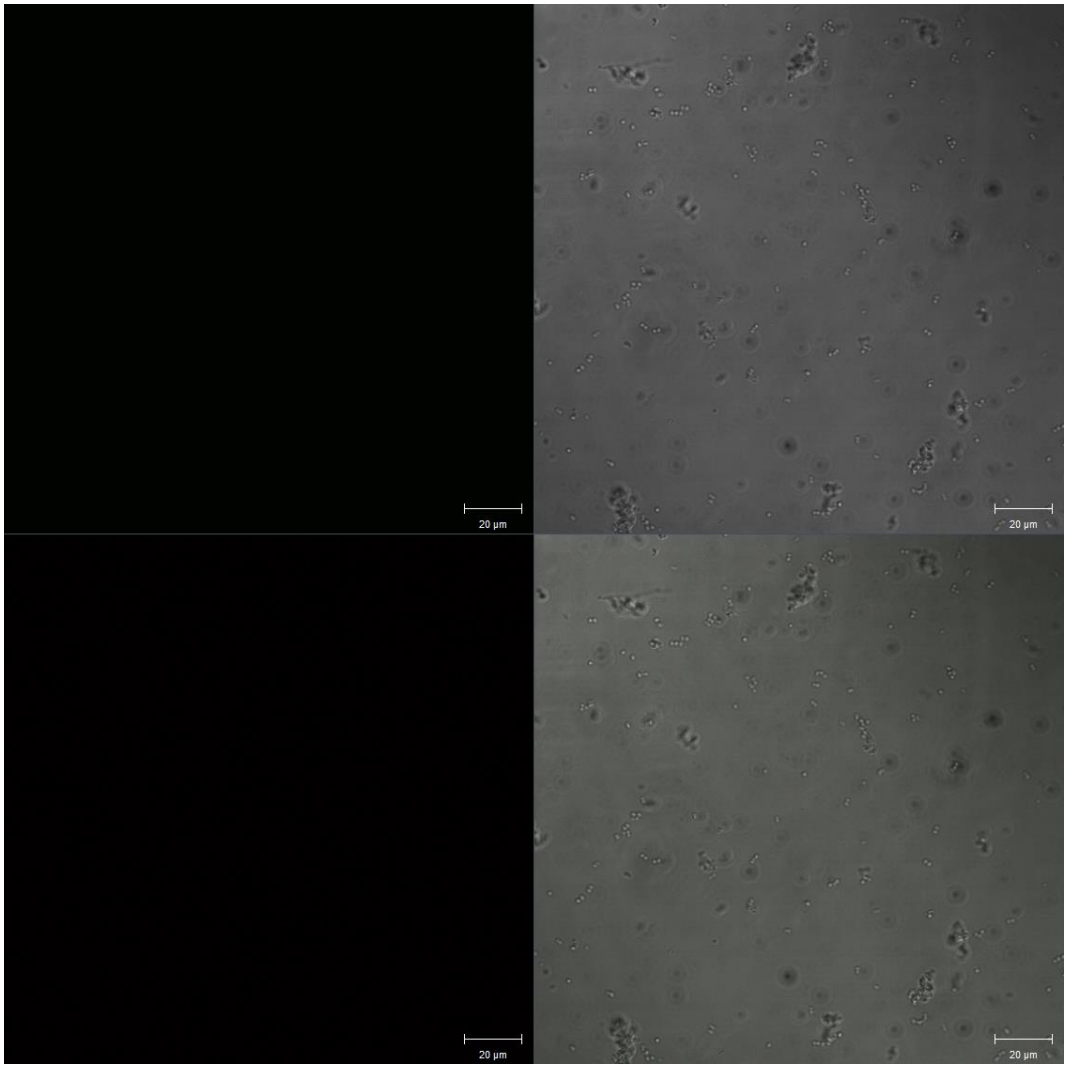

Figure F1: ICC results of BL21 cells. The image obtained by the blue light excited (top-left), bright field (top right), green light excited (bottom-left) and all merged (bottom-right).

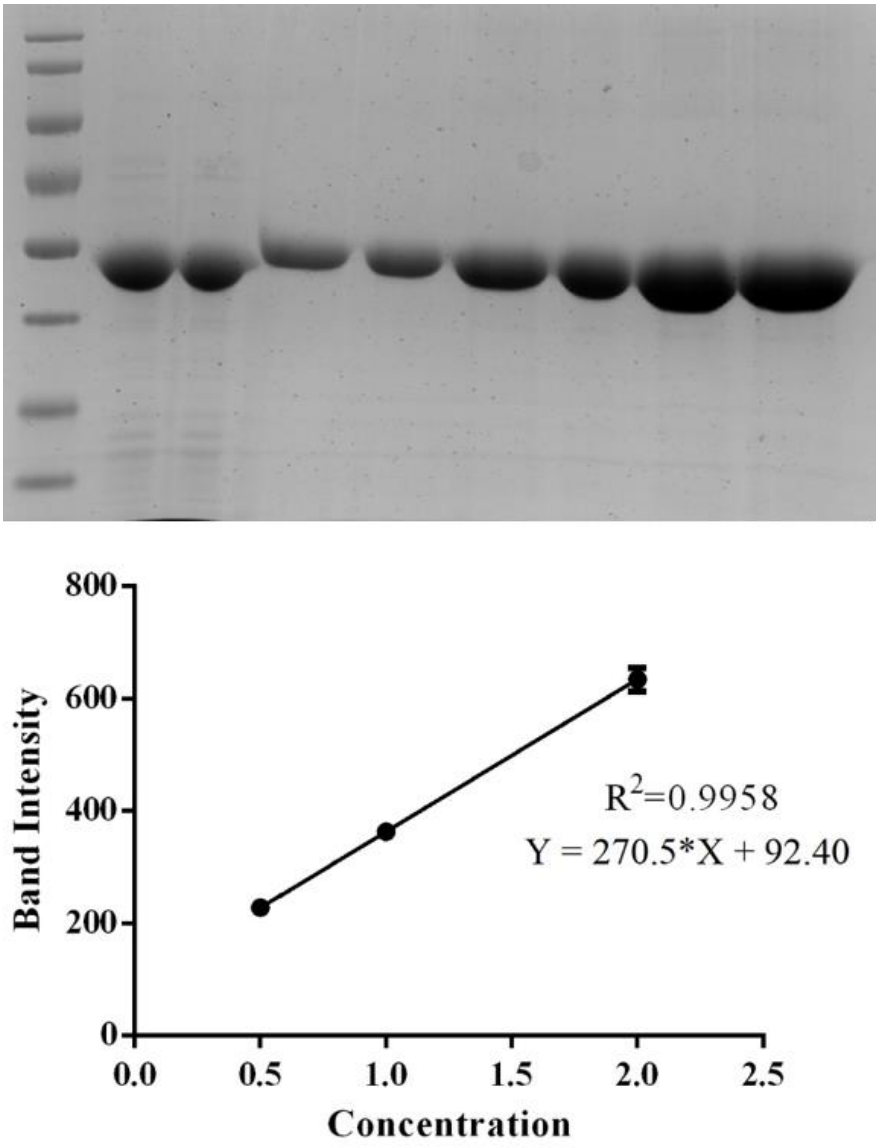

Figure F2: Standard curve obtained from densitometry analysis of BSA bands. The concentration of GST-TEV was calculated as 0.72 μg/μl.